



Muon $g-2$ Experiment at Fermilab

Esra Barlas Yucel

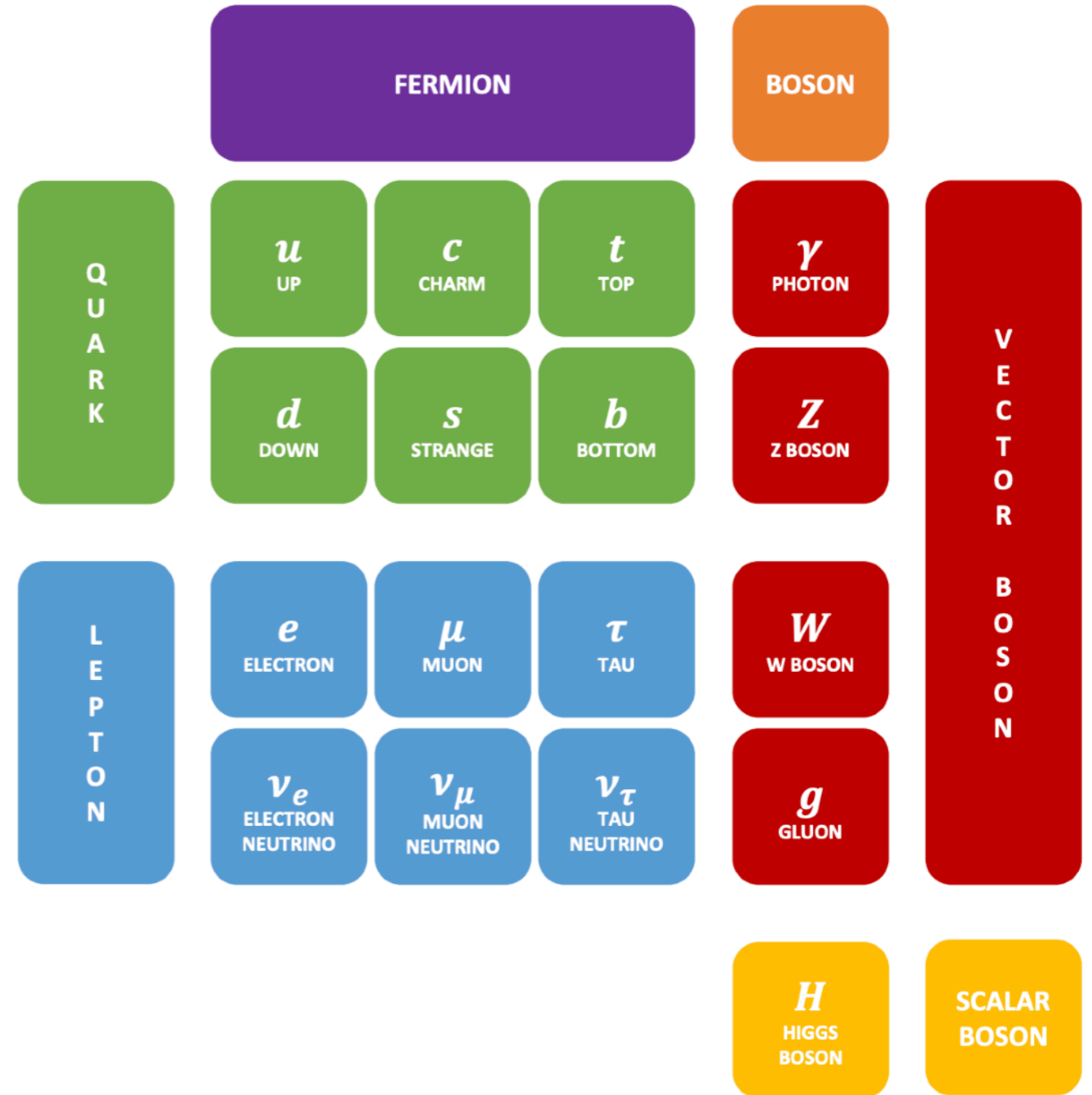
SIST/GEM Summer Lectures

5 July 2022



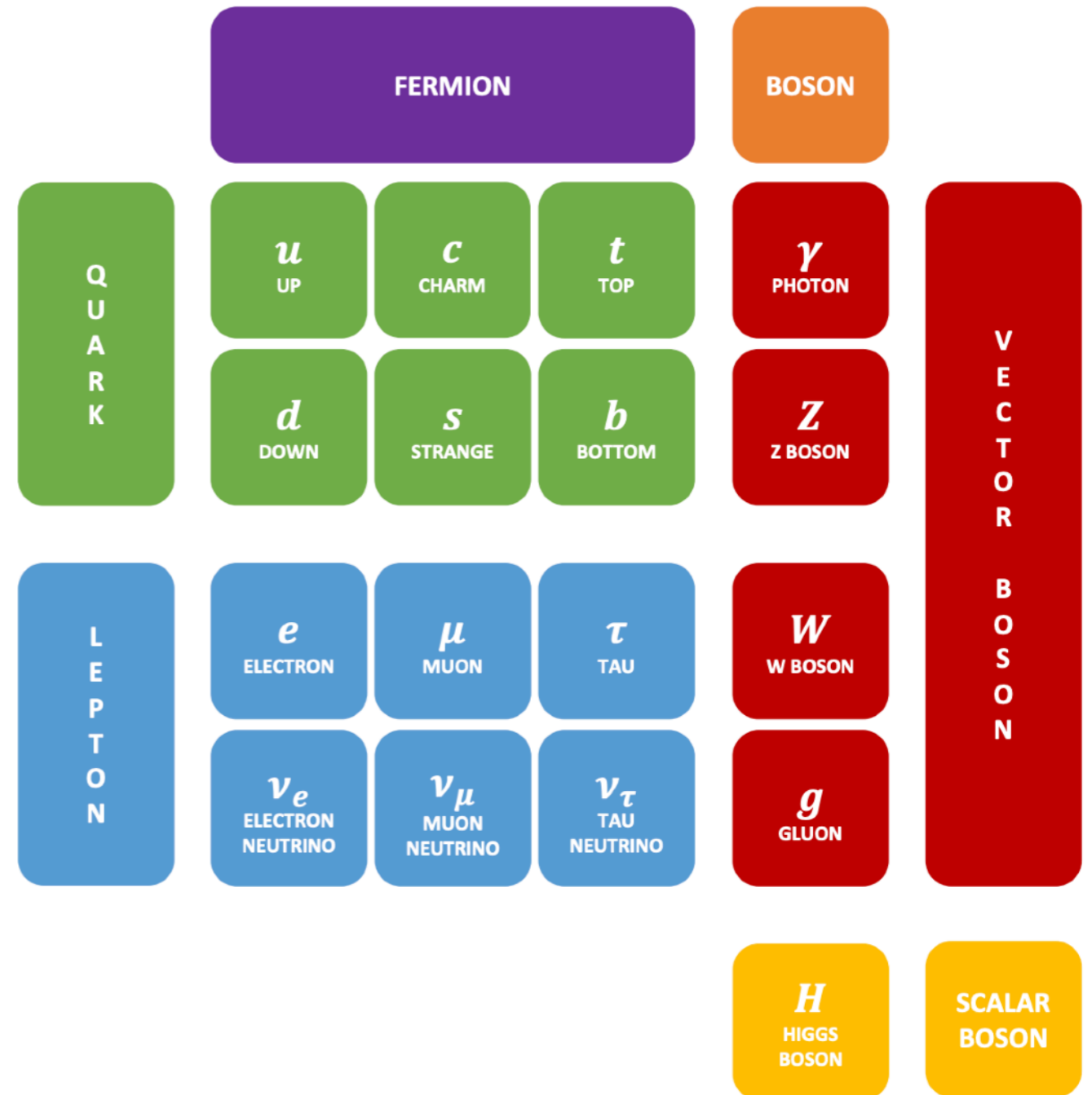
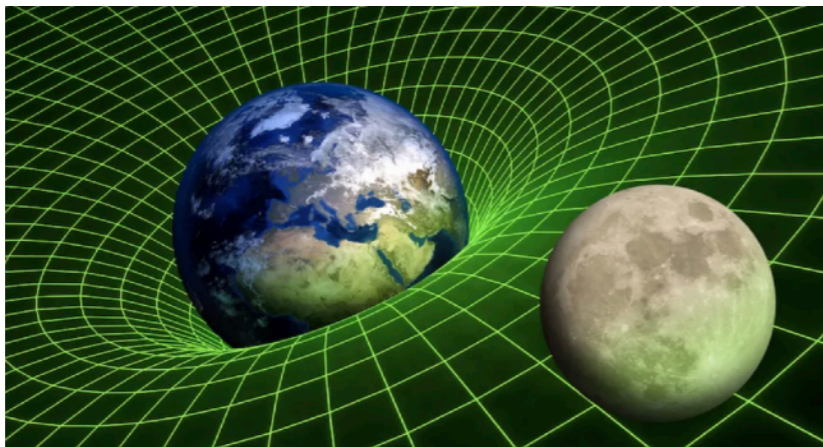
What leads us to searching for new physics

- We have SM to explain
 - Three out of four fundamental forces
 - Classify all elementary particles
 - Successful on providing experimental prediction
- But it is not complete on describing fundamental interactions



What leads us to searching for new physics

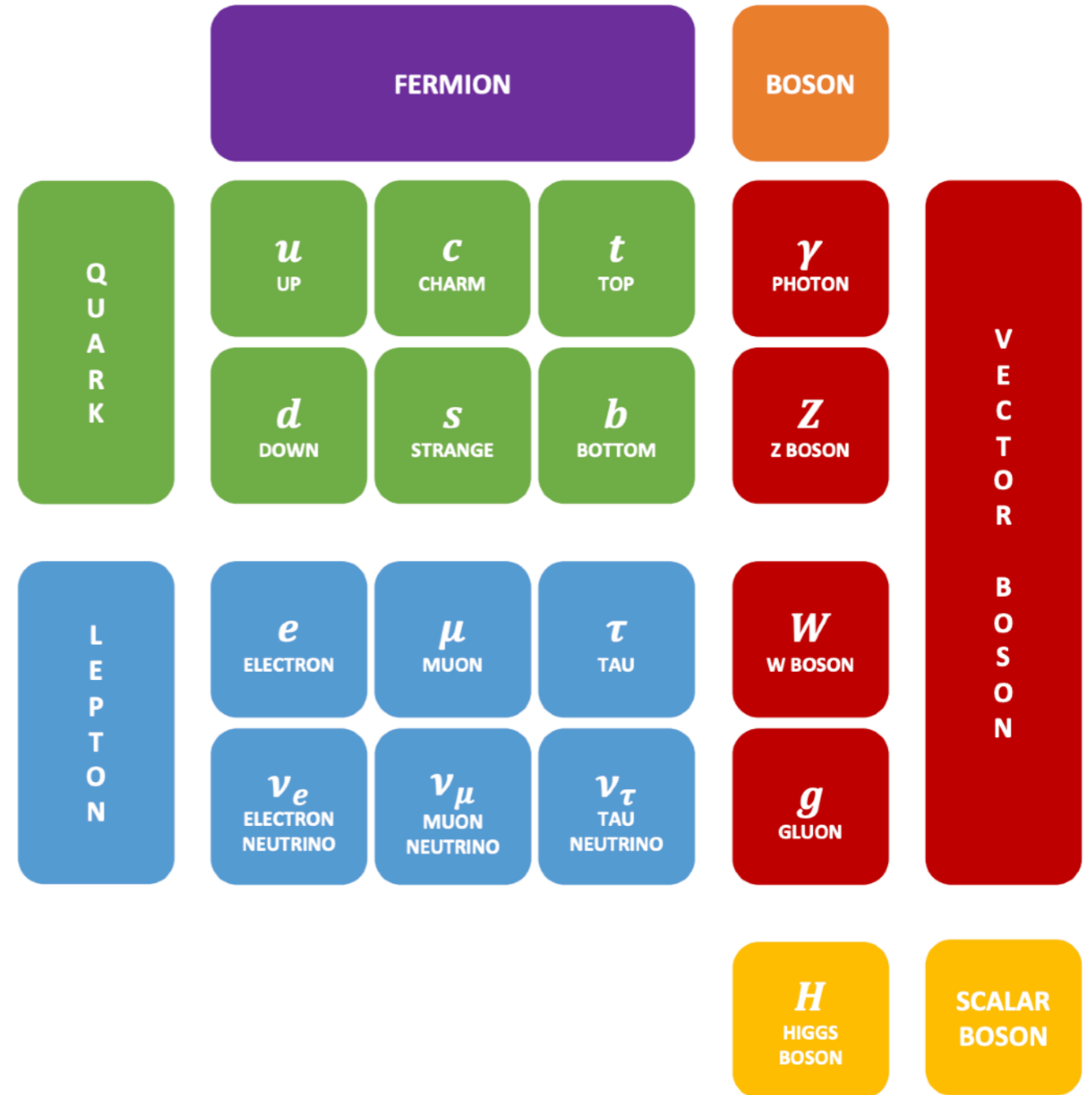
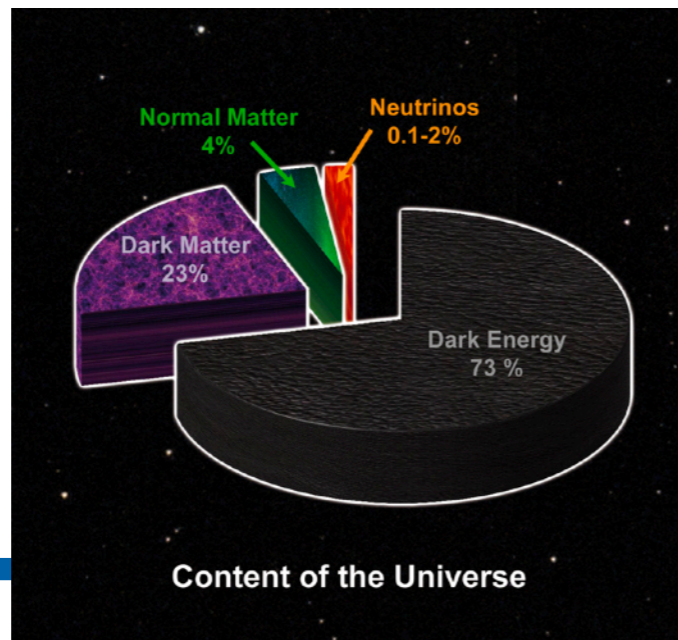
- We have SM to explain
 - Three out of four fundamental forces
 - Classify all elementary particles
 - Successful on providing experimental prediction
- But it is not complete on describing fundamental interactions
 - ❖ Theory of gravitation



What leads us to searching for new physics

- We have SM to explain
 - Three out of four fundamental forces
 - Classify all elementary particles
 - Successful on providing experimental prediction
- But it is not complete on describing fundamental interactions

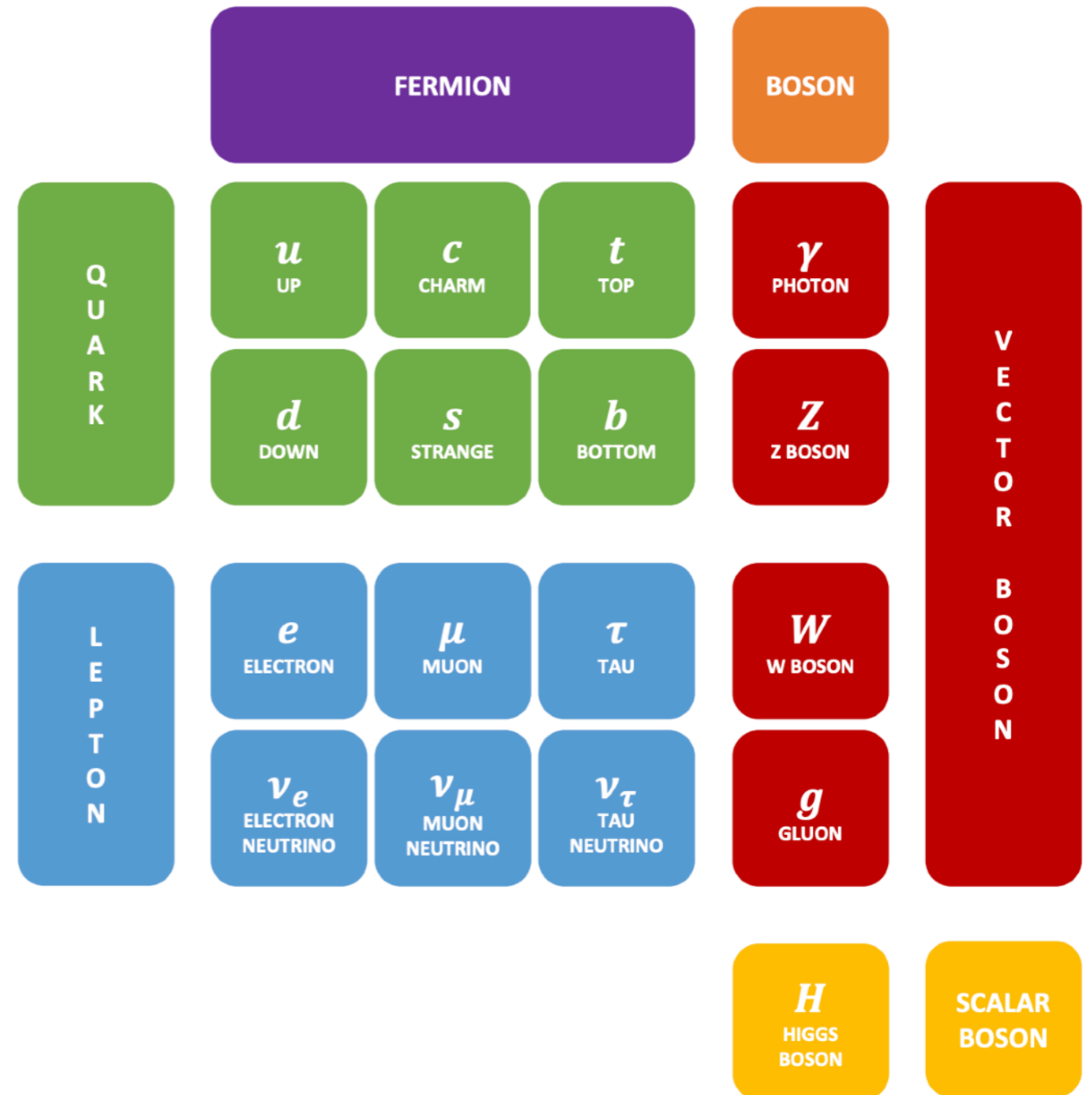
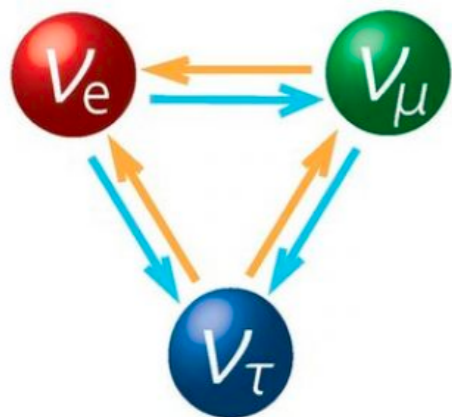
❖ Dark Energy



What leads us to searching for new physics

- We have SM to explain
 - Three out of four fundamental forces
 - Classify all elementary particles
 - Successful on providing experimental prediction
- But it is not complete on describing fundamental interactions

❖ Neutrino oscillations



Searching for new physics

Frontiers of Particle Physics

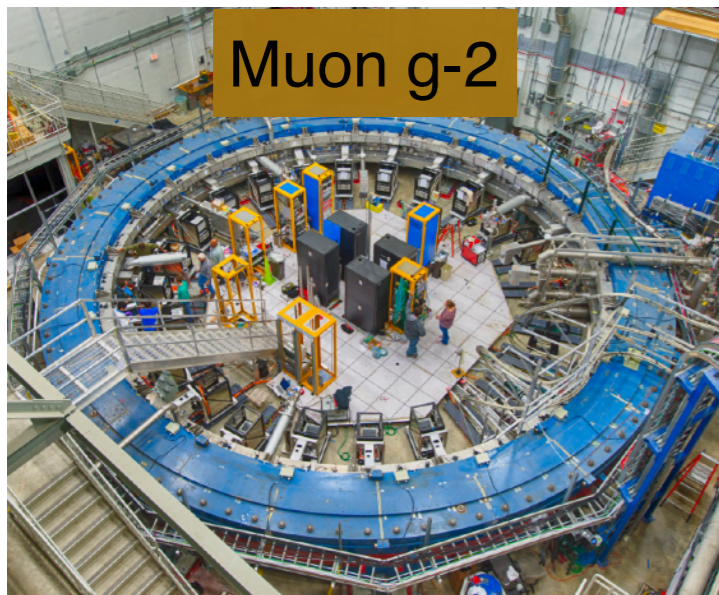
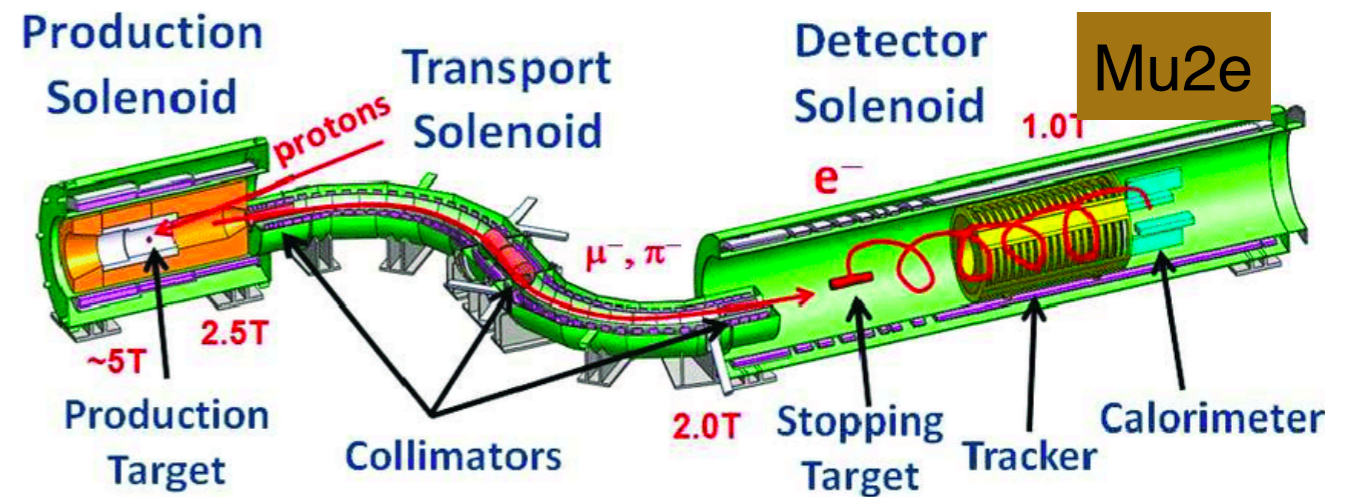
Cosmic Frontier

Intensity Frontier

Energy Frontier

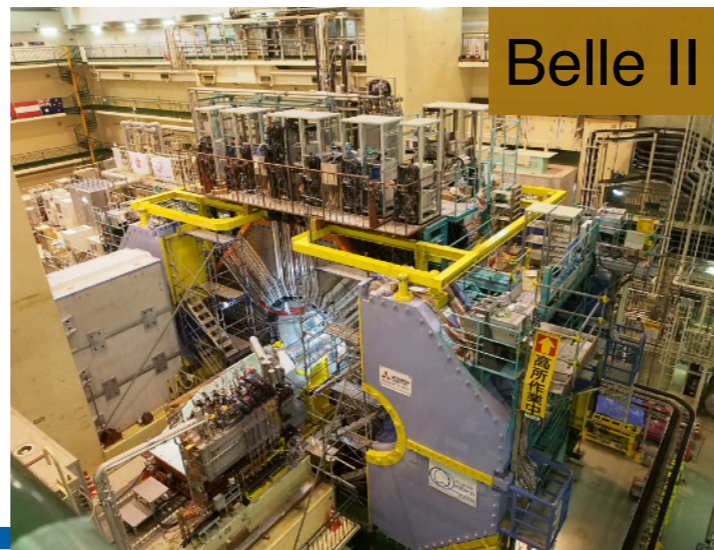
High Intensity:

- Accurate and sensitive measurement to test SM
- Lower energy
- See new particles or forces
- Even forbidden processes...



Muon g-2

Measure the muon magnetic moment Anomaly



Belle II

Study the properties of B mesons

-Exploring with precision measurements-

Searching for new physics

Frontiers of Particle Physics

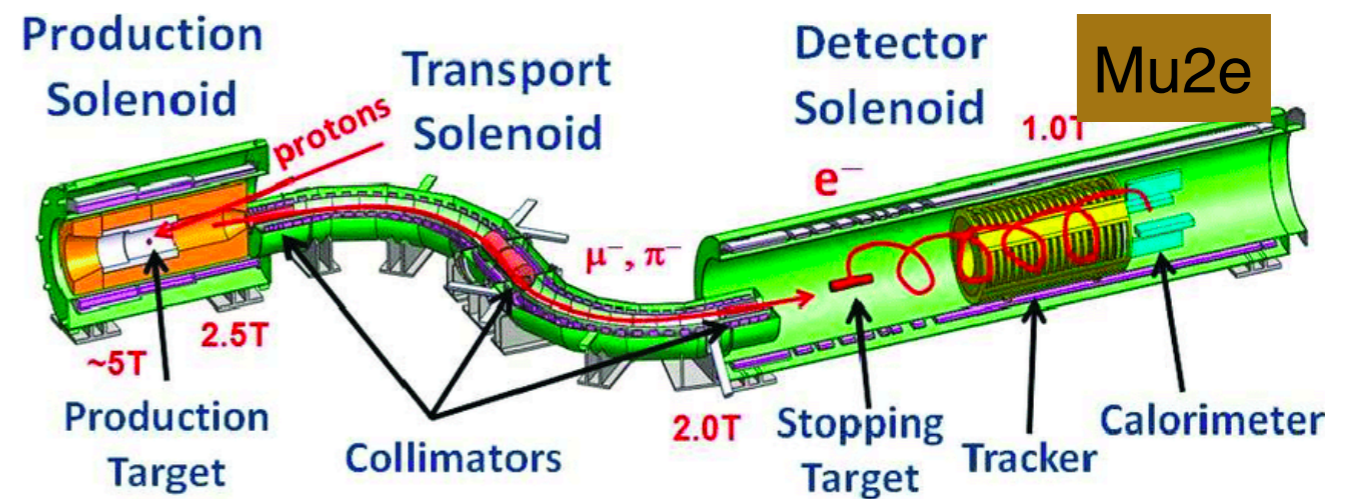
Cosmic Frontier

Intensity Frontier

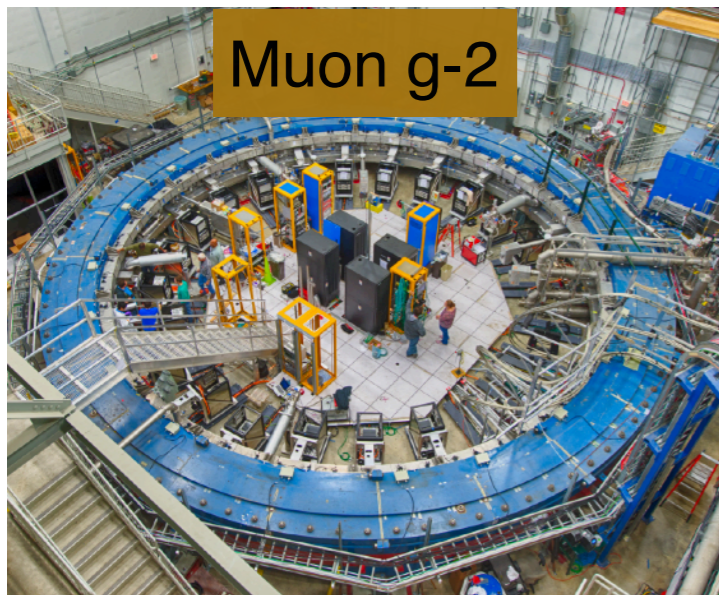
Energy Frontier

High Intensity:

- Accurate and sensitive measurement to test SM
- Lower energy
- See new particles or forces
- Even forbidden processes...

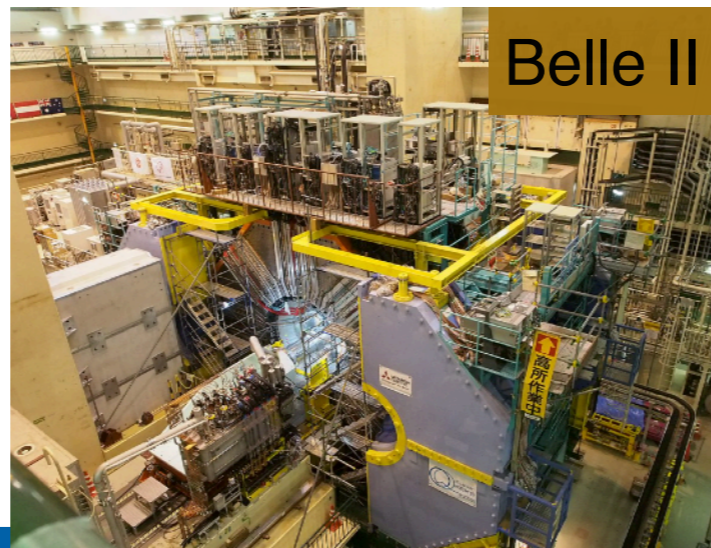


Searching for muon to electron event



Muon g-2

Measure the muon magnetic moment Anomaly

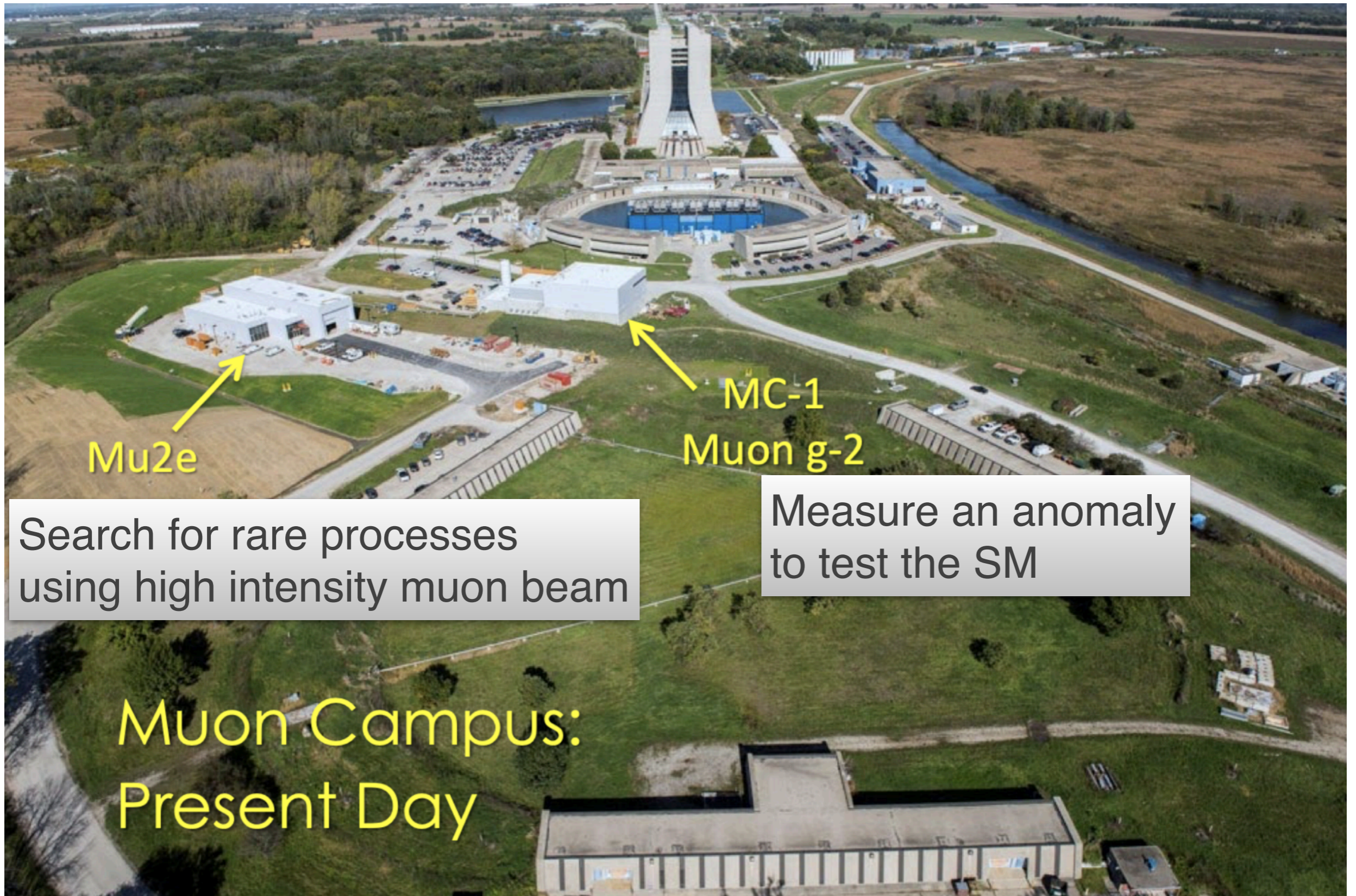


Belle II

Study the properties of B mesons

-Exploring with precision measurements-

Muon Physics at Fermilab



Mu2e

MC-1
Muon g-2

Search for rare processes
using high intensity muon beam

Measure an anomaly
to test the SM

Muon Campus:
Present Day

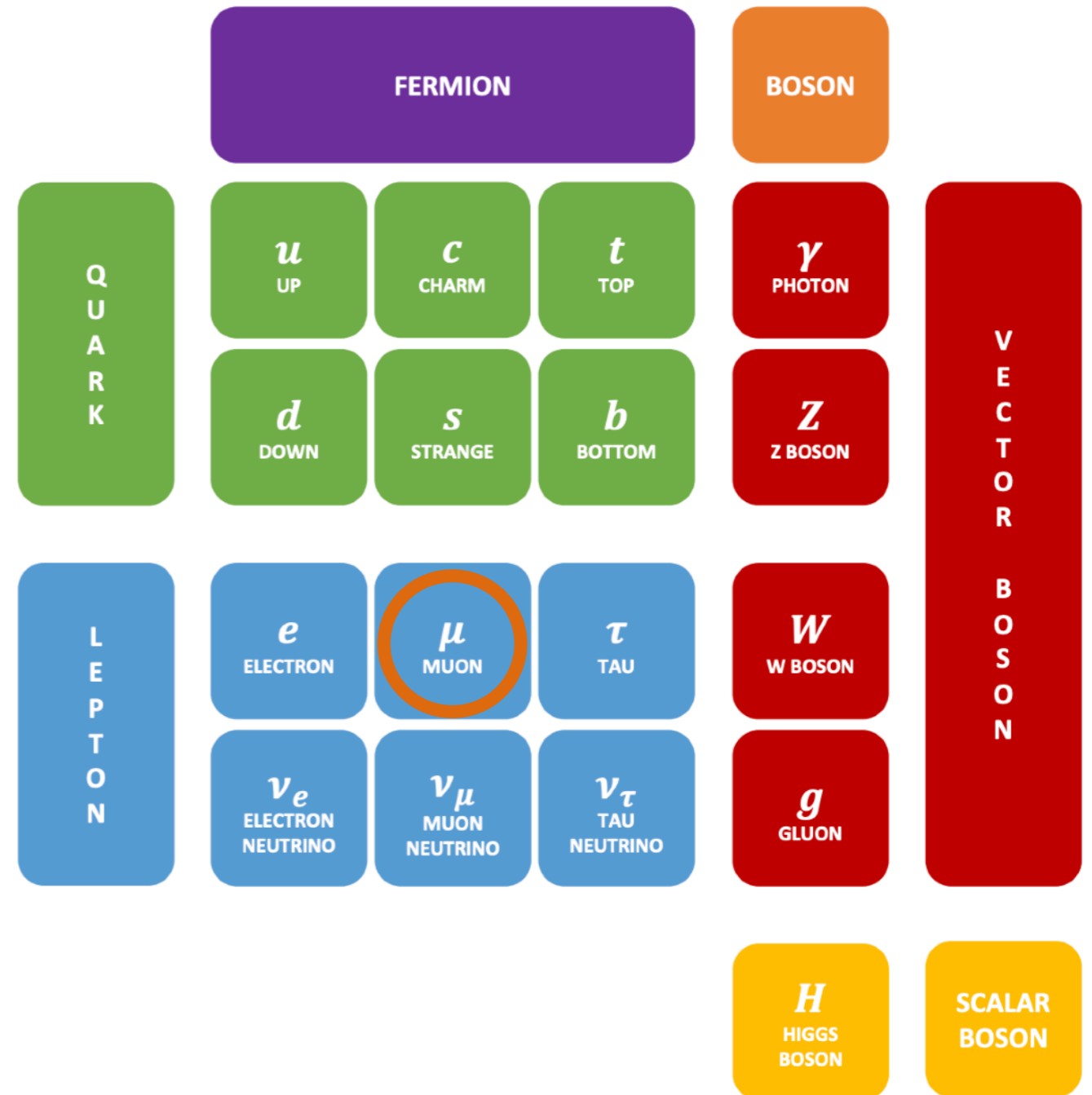
Why the Muons?

Muons are useful!

- $(m_\mu/m_e)^2 = 40000 \rightarrow$ More sensitive to new physics.
- Easy to produce, muon beams from pion decays(99.9%).
- Relatively long lifetime ($2.2 \mu s$) \rightarrow In the lab frame $64.4 \mu s$

Why measure the muon anomaly

- An accurate way to test SM validity
- BNL measurement hints at the possibility of new physics.

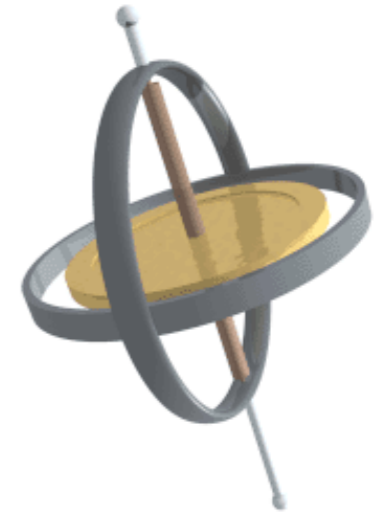


Muon Magnetic Moment and Defining the Anomaly

Magnetic Moment of Muon

$$\vec{\mu} = g_{\mu} \frac{e}{2m} \vec{s}$$

g : Proportionality constant between spin and magnetic moment (shows strength of the magnetic moment)



Anomalous Magnetic Moment of Muon

$$a_{\mu} = \frac{g_{\mu} - 2}{2}, \quad \vec{\mu} = (1 + a_{\mu}) \frac{e}{m} \vec{s}$$



Shows how much g differs fractionally from 2!

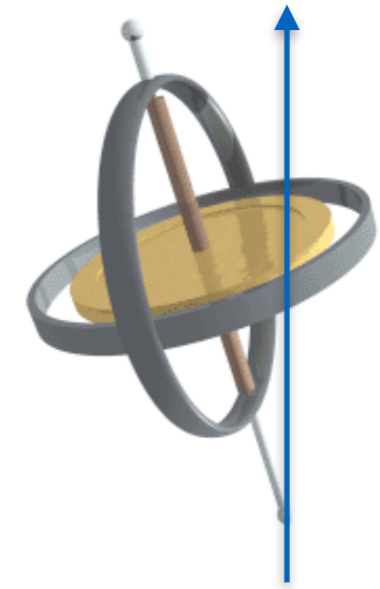
Measuring this anomaly could tell us if there are new particles or even forces that contribute to a_{μ}

Muon Magnetic Moment and Defining the Anomaly

Magnetic Moment of Muon

$$\vec{\mu} = g_{\mu} \frac{e}{2m} \vec{s}$$

g : Proportionality constant between spin and magnetic moment (shows strength of the magnetic moment)



Magnetic Field

Anomalous Magnetic Moment of Muon

$$a_{\mu} = \frac{g_{\mu} - 2}{2}, \quad \vec{\mu} = (1 + a_{\mu}) \frac{e}{m} \vec{s}$$



Shows how much g differs fractionally from 2!

Measuring this anomaly could tell us if there are new particles or even forces that contribute to a_{μ}

Muon Magnetic Moment and Defining the Anomaly

Magnetic Moment of Muon

$$\vec{\mu} = g_{\mu} \frac{e}{2m} \vec{s}$$

g : Proportionality constant between spin and magnetic moment (shows strength of the magnetic moment)

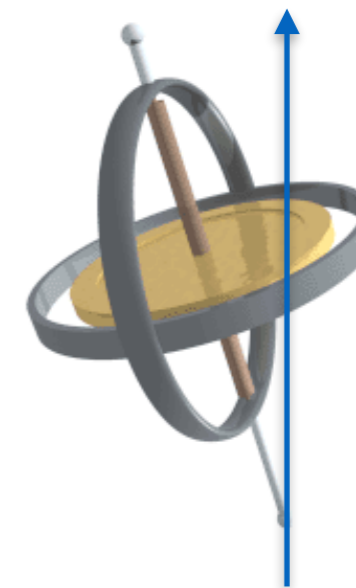
Anomalous Magnetic Moment of Muon

$$a_{\mu} = \frac{g_{\mu} - 2}{2}, \quad \vec{\mu} = (1 + a_{\mu}) \frac{e}{m} \vec{s}$$

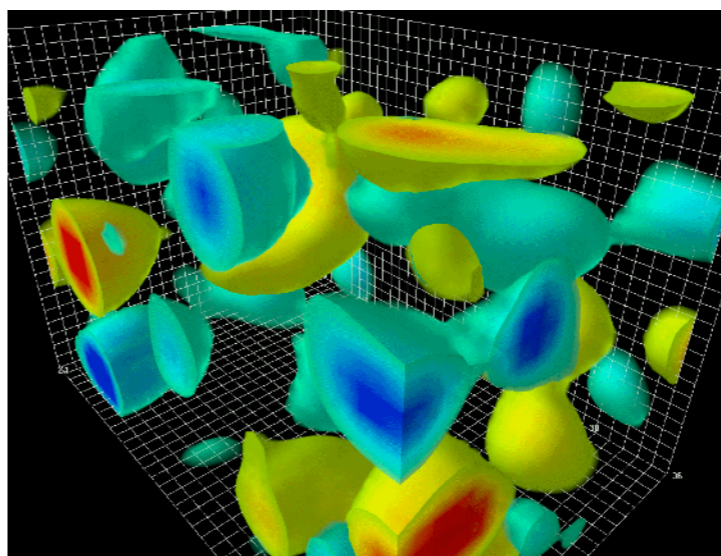


Shows how much g differs fractionally from 2!

Measuring this anomaly could tell us if there are new particles or even forces that contribute to a_{μ}



Magnetic Field

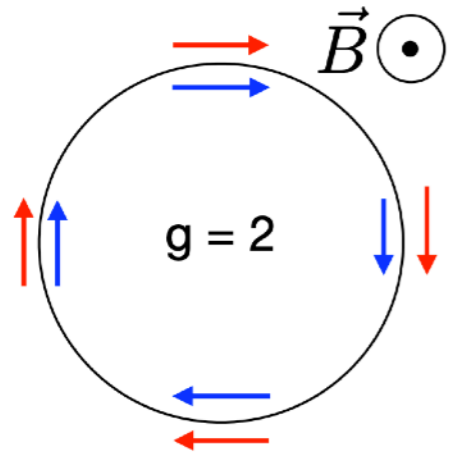


- Particles don't exist by themselves
- They are surrounded by a quantum vacuum where virtual particles exist for a short time
- That could explain muon's interaction with the magnetic field

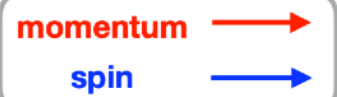
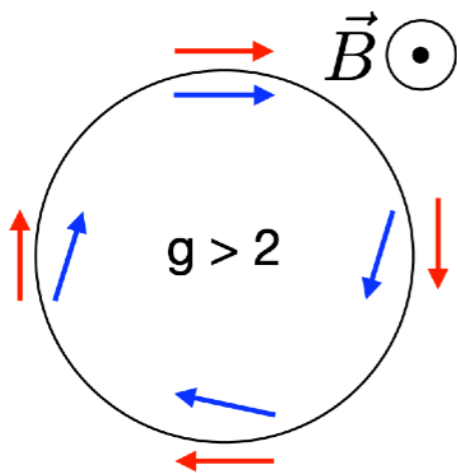
Muon Magnetic Moment and Measuring the Anomaly

polarized muons in a magnetic field

$$\text{If } g = 2 \Rightarrow \vec{\omega}_a = 0$$



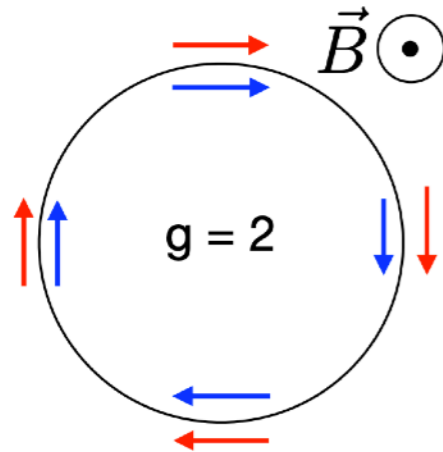
$$g \neq 2 \Rightarrow \vec{\omega}_a \cong a_\mu \frac{e}{m} \vec{B}$$



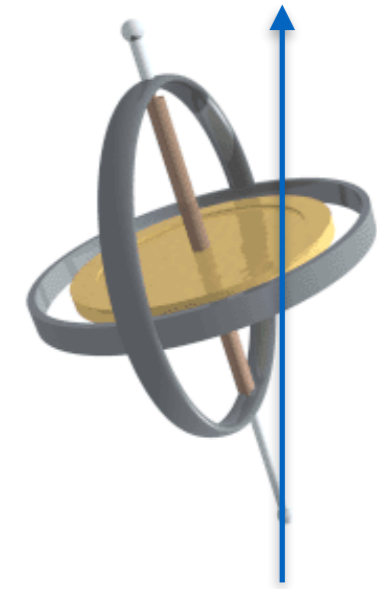
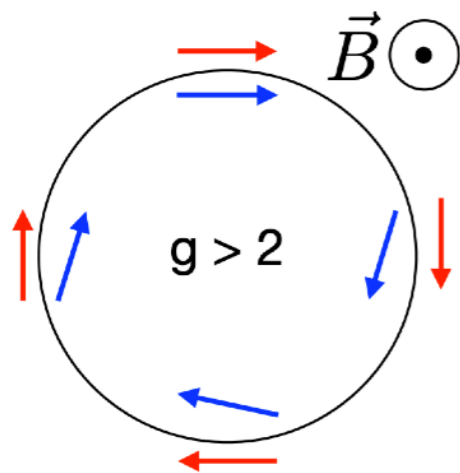
Muon Magnetic Moment and Measuring the Anomaly

polarized muons in a magnetic field

$$\text{If } g = 2 \Rightarrow \vec{\omega}_a = 0$$



$$g \neq 2 \Rightarrow \vec{\omega}_a \cong a_\mu \frac{e}{m} \vec{B}$$



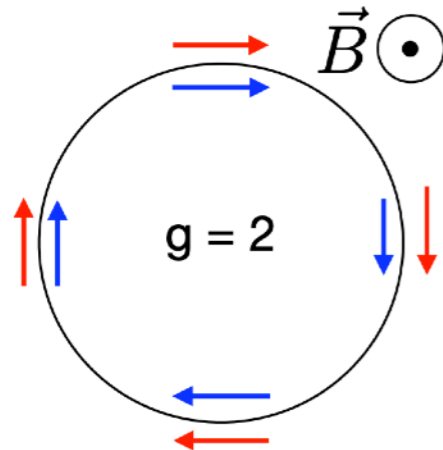
Magnetic Field

$$\vec{\omega}_c = -\frac{e}{\gamma m} \vec{B}, \text{ cyclotron frequency (freq. of charged particle under magnetic field)}$$

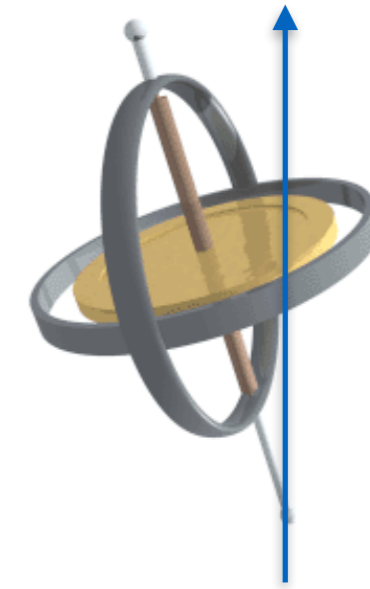
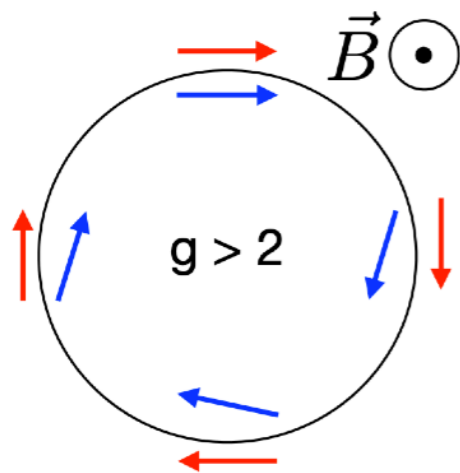
Muon Magnetic Moment and Measuring the Anomaly

polarized muons in a magnetic field

$$\text{If } g = 2 \Rightarrow \vec{\omega}_a = 0$$



$$g \neq 2 \Rightarrow \vec{\omega}_a \cong a_\mu \frac{e}{m} \vec{B}$$



Magnetic Field

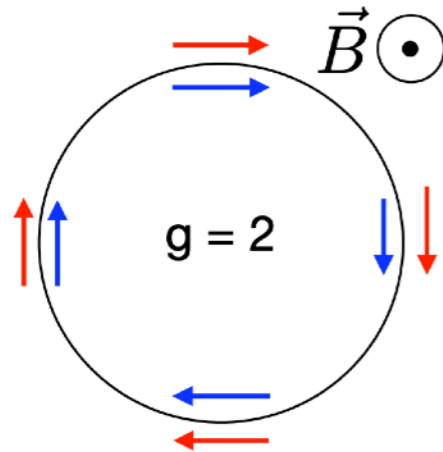
$$\vec{\omega}_c = -\frac{e}{\gamma m} \vec{B}, \text{ cyclotron frequency (freq. of charged particle under magnetic field)}$$

$$\vec{\omega}_s = -\frac{e}{\gamma m} \vec{B} (1 + \gamma a_\mu), \text{ Larmor precession frequency (total spin precession freq.)}$$

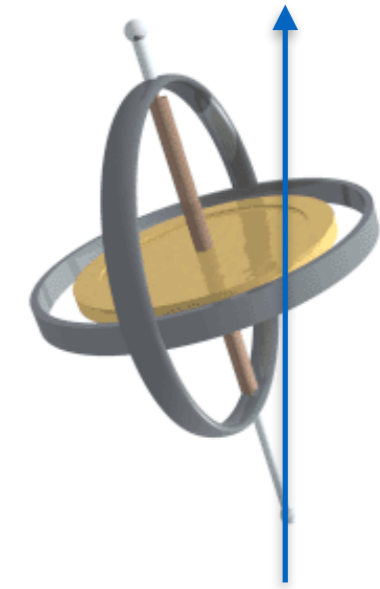
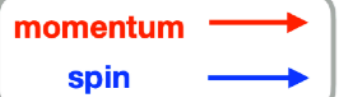
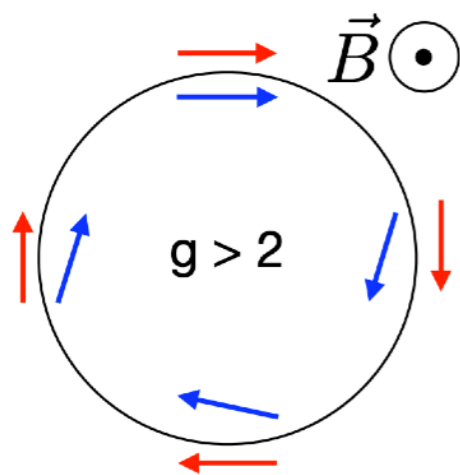
Muon Magnetic Moment and Measuring the Anomaly

polarized muons in a magnetic field

$$\text{If } g = 2 \Rightarrow \vec{\omega}_a = 0$$



$$g \neq 2 \Rightarrow \vec{\omega}_a \cong a_\mu \frac{e}{m} \vec{B}$$



Magnetic Field

$$\vec{\omega}_c = -\frac{e}{\gamma m} \vec{B}, \text{ cyclotron frequency (freq. of charged particle under magnetic field)}$$

$$\vec{\omega}_s = -\frac{e}{\gamma m} \vec{B} (1 + \gamma a_\mu), \text{ Larmor precession frequency (total spin precession freq.)}$$

$$\vec{\omega}_a \cong \vec{\omega}_s - \vec{\omega}_c, \text{ anomalous precession frequency}$$

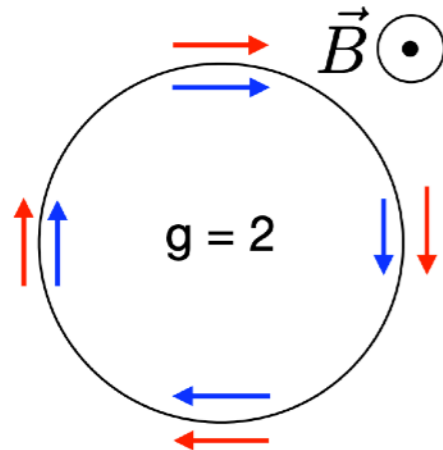
$$\vec{\omega}_a \cong a_\mu \frac{e}{m} \vec{B}$$

Measure them to extract anomaly

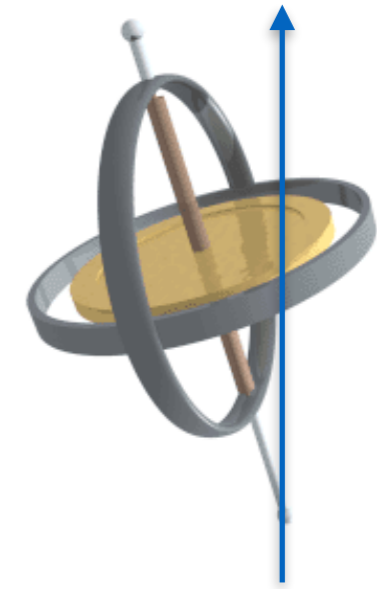
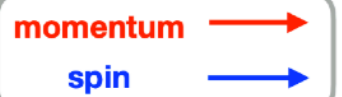
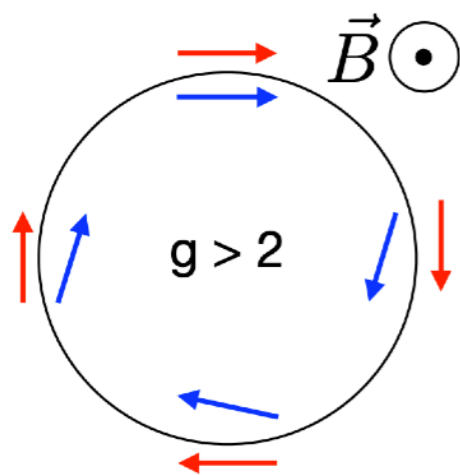
Muon Magnetic Moment and Measuring the Anomaly

polarized muons in a magnetic field

$$\text{If } g = 2 \Rightarrow \vec{\omega}_a = 0$$



$$g \neq 2 \Rightarrow \vec{\omega}_a \cong a_\mu \frac{e}{m} \vec{B}$$



Magnetic Field

$$\vec{\omega}_c = -\frac{e}{\gamma m} \vec{B}, \text{ cyclotron frequency (freq. of charged particle under magnetic field)}$$

$$\vec{\omega}_s = -\frac{e}{\gamma m} \vec{B} (1 + \gamma a_\mu), \text{ Larmor precession frequency (total spin precession freq.)}$$

$$\vec{\omega}_a \cong \vec{\omega}_s - \vec{\omega}_c, \text{ anomalous precession frequency}$$

$$\vec{\omega}_a \cong a_\mu \frac{e}{m} \vec{B}$$

Measure them to extract anomaly


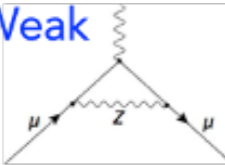
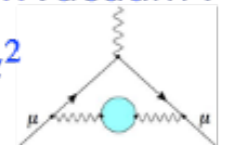
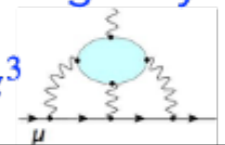
$$a_\mu = \left(\frac{g_e}{2} \right) \left(\frac{\omega_a}{\langle \omega_p \rangle} \right) \left(\frac{\mu_p}{\mu_e} \right) \left(\frac{m_\mu}{m_e} \right)$$

Muon Magnetic Moment and Standard Model

- g-factor was expected to be 1 around 1900
- Dirac predicted g-factor as 2 for spin 1/2 particles
- But then Kusch & Foley measured electron spin factor as 2.00238
- Julian Schwinger calculated this deviation in QED (1948)

$$a = (g - 2)/2 = \alpha/2\pi = 0.0011636, \text{ where } \alpha = 1/137$$

More loops of calculations are added today

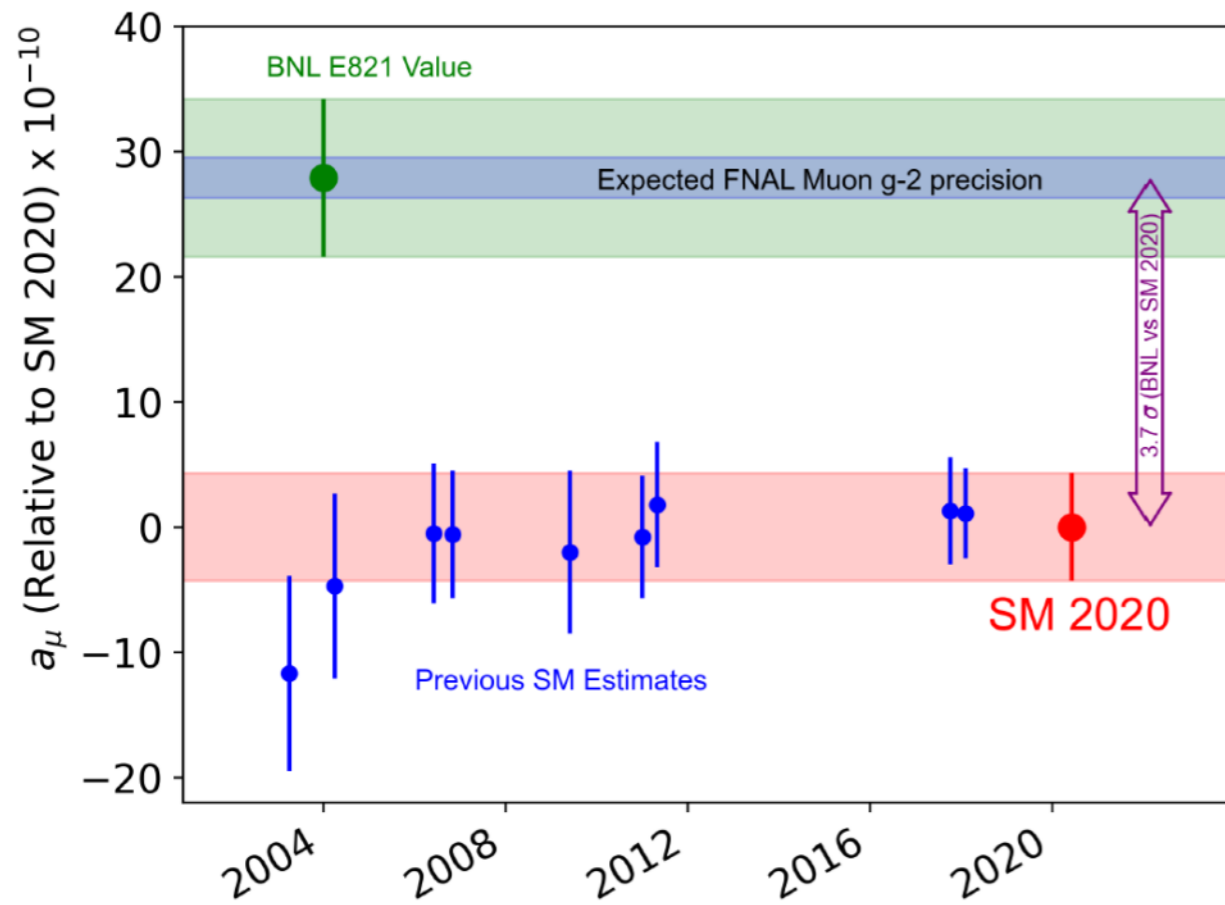
| | | | |
|---|--------------------------------------|-----------|---|
|  <p>QED + ...</p> | $116\,584\,718.9(1) \times 10^{-11}$ | 0.001 ppm | Well-known |
|  <p>Weak + ...</p> | $153.6(1.0) \times 10^{-11}$ | 0.01 ppm | |
| <p>Hadronic...</p> <p>...Vacuum Polarization (HVP)</p>  <p>α^2 + ...</p> | $6845(40) \times 10^{-11}$ | 0.37 ppm | Non-perturbative (Data-driven & lattice QCD) |
| <p>...Light-by-Light (HLbL)</p>  <p>α^3 + ...</p> | $92(18) \times 10^{-11}$ | 0.15 ppm | |

Hadronic Contribution:
FPCP talk from Maarten Golterman

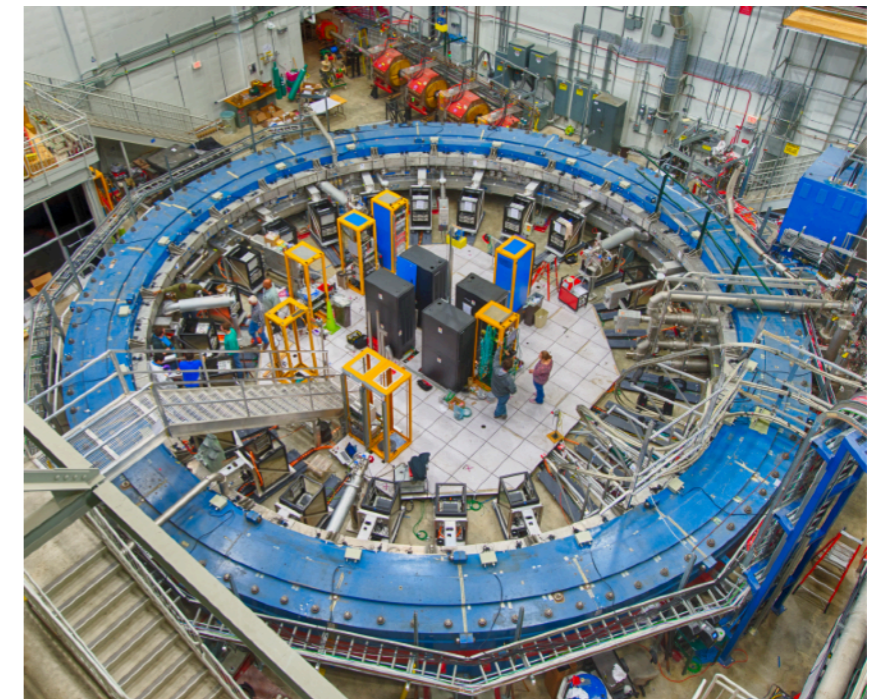
A bit of History: CERN and BNL g-2 Experiments

- Muon g-2 experiments were launched at CERN to measure a_μ
 - Launched a measurement(with a long dipole magnet) with precision of 2% and finally **0.4%** (1961,1962)
 - Second measurement with a storage ring-> x25 more precise- **270ppm**-> Revealed a quantitative discrepancy with the theory (1966)
 - Third measurement with a storage ring + electrostatic quadrupole field-> **7.3 ppm** precision (1969-1979)
- BNL took over the effort on measuring the anomaly more precisely (1997-2001)
 - Storage ring magnet + electrostatic quadrupole field + Fast Kickers +24 calorimeters
 - μ^+ and μ^- running
 - A factor of 14 improvement on precision after latest CERN measurement - **0.54ppm**

Fermilab Muon g-2 Experiment



BNL measured the anomaly with 2.7σ discrepancy and later it increased to 3.7σ with new theory results



Muon Delivery to g-2 Experiment

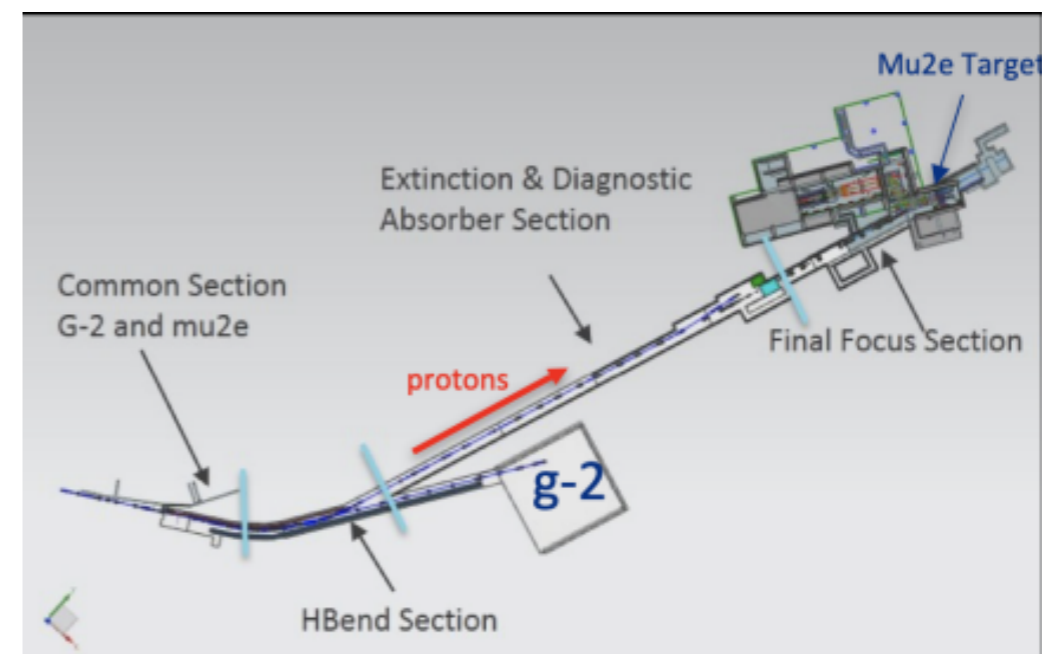


- 8 GeV protons are delivered to Recycler Ring from Booster
- Split the proton bunch into four bunches with RF system.
- Direct the proton punches to pion production target and obtain pions.
- Muons produced by pion decays circulate in the delivery ring until proton contamination is removed.
- Deliver muons to g-2 storage ring.

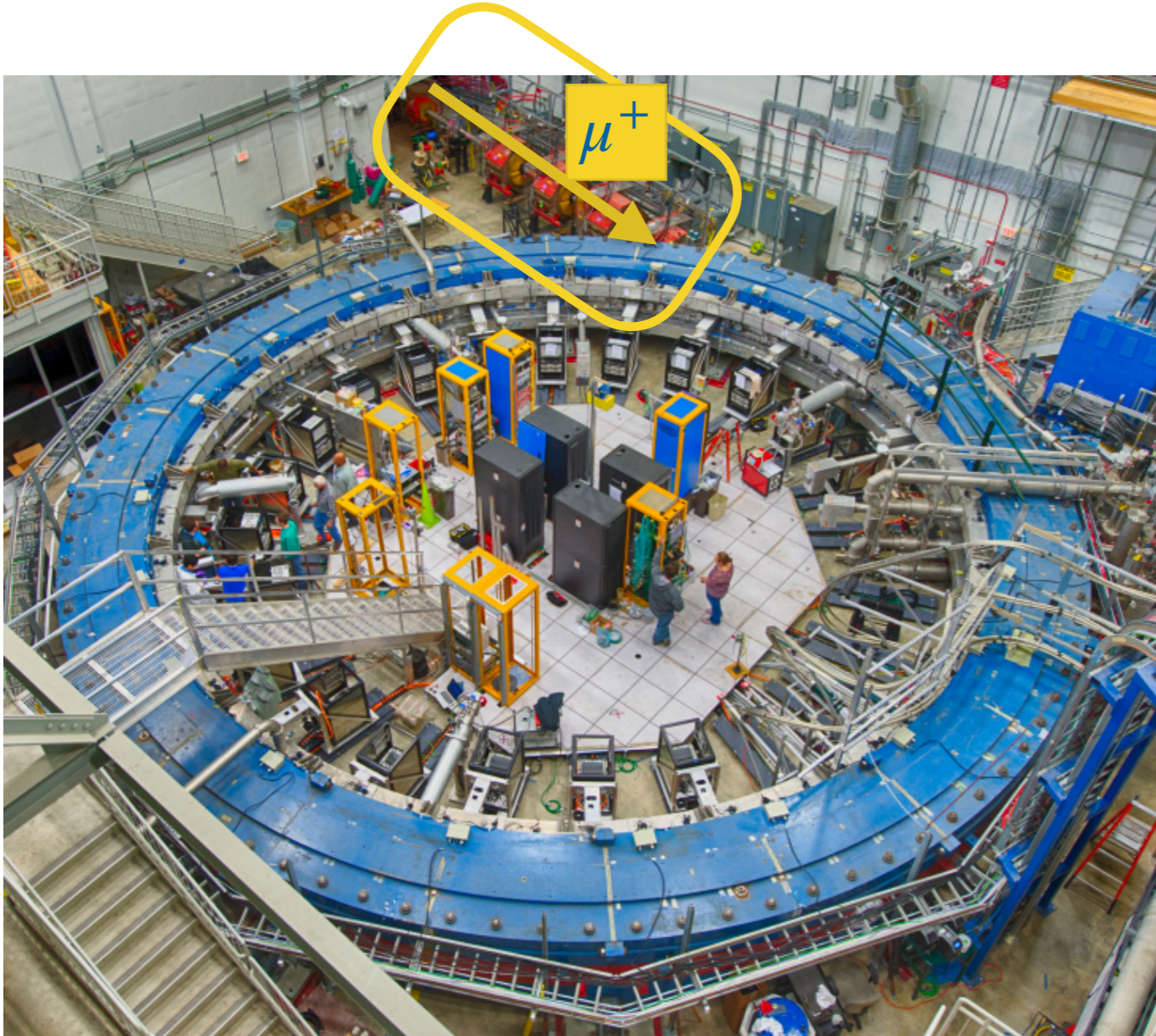
Muon Delivery to g-2 Experiment



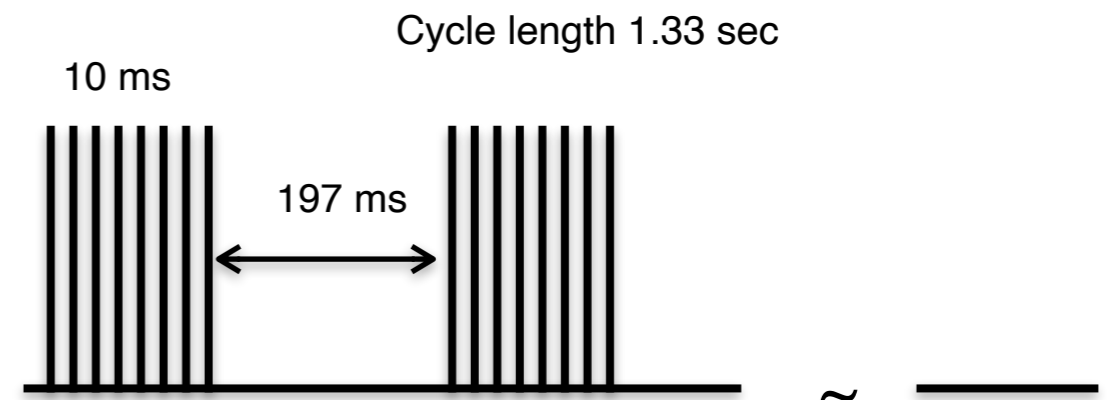
- 8 GeV protons are delivered to Recycler Ring from Booster
- Split the proton bunch into four bunches with RF system.
- Direct the proton punches to pion production target and obtain pions.
- Muons produced by pion decays circulate in the delivery ring until proton contamination is removed.
- Deliver muons to g-2 storage ring.



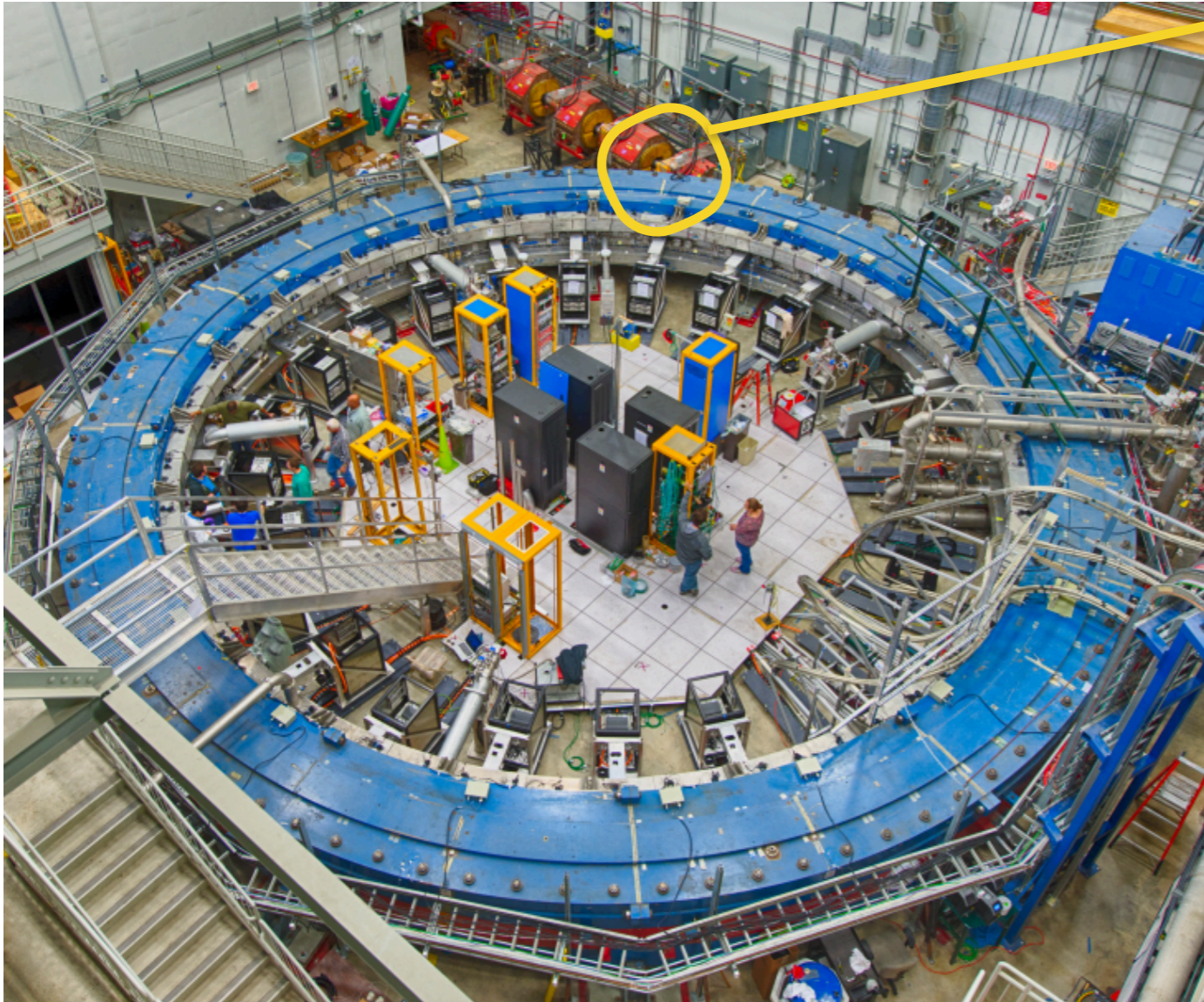
Muons at the Experimental Hall !



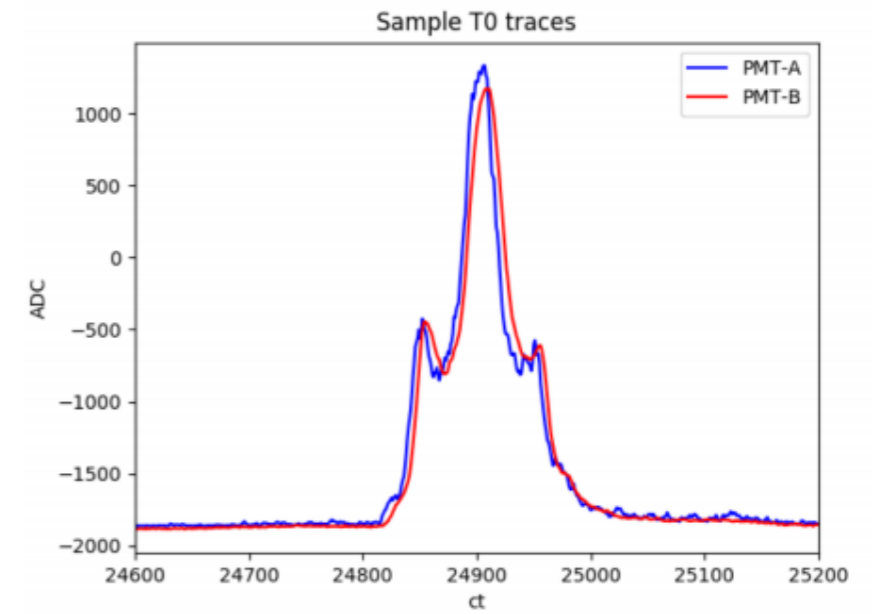
- Polarized muons at 3.1 GeV



Monitoring the Injected Beam: T0 counter

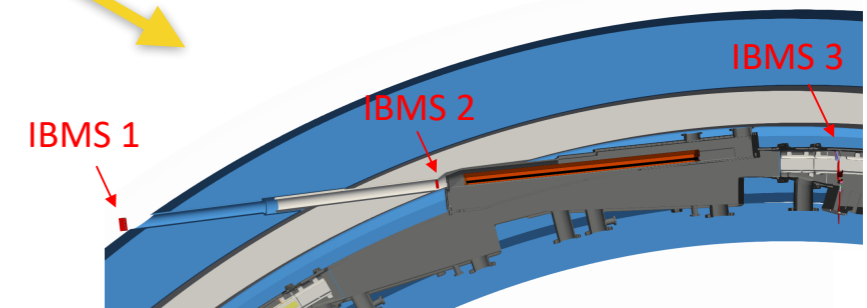
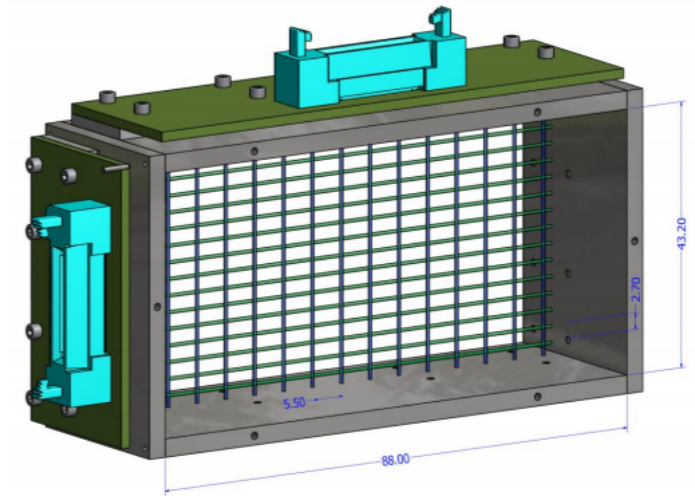
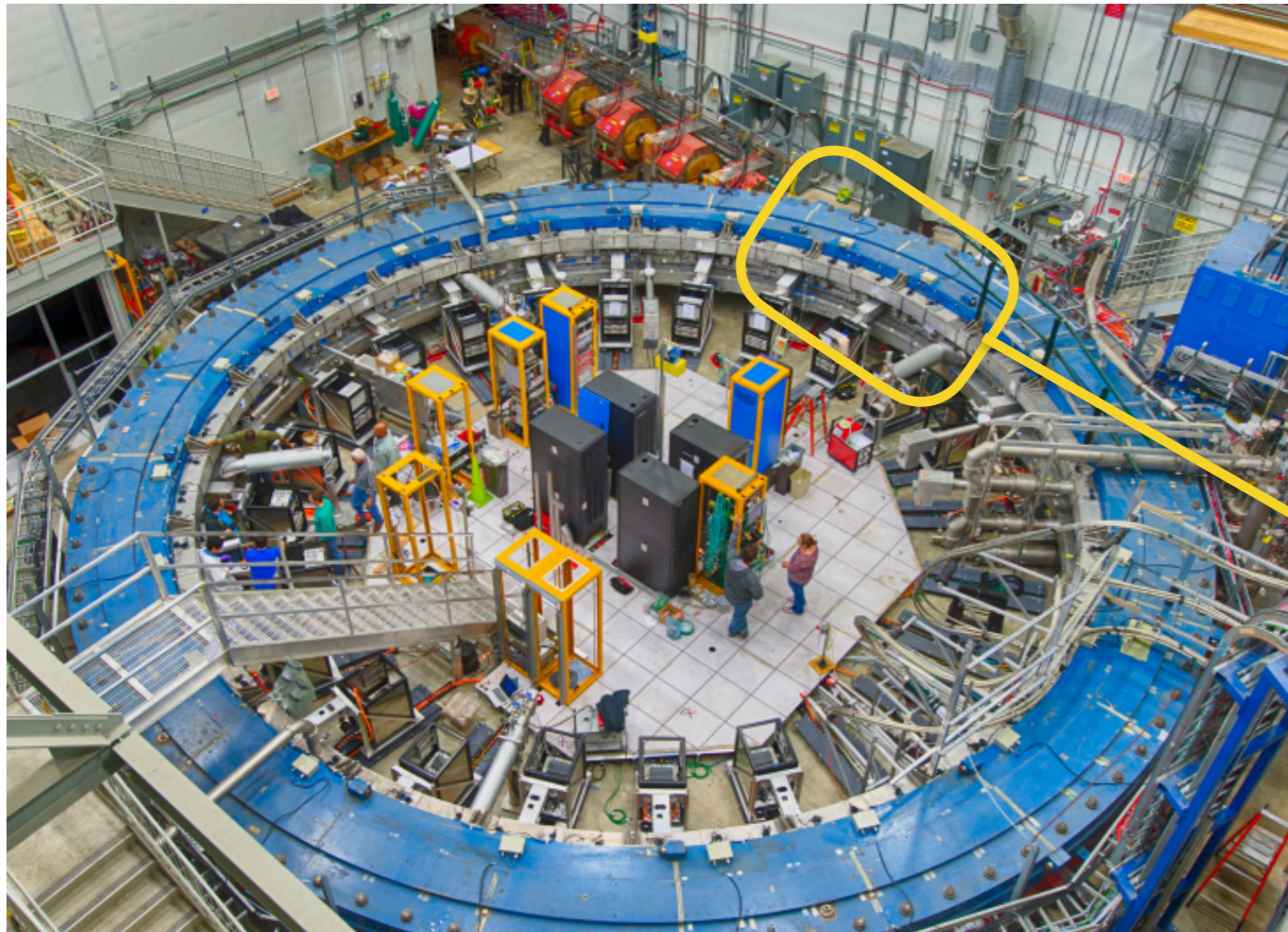


- **T0 Counter**
 - Thin scintillator with 2 PMT readouts
 - Provides beam time profile before beam enters the storage ring



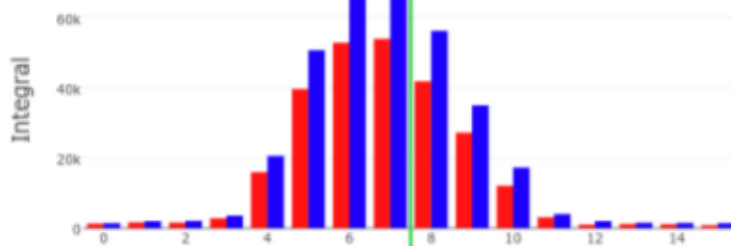
Monitoring the Injected Beam: IBMS detectors

- IBMS (Inflector beam monitoring systems)
 - Check beam injection characteristics
 - 2 planes of scintillation fibers

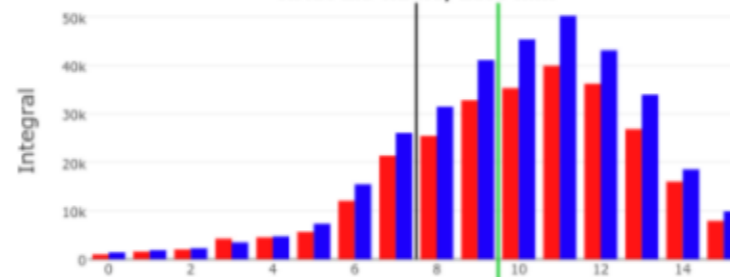


IBMS spatial beam profiles

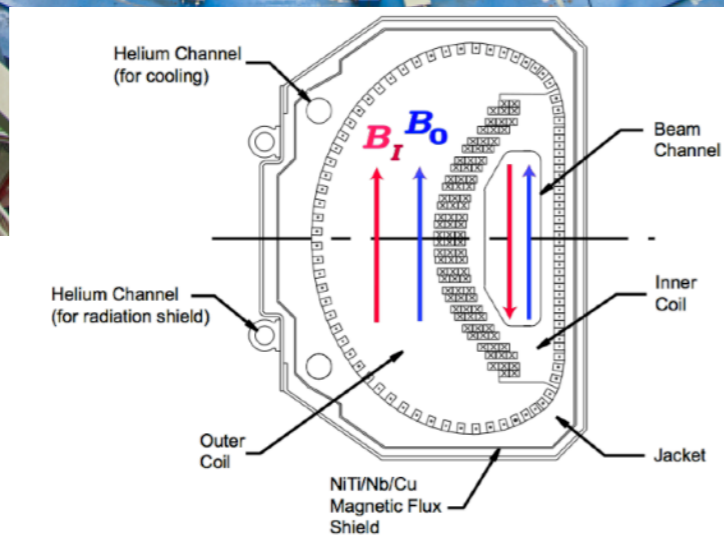
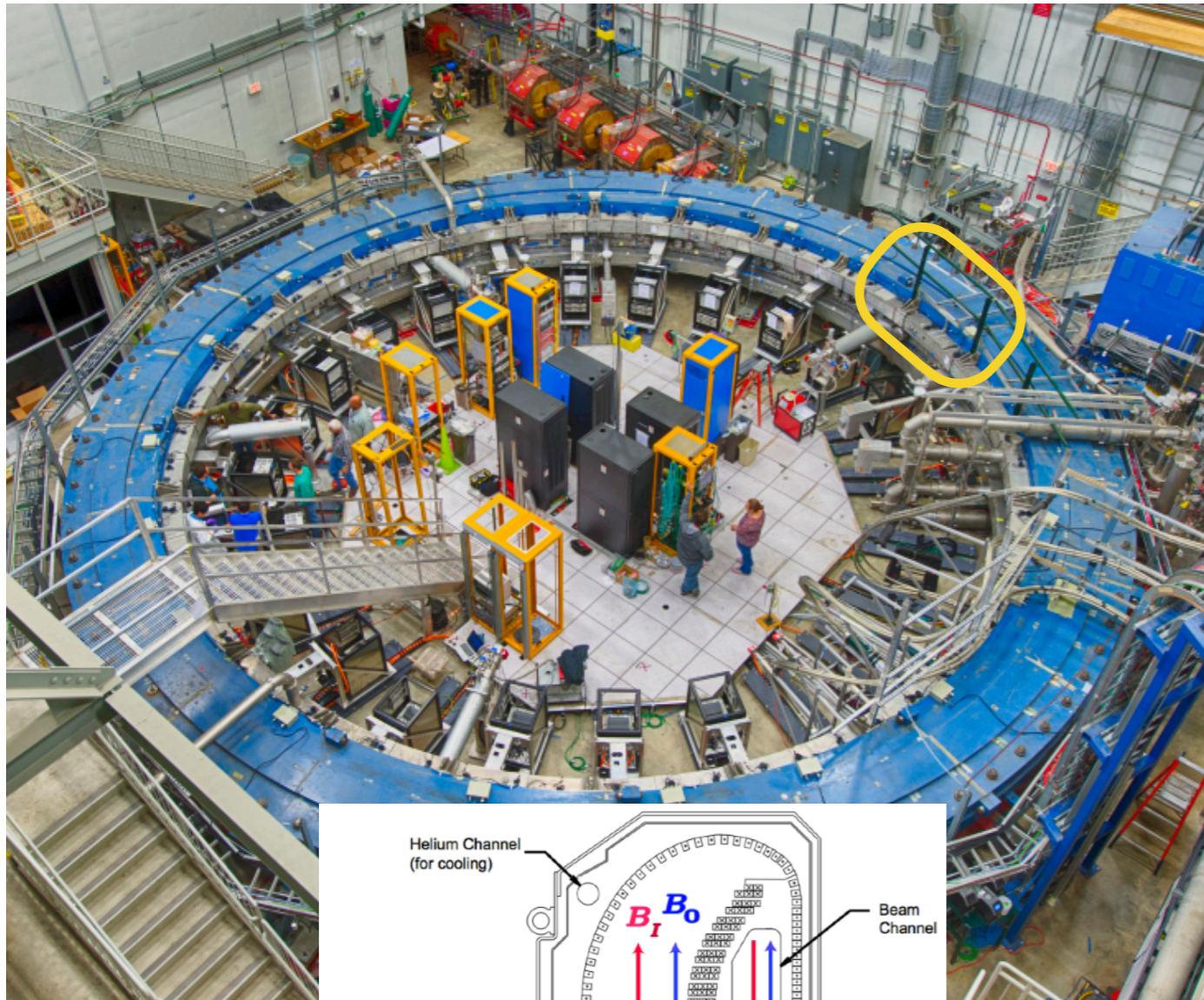
IBMS 1 Y
mean: 6.8 fibers, -1.8 mm
RMS: 2.0 fibers, 5.4 mm



IBMS 1 X
mean: 9.9 fibers, 13.3 mm
RMS: 2.9 fibers, 15.8 mm

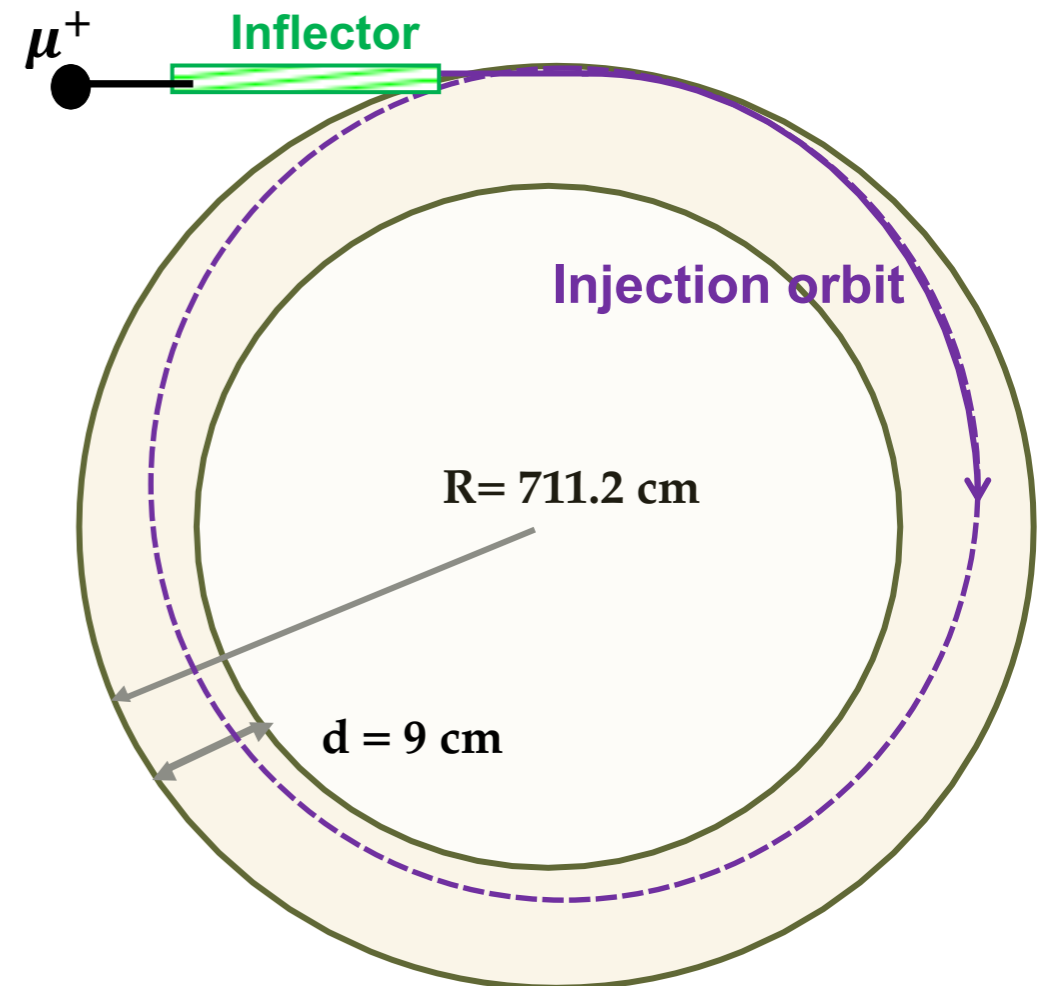


Storing the Muons : **Inflector** and Kickers



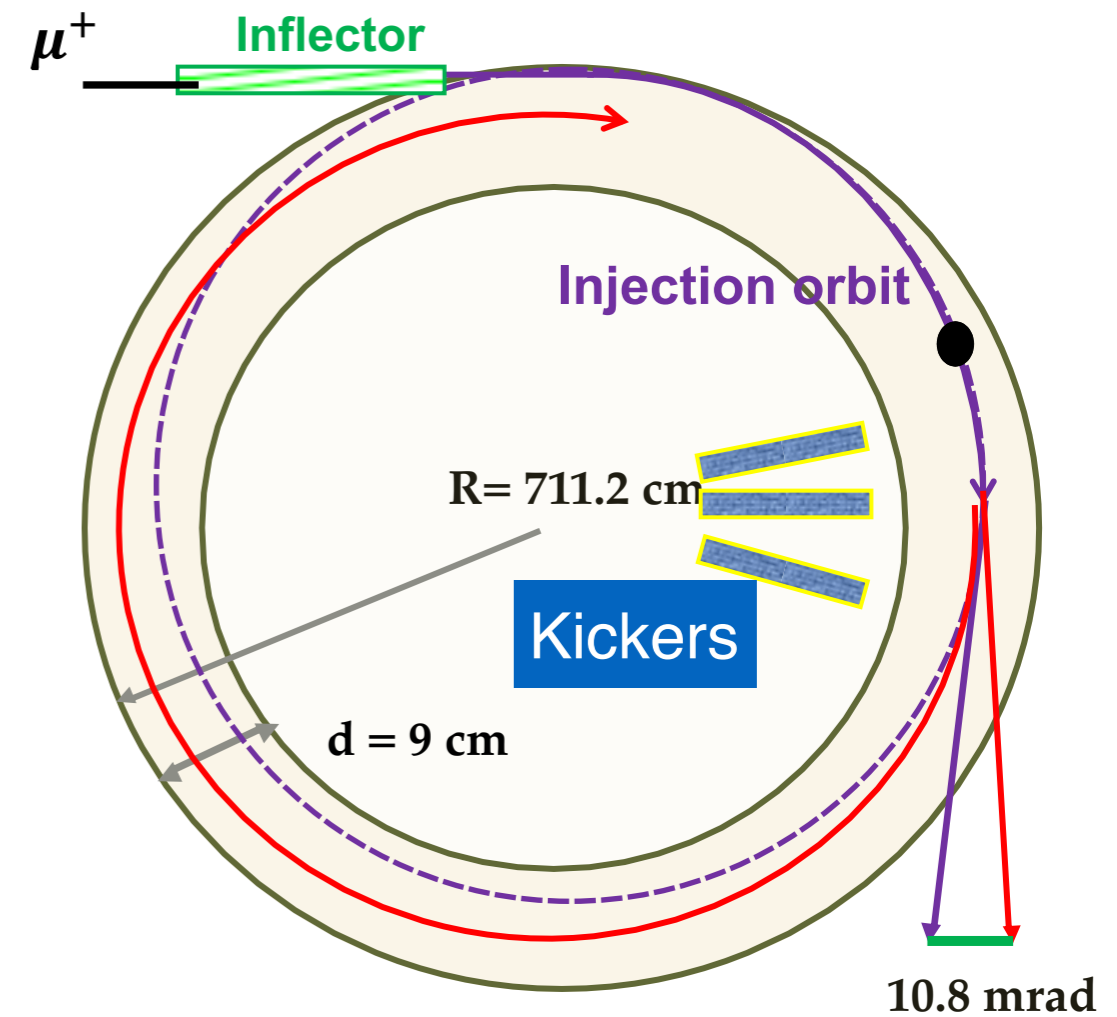
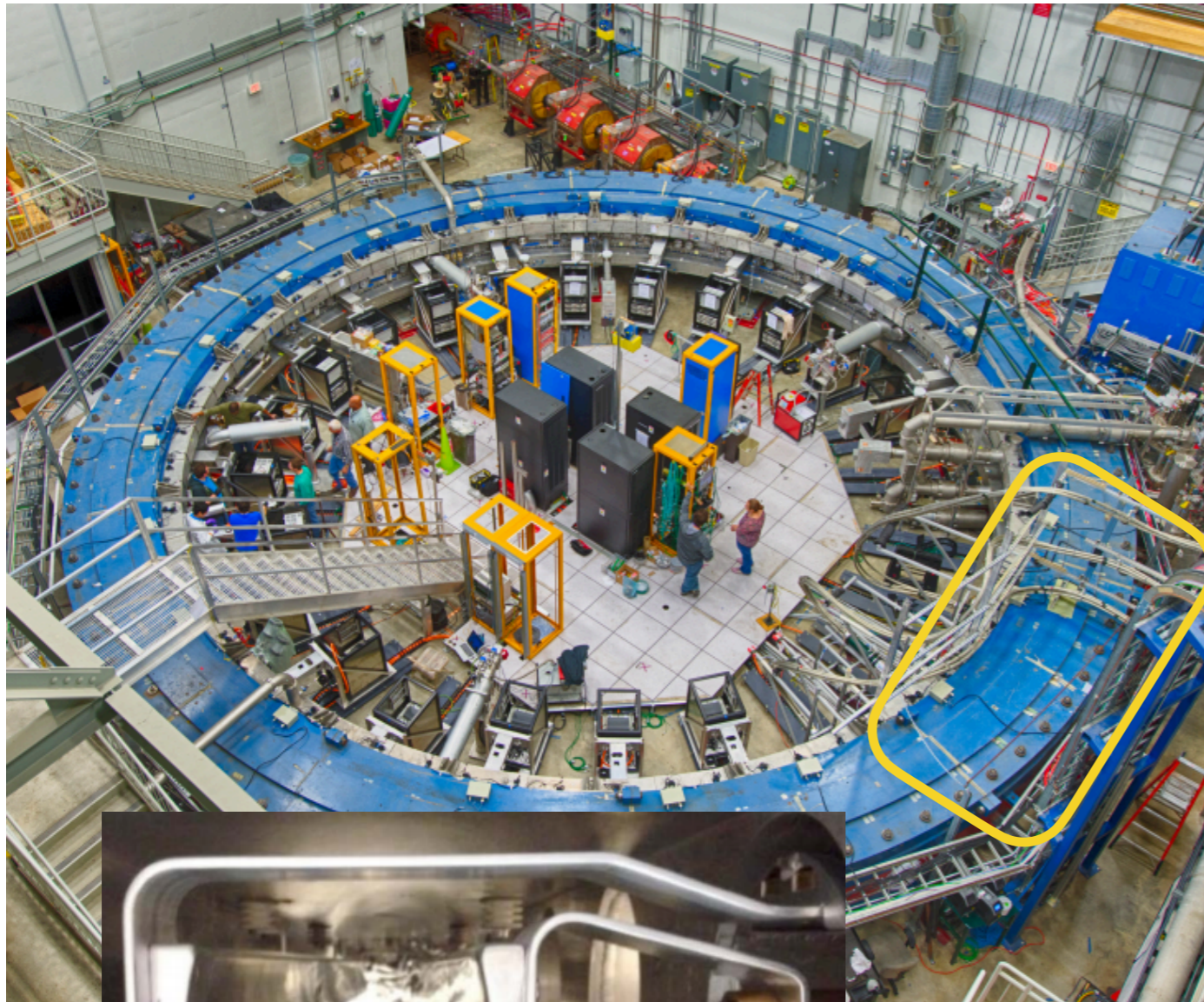
- **Inflector**

- Super conducting magnet
- Cancels B field(1.45T) in the magnet gap and let the beam enter the storage ring without being deflected.
- They are at $r=77\text{mm}$ outside central closed orbit

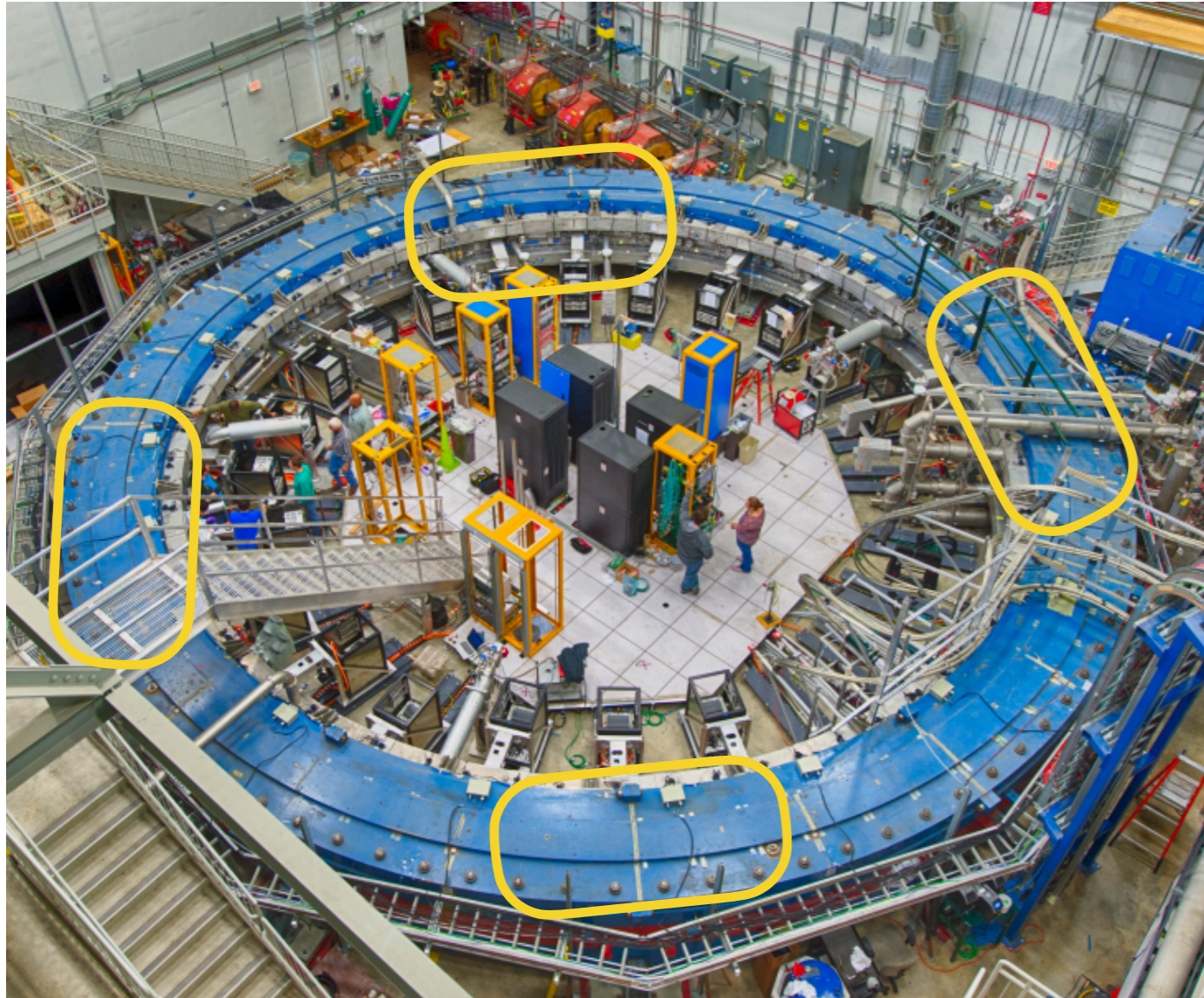


Storing the Muons : Inflector and Kickers

- **Magnetic Kickers**
 - Kick some more to direct the muons into ideal orbit.
 - Use 10.8 mrad pulsed kicks (<149 ns)



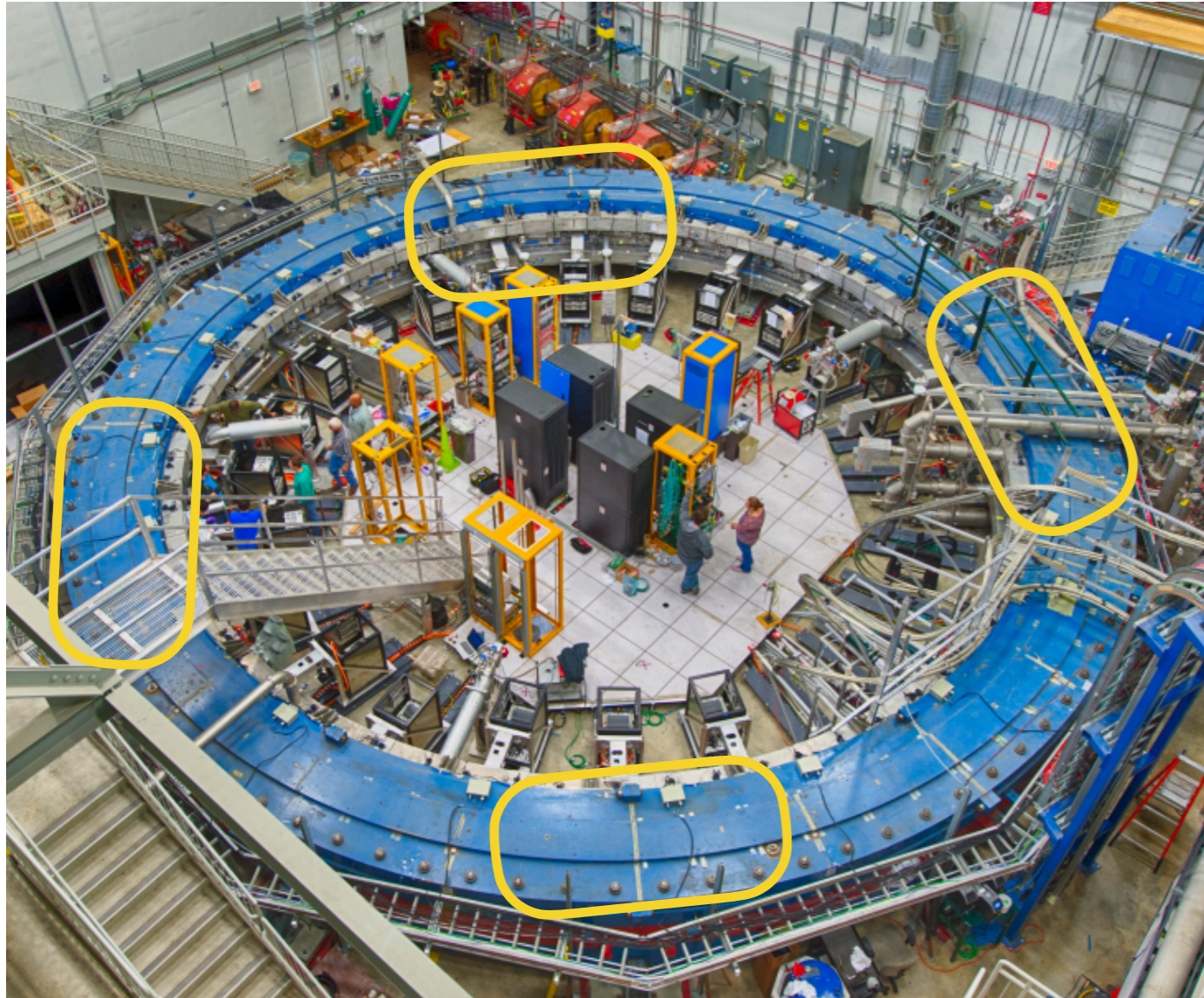
Storing the Muons: **Electrostatic Quadrupoles**



- **Electrostatic Quadrupoles**
 - 4 sets of quads which cover 43% of the ring
 - Electrostatic quadrupoles are used to focus the beam vertically while the storage ring field provides horizontal focusing
 - Cancels out leading order of electric field contribution running at magic momentum $p = 3.094 \text{ GeV}/c$



Storing the Muons: **Electrostatic Quadrupoles**



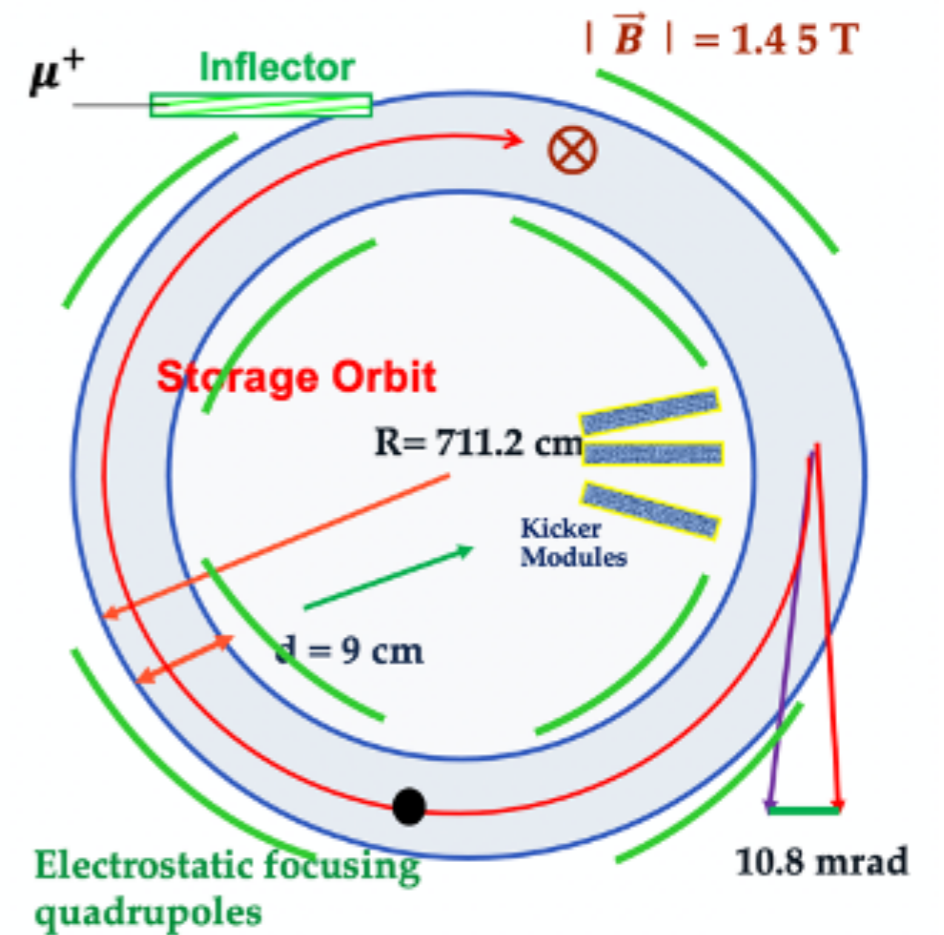
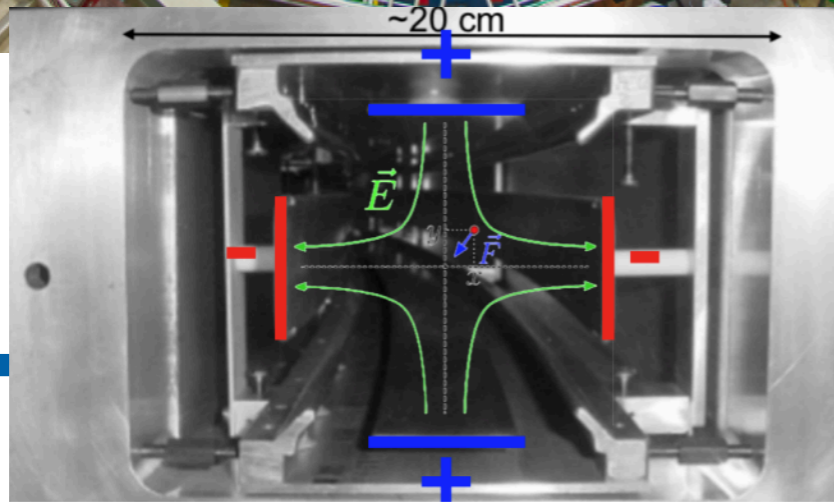
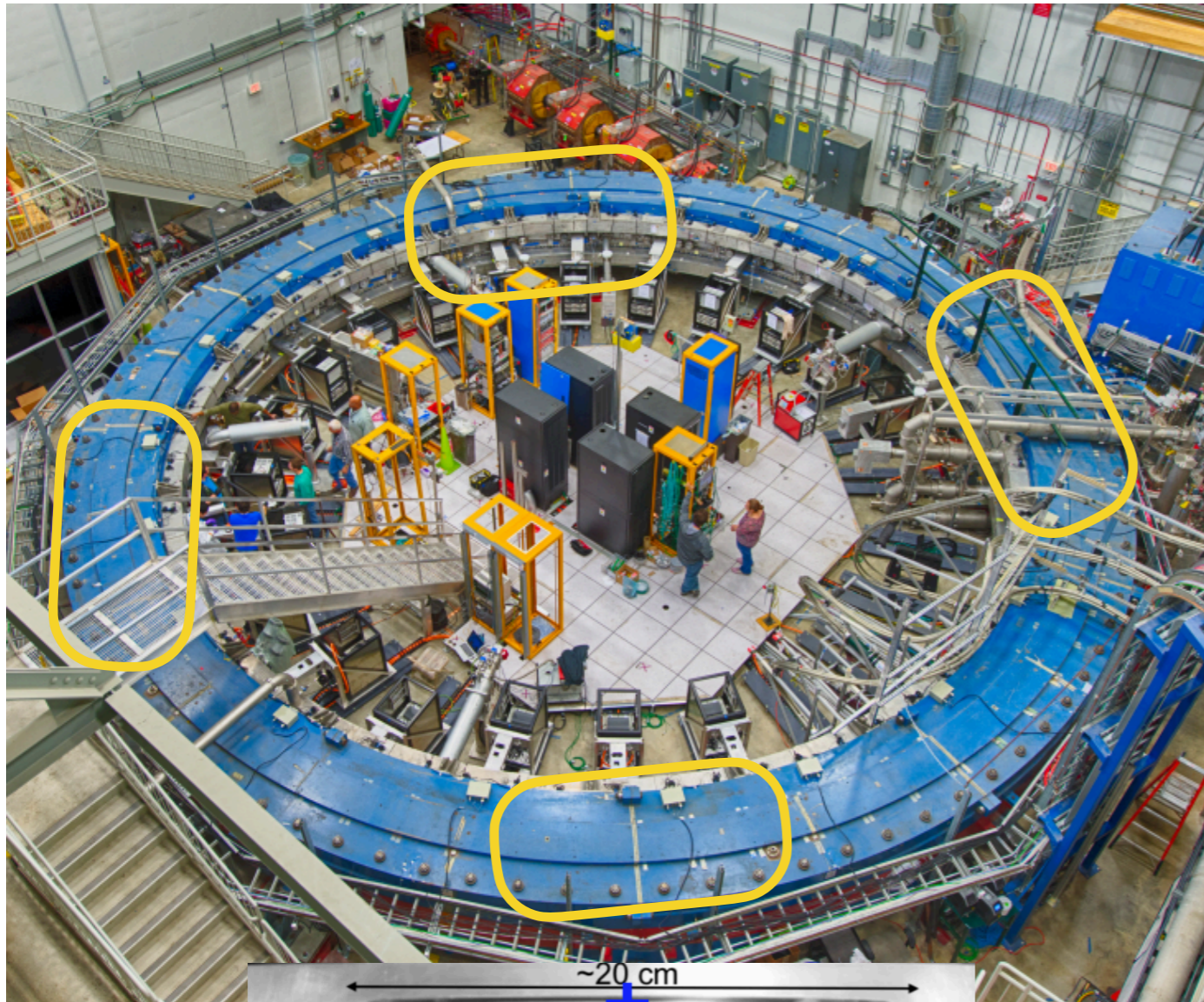
- **Electrostatic Quadrupoles**
 - 4 sets of quads which cover 43% of the ring
 - Electrostatic quadrupoles are used to focus the beam vertically while the storage ring field provides horizontal focusing
 - Cancels out leading order of electric field contribution running at magic momentum $p = 3.094 \text{ GeV}/c$



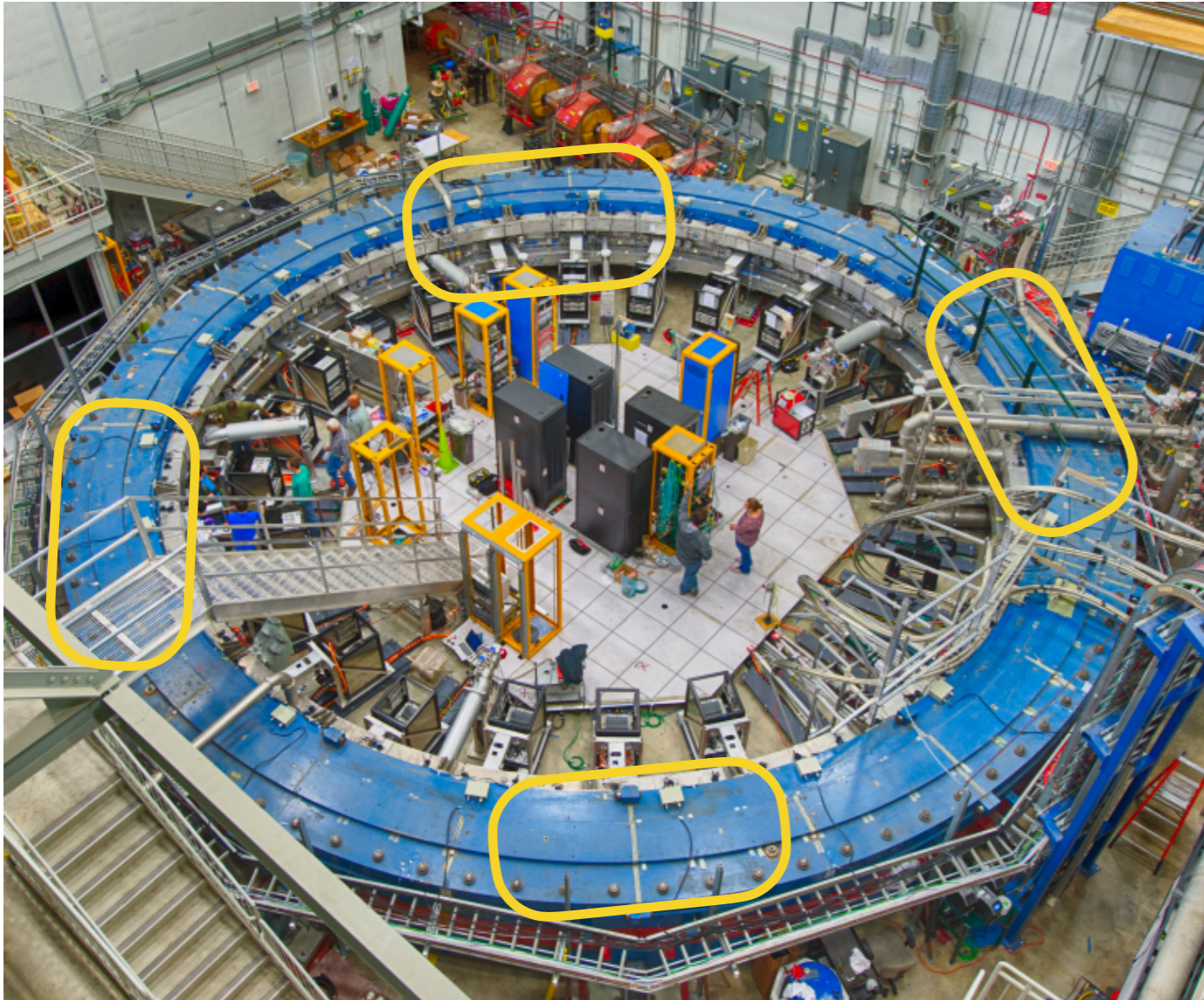
Storing the Muons: Electrostatic Quadrupoles

- **Electrostatic Quadrupoles**

- 4 sets of quads which cover 43% of the ring
- **Electrostatic quadrupoles are used to focus the beam vertically while the storage ring field provides horizontal focusing**
- Cancels out leading order of electric field contribution running at magic momentum $p = 3.094 \text{ GeV}/c$



Storing the Muons: Electrostatic Quadrupoles



- **Electrostatic Quadrupoles**

- 4 sets of quads which cover 43% of the ring
- Electrostatic quadrupoles are used to focus the beam vertically while the storage ring field provides horizontal focusing
- **Cancels out leading order of electric field contribution running at magic momentum $p = 3.094 \text{ GeV}/c$**

$$\vec{\omega}_a = \frac{e}{m} \left[a_\mu \vec{B} - a_\mu \frac{\gamma}{\gamma+1} (\vec{\beta} \cdot \vec{B}) \vec{\beta} - \left(a_\mu - \frac{1}{\gamma^2-1} \right) \vec{\beta} \times \vec{E} \right]$$

0 if in plane

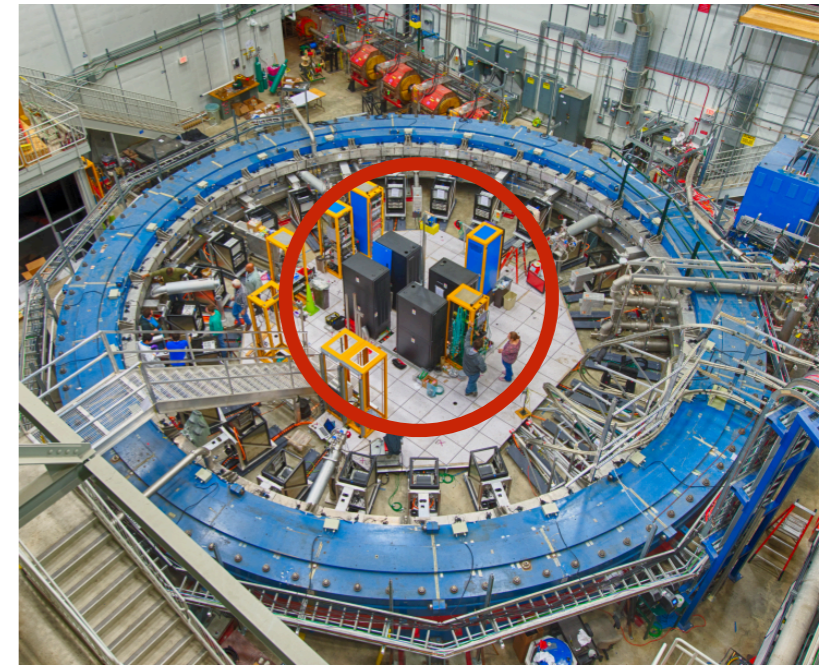
Term cancels at the magic momentum

Cheat-Sheet for Electrostatic Quadrupoles

- **Electrostatic Quadrupoles**
 - 4 Pulsers : 2 Positive, 2 Negative Polarities
 - Each has one step and two steps voltage configurations

Cheat-Sheet for Electrostatic Quadrupoles

- **Electrostatic Quadrupoles**
 - 4 Pulsers : 2 Positive, 2 Negative Polarities
 - Each has one step and two steps voltage configurations

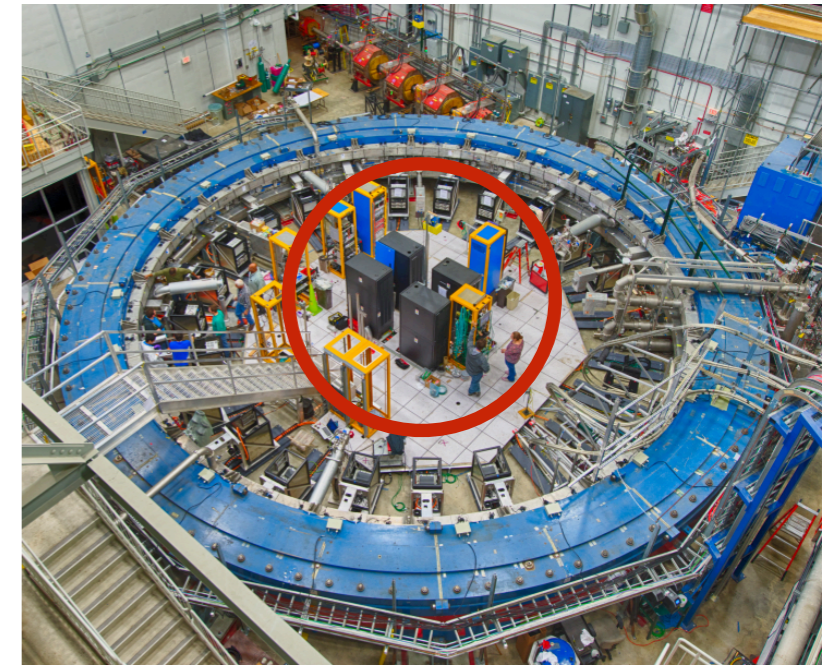
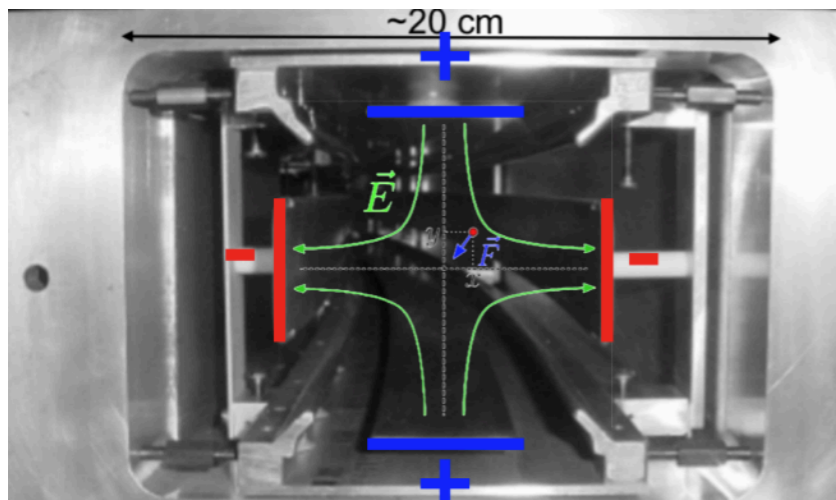


Cheat-Sheet for Electrostatic Quadrupoles

- **Electrostatic Quadrupoles**
 - 4 Pulsers : 2 Positive, 2 Negative Polarities
 - Each has one step and two steps voltage configurations

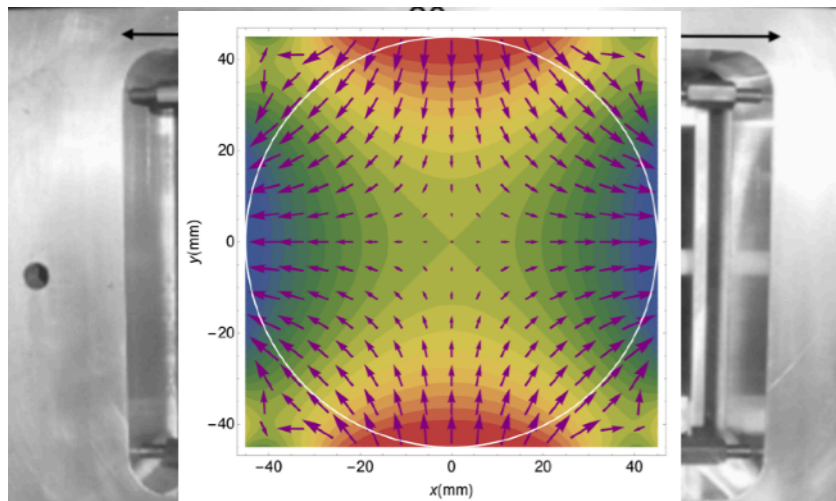
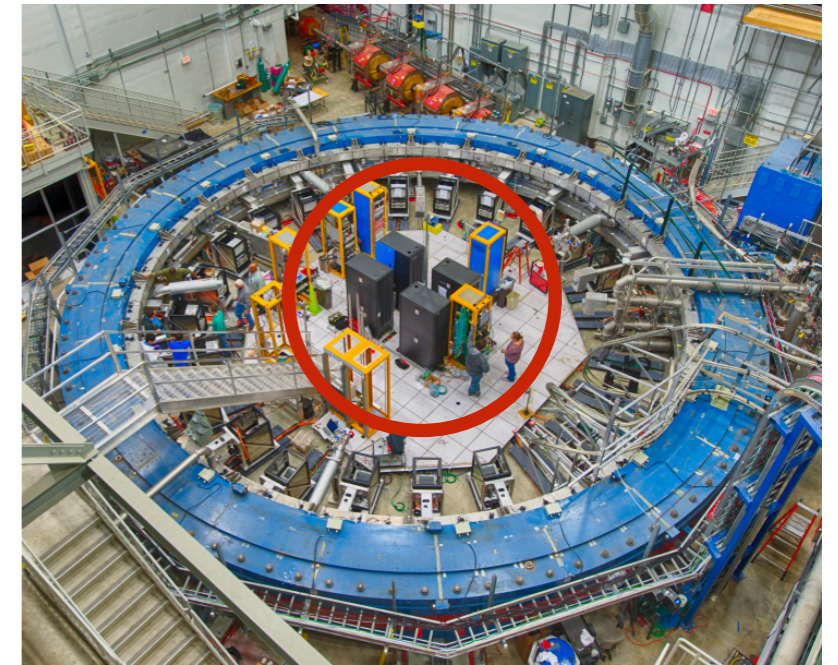
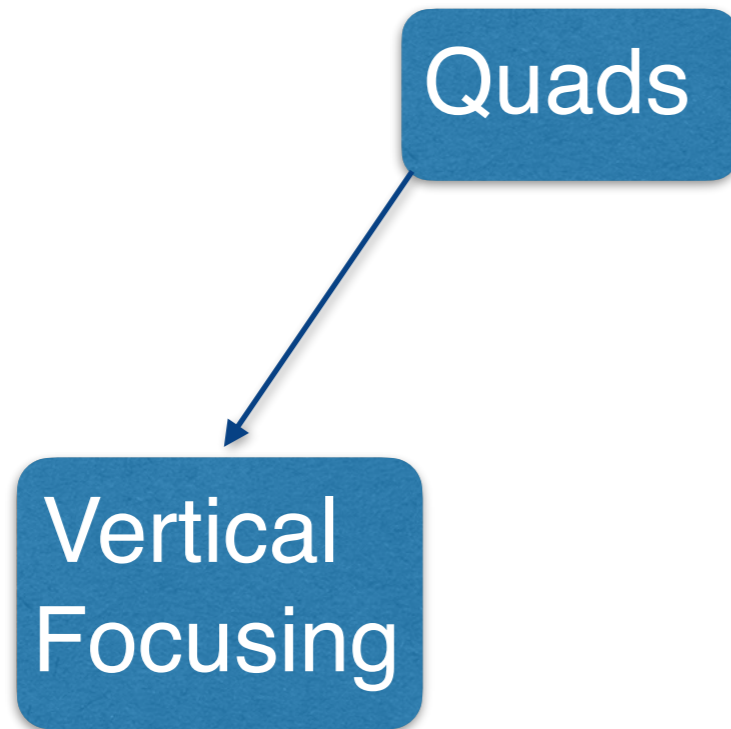
Quads

Vertical
Focusing



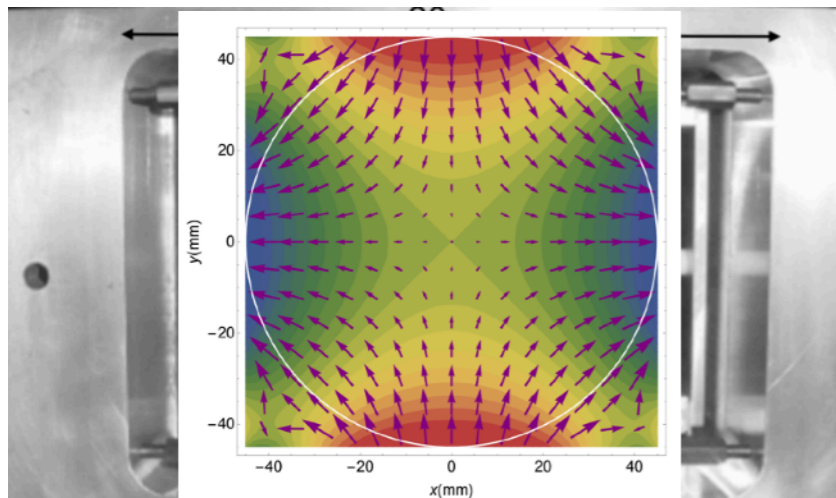
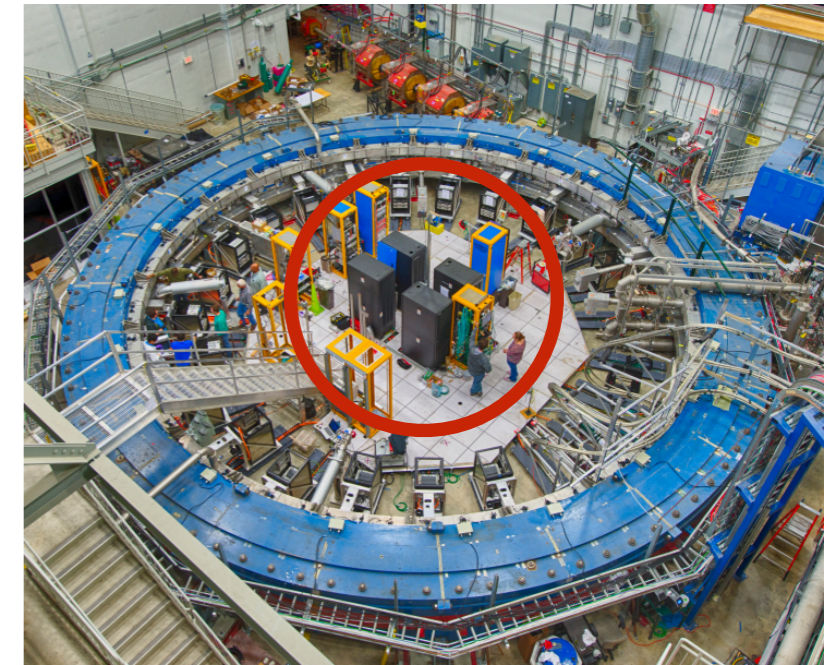
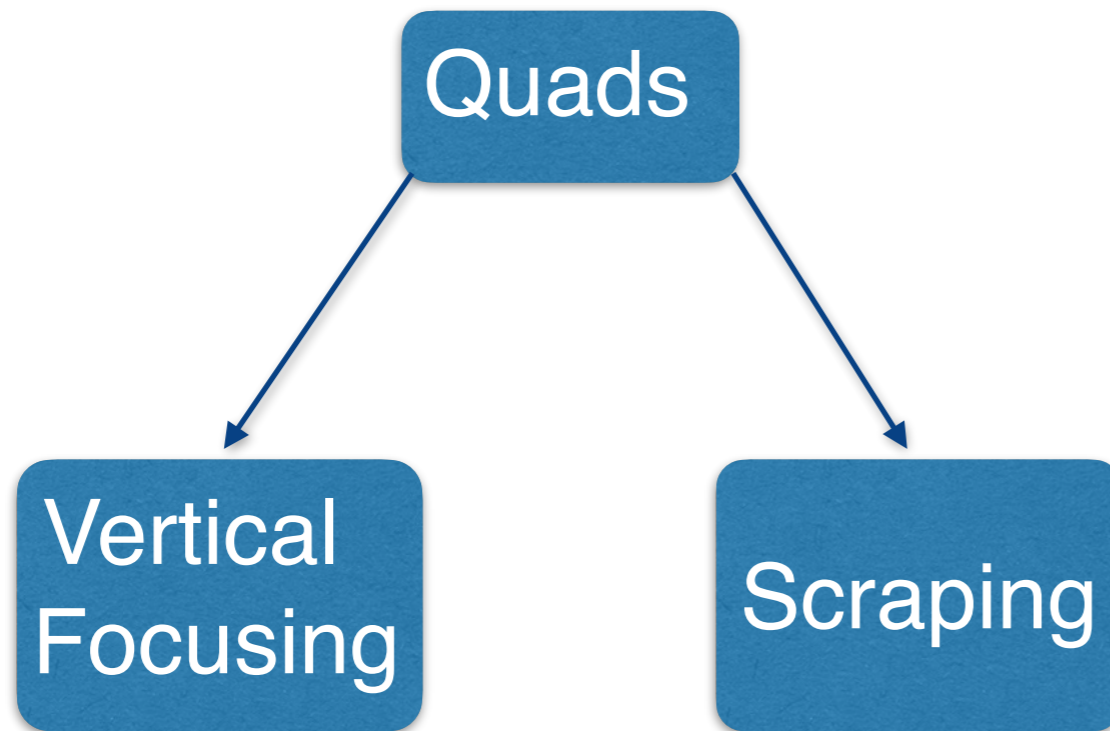
Cheat-Sheet for Electrostatic Quadrupoles

- **Electrostatic Quadrupoles**
 - 4 Pulsers : 2 Positive, 2 Negative Polarities
 - Each has one step and two steps voltage configurations



Cheat-Sheet for Electrostatic Quadrupoles

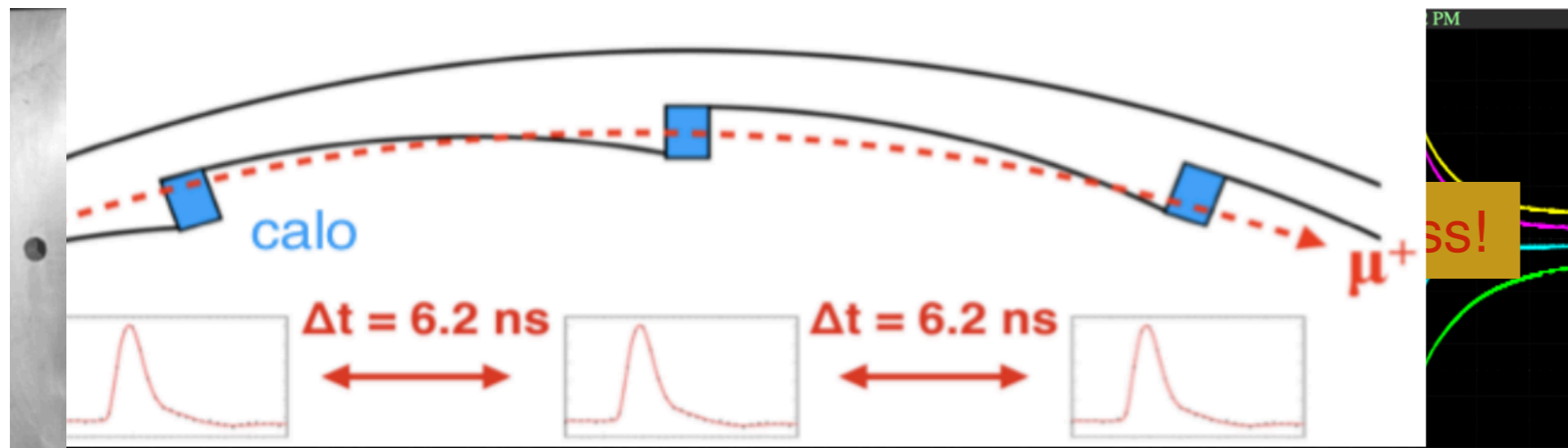
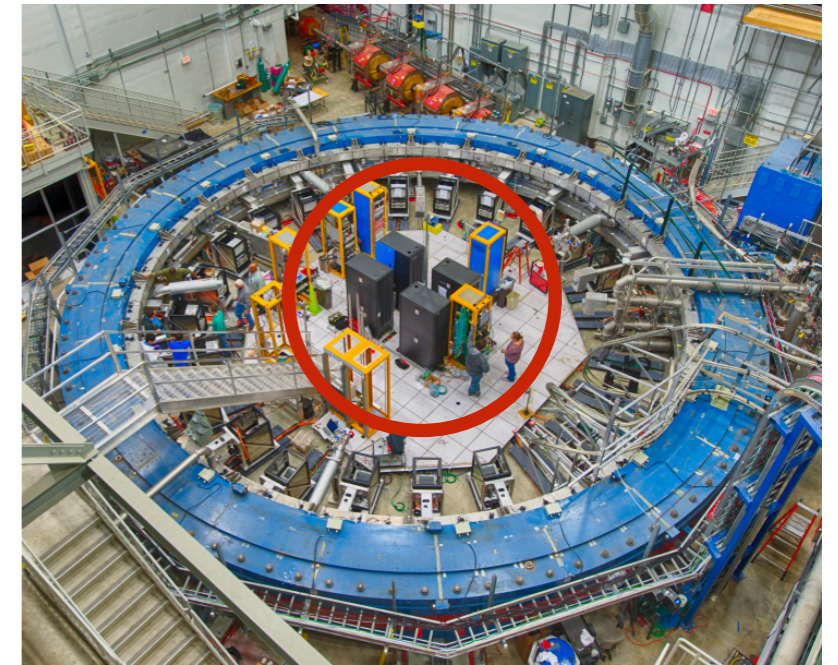
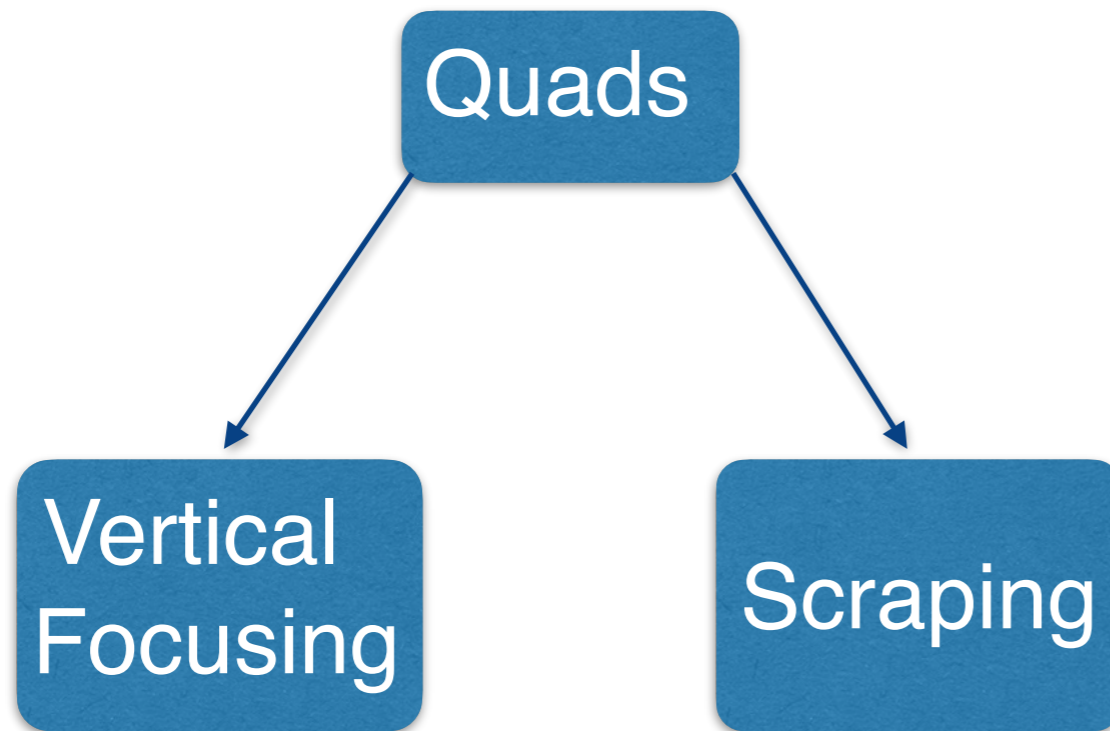
- **Electrostatic Quadrupoles**
 - 4 Pulsers : 2 Positive, 2 Negative Polarities
 - Each has one step and two steps voltage configurations



- Power quad plates asymmetrically
- Displace closed orbit from the center by 2.6mm
- Scrape off the muons outside the reduced aperture
- Restore the quad symmetry after $30\mu s$

Cheat-Sheet for Electrostatic Quadrupoles

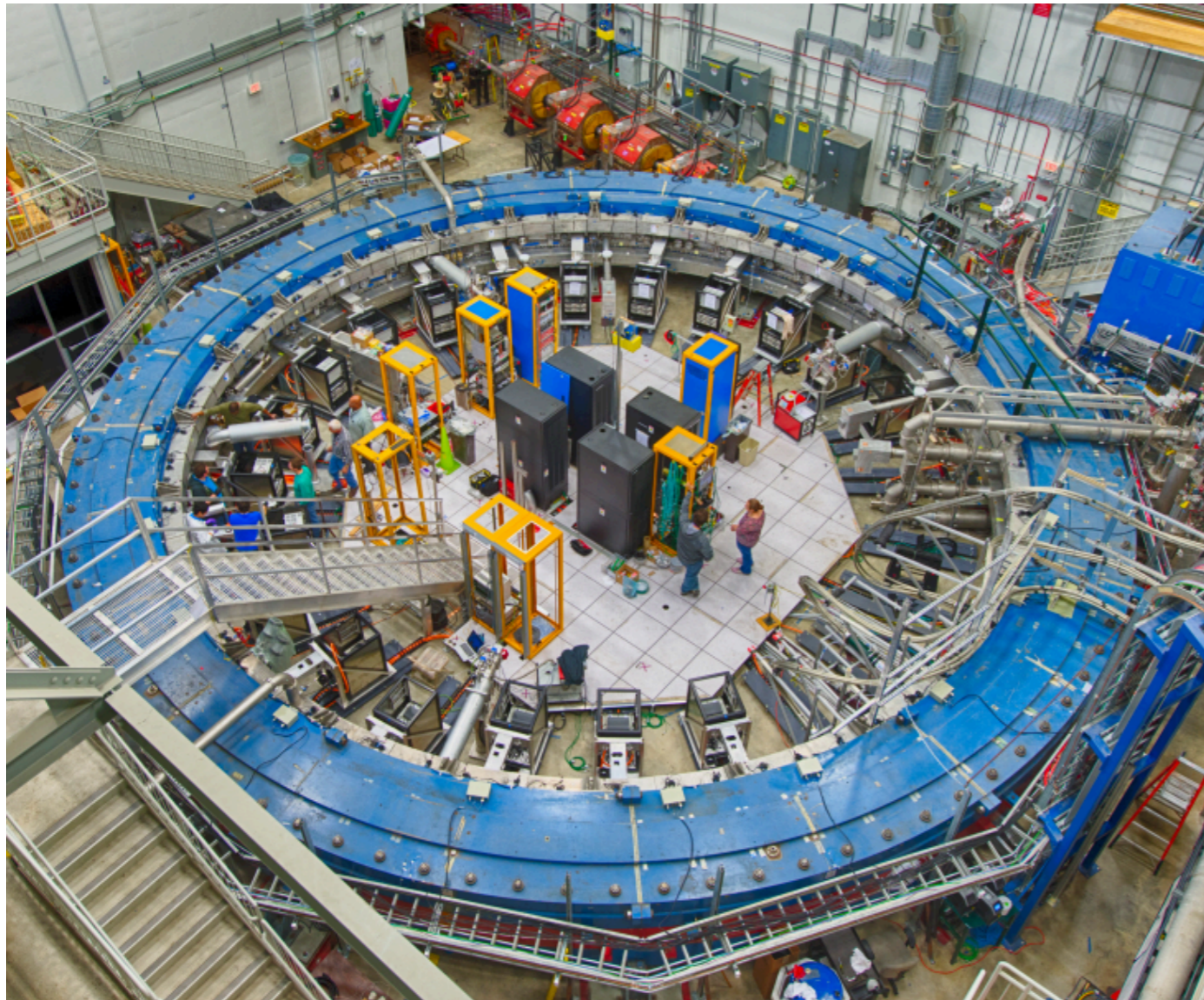
- **Electrostatic Quadrupoles**
 - 4 Pulsers : 2 Positive, 2 Negative Polarities
 - Each has one step and two steps voltage configurations



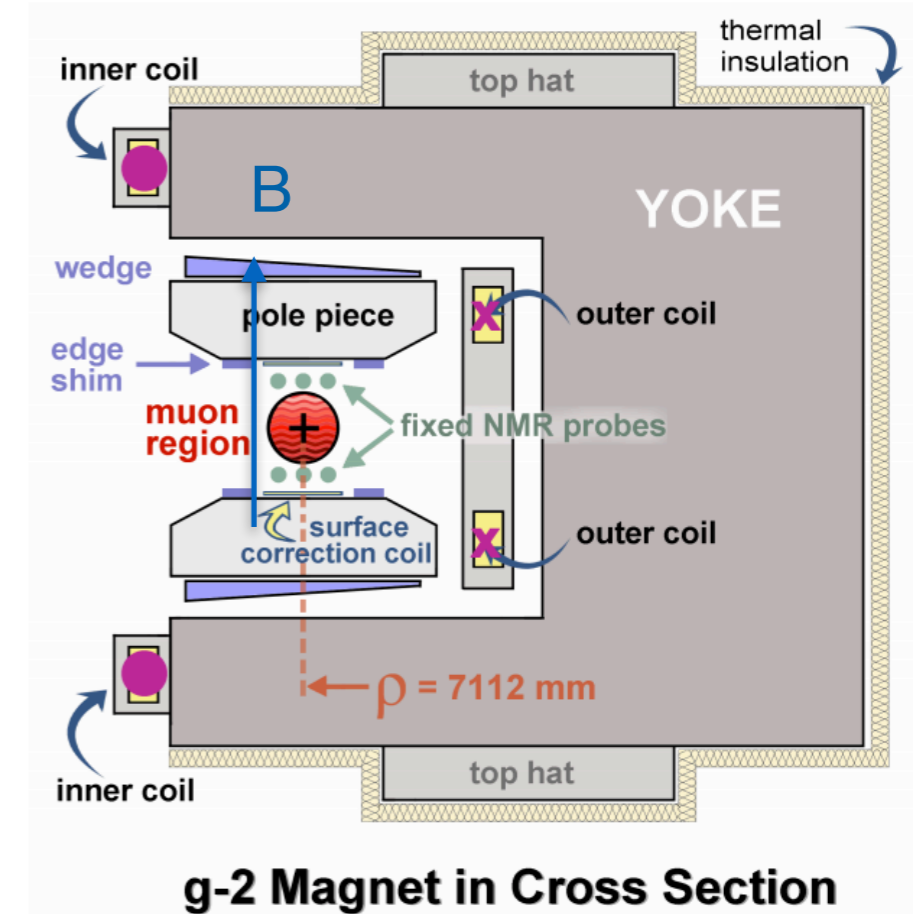
- Power quad plates asymmetrically
- Displace closed orbit from the center by 2.6mm
- Scrape off the muons outside the reduced aperture
- Restore the quad symmetry after $30\mu s$

Several mechanisms contribute to Muon Loss Rate: Muons that were scattered from different materials before decaying and then punch through multiple calorimeters. They have different phase than stored muons so they modulate ω_q , producing a systematic error. We need to identify them in the data!

Storing the Muons: Magnet



Achieved 25 ppm on field uniformity

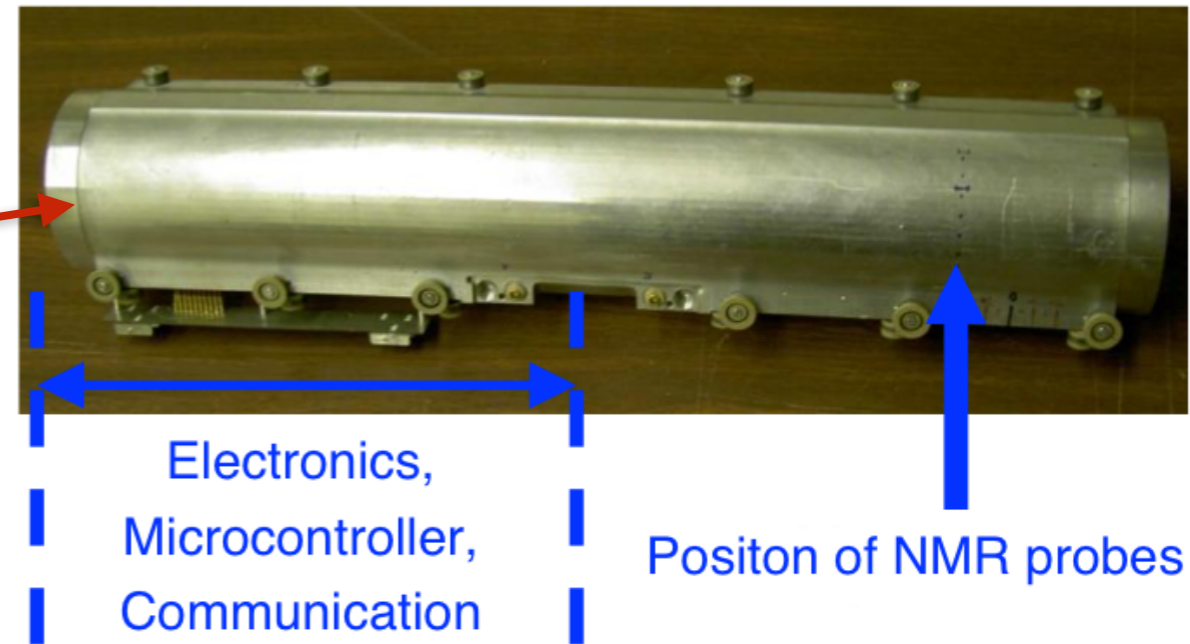
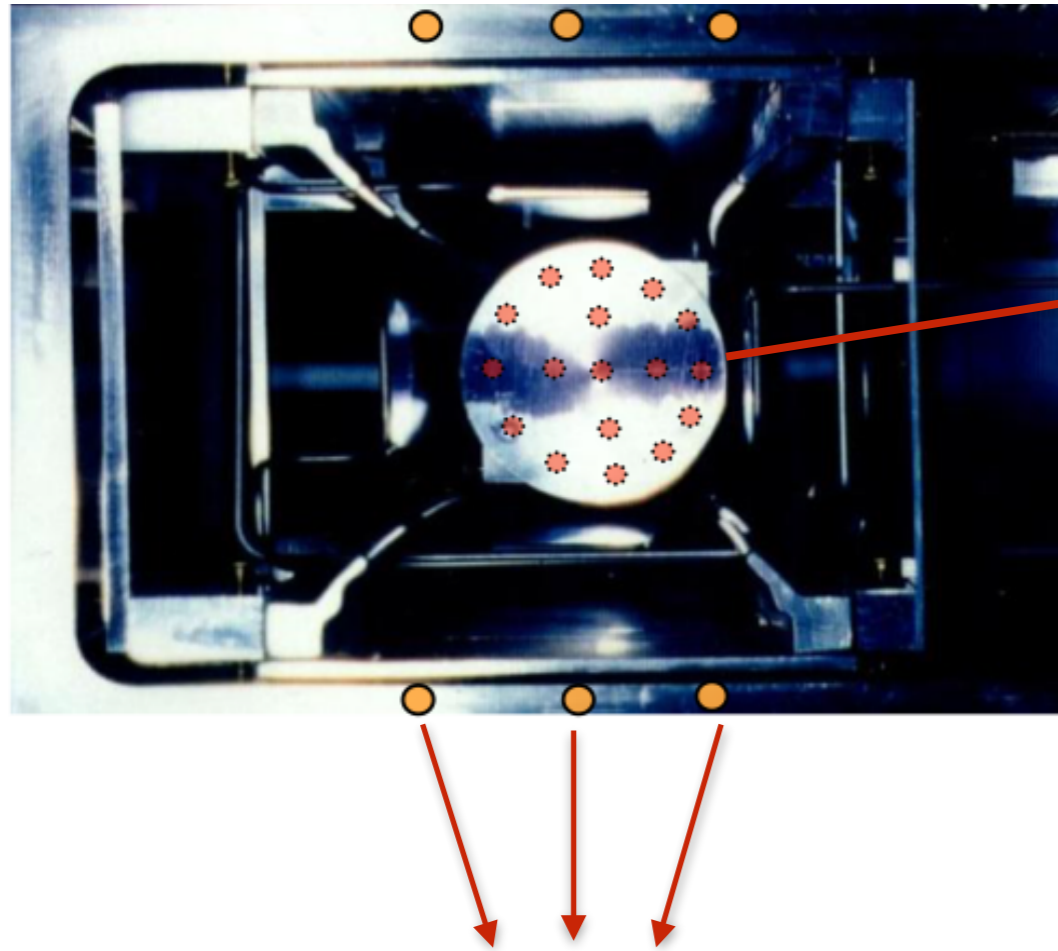


Superconducting C shaped magnet

Provides 1.45T B field (vertical and uniform)

- **12 Yokes:** Open on the inside, allows the decay positrons to reach to the detectors.
- **72 poles:** Low-carbon steel to minimize the impurity
- **144 Edge shims:** Minimize the local sextupole field by changing edge shim thickness
- **864 Steel wedges:** Angle adjustment (compensate quadrupole component), radial adjustment (shim local dipole field).
- **Surface correction coil:** Reduces non-uniformities on higher moment of field.

Measuring ω_p : **Monitoring** and Measuring the Magnetic Field



- **Fixed probes:**

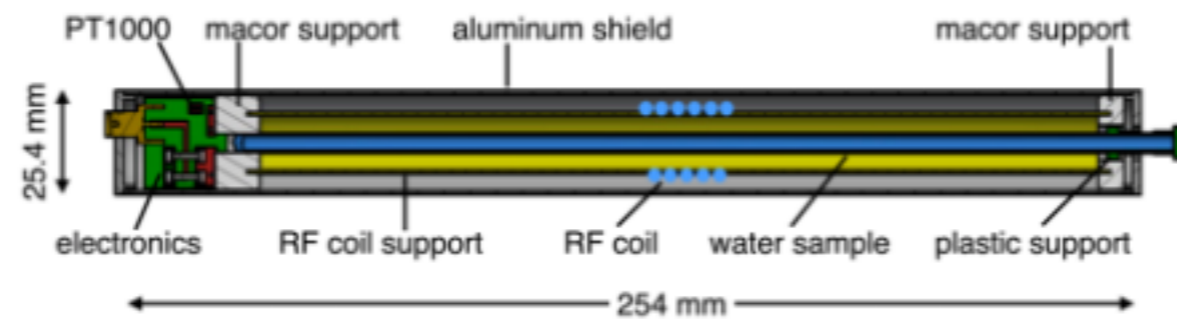
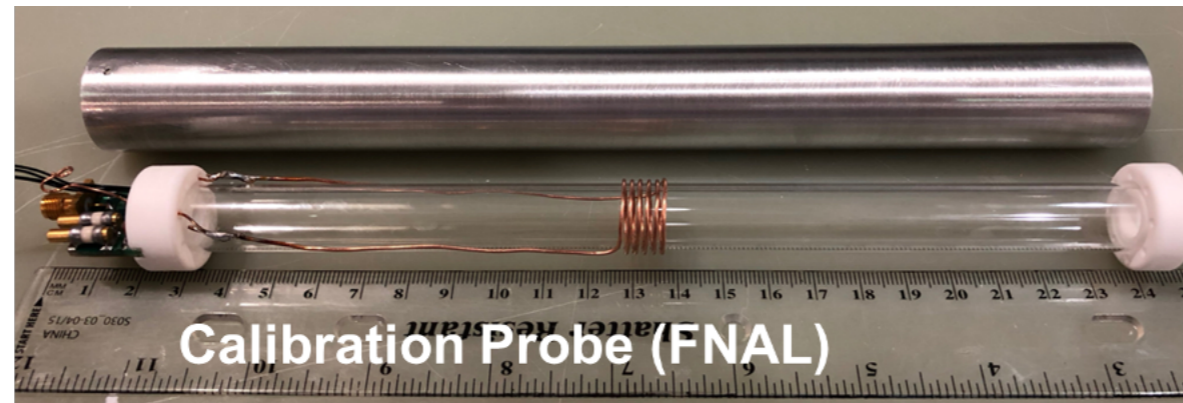
- 378 probes located on vacuum chamber
- Measure the magnetic field while muons are inside the storage ring

- **Trolley(Motorized cart):**

- 17 NMR probes
- Circles around the ring on periodically
- Measures the magnetic field in the storage region
- Used to calibrate FP measurements

NMR Probes

Calibration Uncertainty

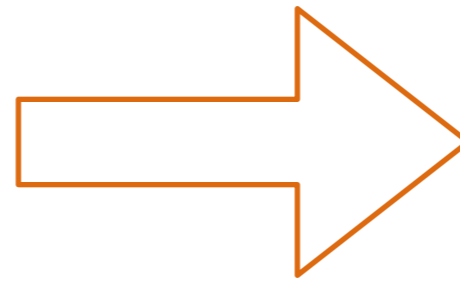
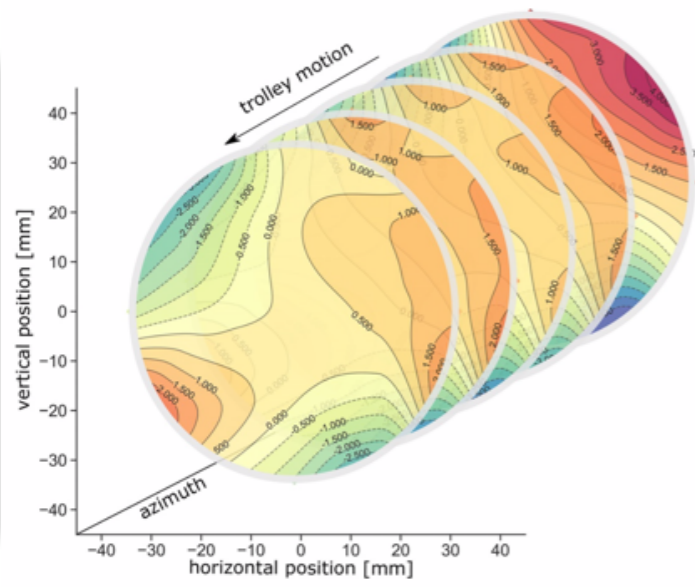
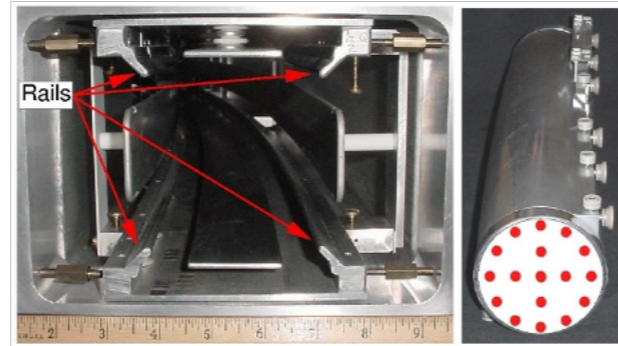


ω_p : free proton precession frequency
Using proton NMR
 $\hbar\omega_p = 2\mu_p B$

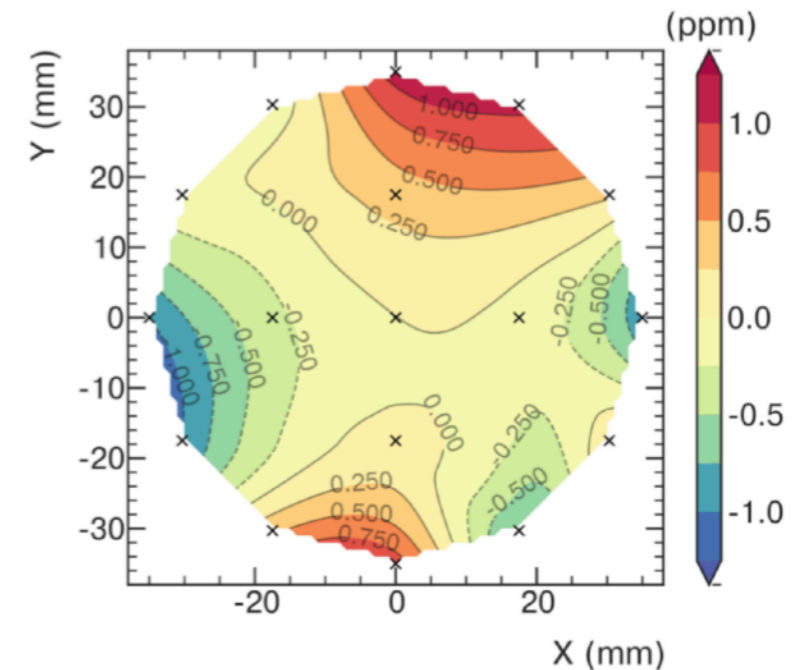
Absolute field calibration:

- Absolute probes were used to calibrate NMR probes
- Proton NMR, calibrated in terms of $\omega_p(T_r)$ of a proton shielded in a spherical sample of water at an exact temperature.

Measuring ω_p : Monitoring and Measuring the Magnetic Field



azimuthally averaged field



To determine ω_p at all times:

- Map the magnetic field in the storage region with trolley runs every 3 days
- Use fixed probes to interpolate the field between trolley runs

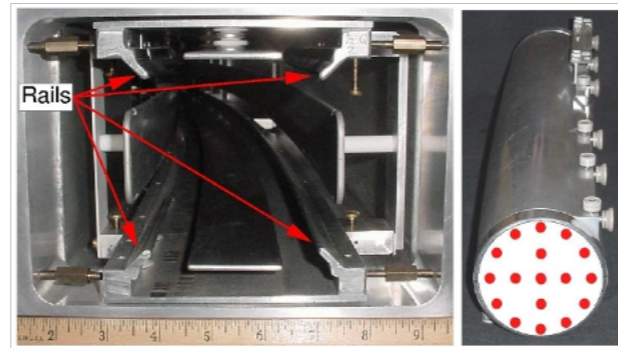
$$a_\mu = \left(\frac{g_e}{2}\right) \left(\frac{\omega_a}{\langle\omega_p\rangle}\right) \left(\frac{\mu_p}{\mu_e}\right) \left(\frac{m_\mu}{m_e}\right)$$

$$\langle\omega_p\rangle \approx \omega_p \otimes \rho(r)$$

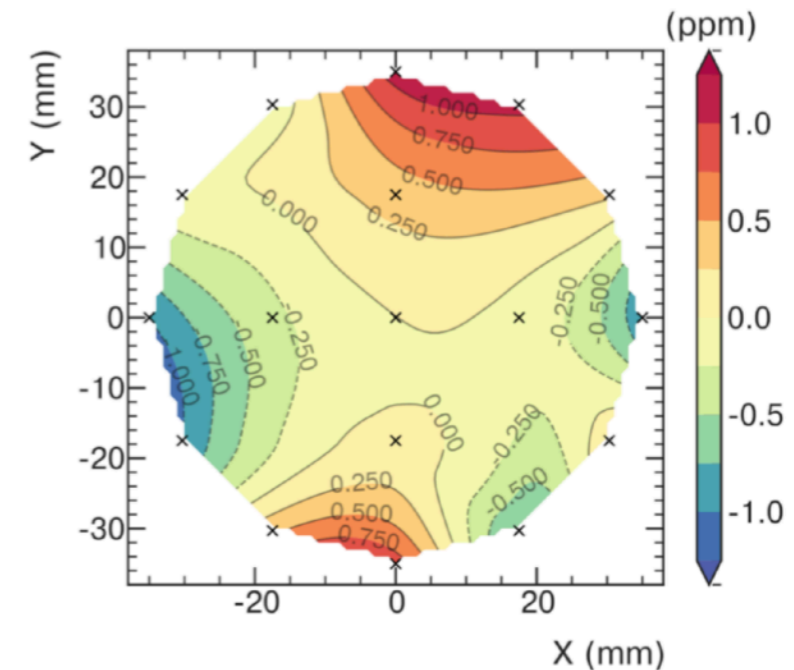
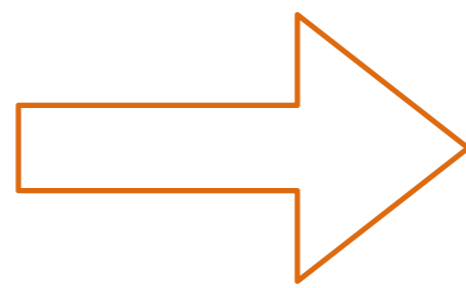
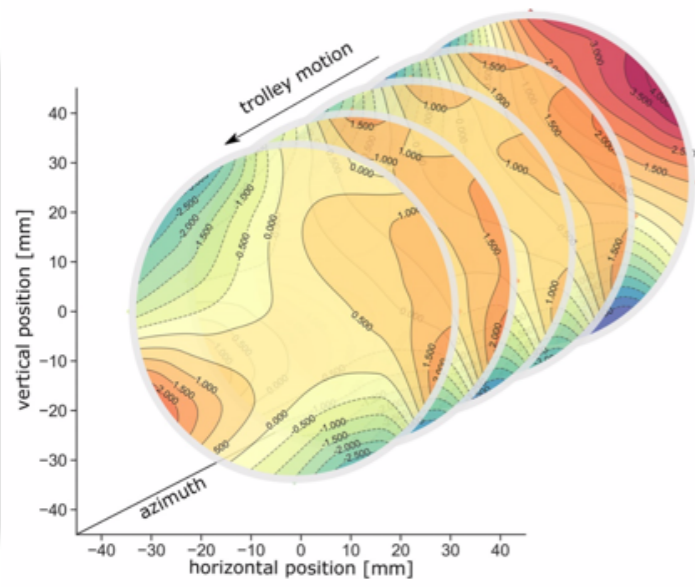
ω_p : free proton precession frequency

Using proton NMR $\hbar\omega_p = 2\mu_p B$

Measuring ω_p : Monitoring and Measuring the Magnetic Field



azimuthally averaged field

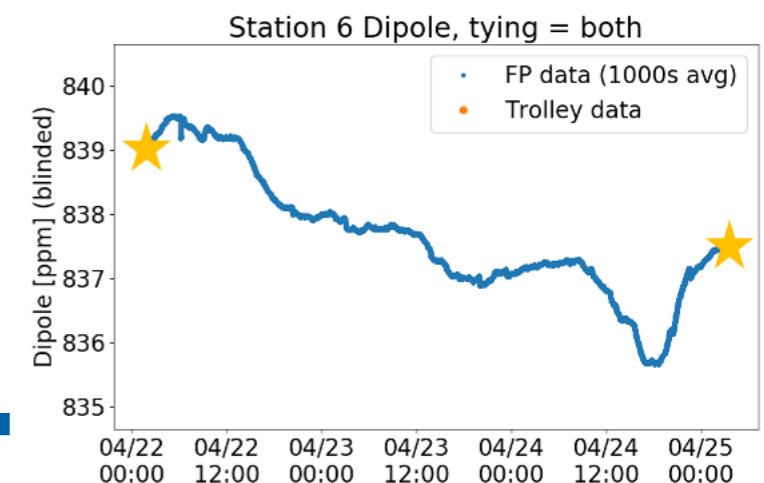


To determine ω_p at all times:

- Map the magnetic field in the storage region with trolley runs every 3 days
- Use fixed probes to interpolate the field between trolley runs

$$a_\mu = \left(\frac{g_e}{2}\right) \left(\frac{\omega_a}{\langle\omega_p\rangle}\right) \left(\frac{\mu_p}{\mu_e}\right) \left(\frac{m_\mu}{m_e}\right)$$

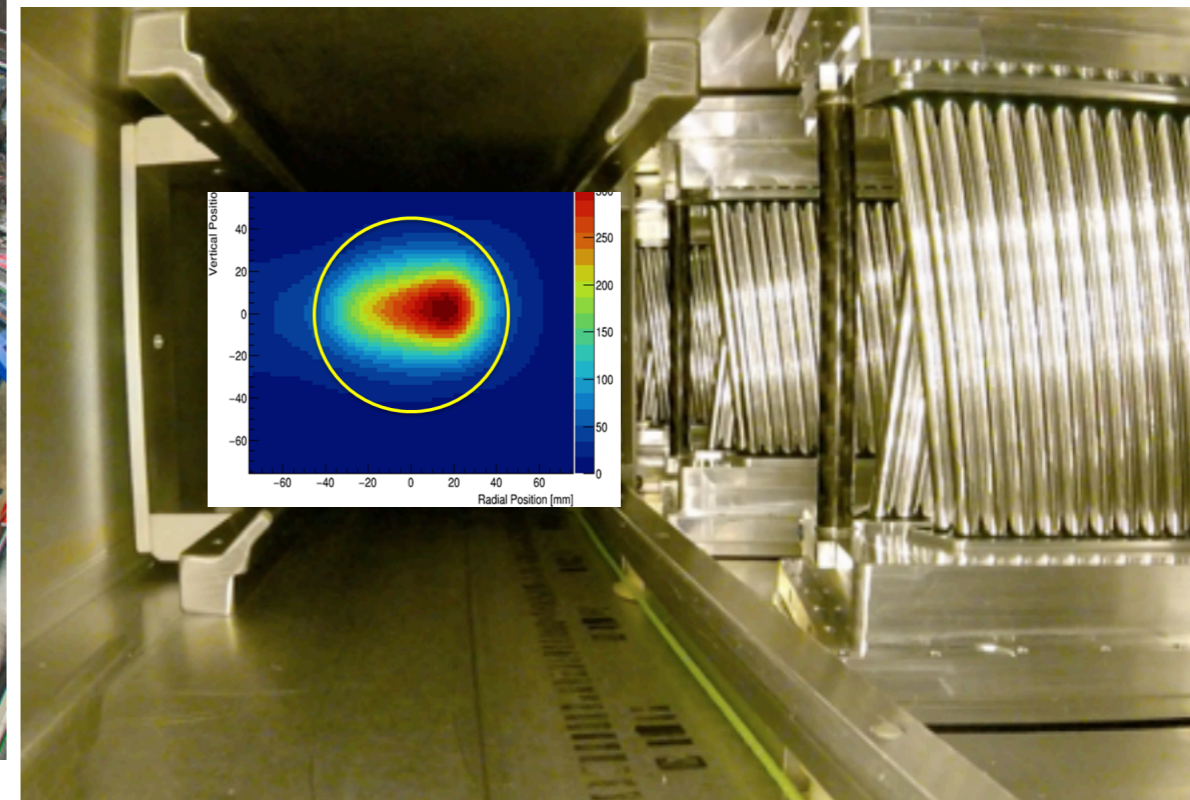
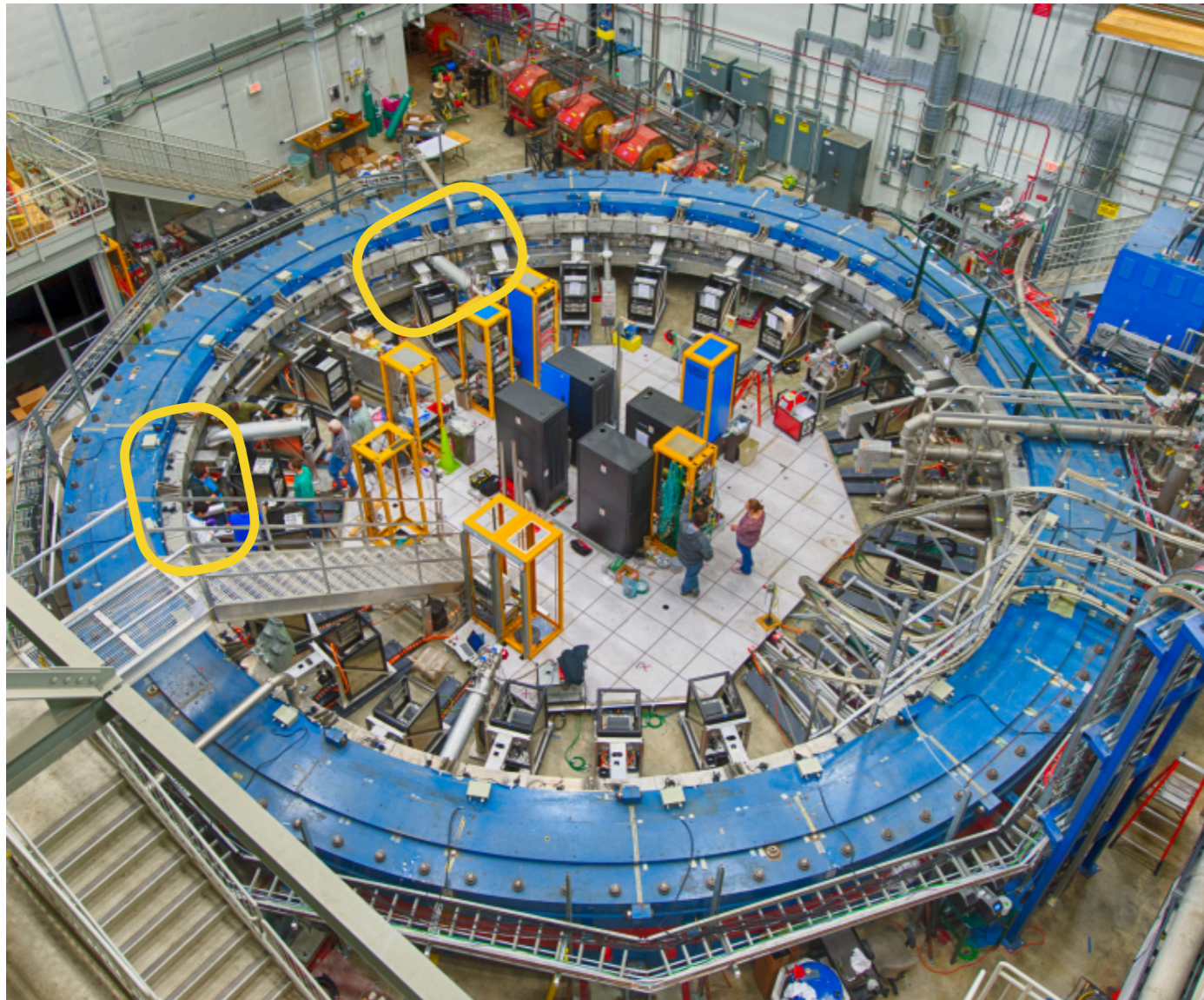
$$\langle\omega_p\rangle \approx \omega_p \otimes \rho(r)$$



Detectors: Trackers for Reconstructing the Beam Profile



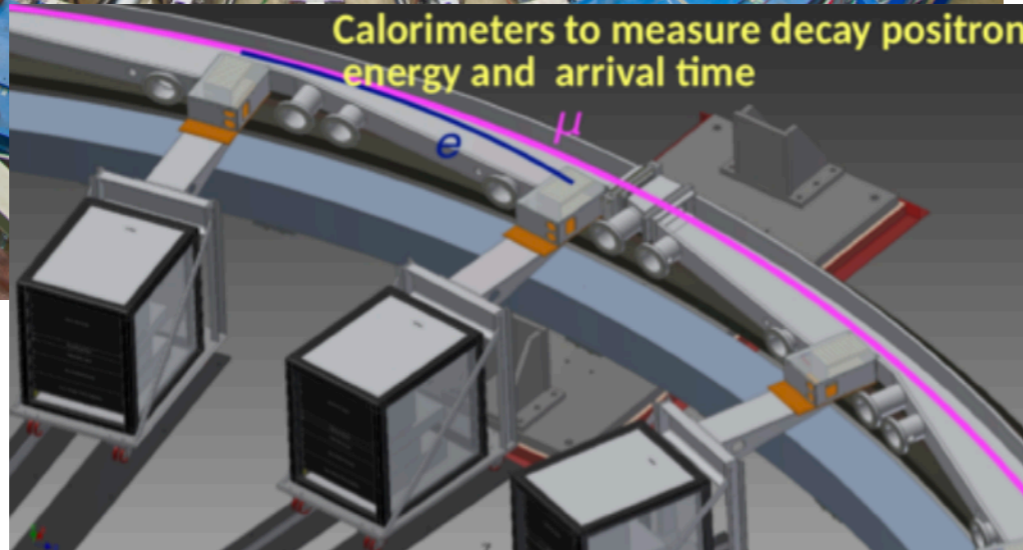
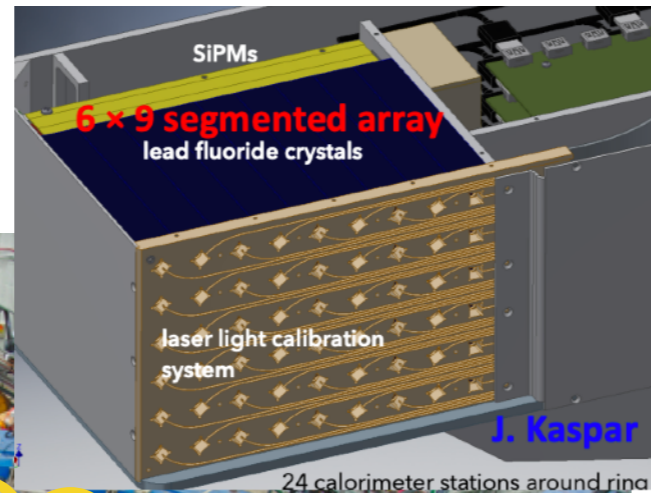
- Trackers
 - 2 straw-tracker stations
 - 8 modules per station each with 128 straws
 - Reconstruct muon beam profile from positron trajectories



$$a_{\mu} = \left(\frac{g_e}{2} \right) \left(\frac{\omega_a}{\langle \omega_p \rangle} \right) \left(\frac{\mu_p}{\mu_e} \right) \left(\frac{m_{\mu}}{m_e} \right)$$

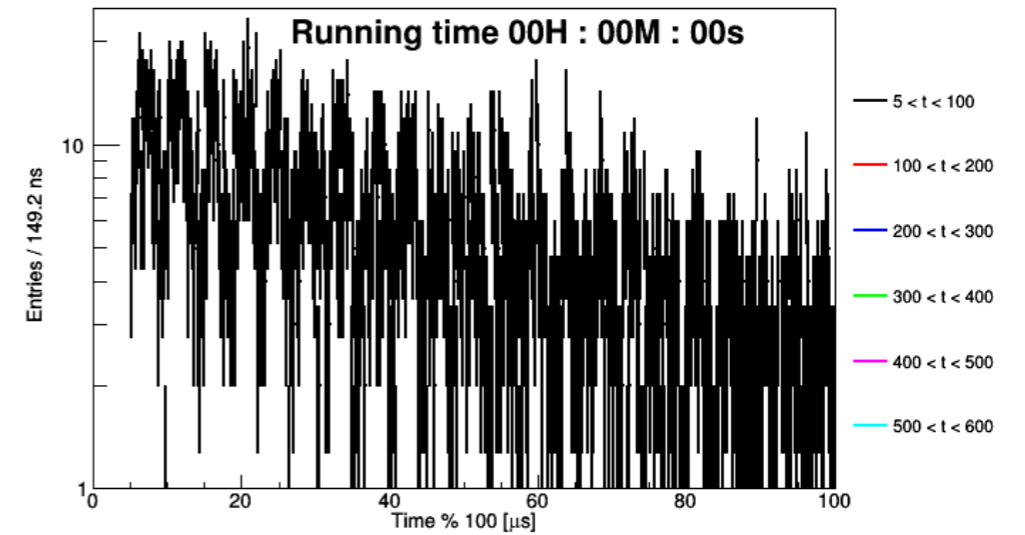
$$\langle \omega_p \rangle \approx \omega_p \otimes \rho(r)$$

Detectors : Calorimeters

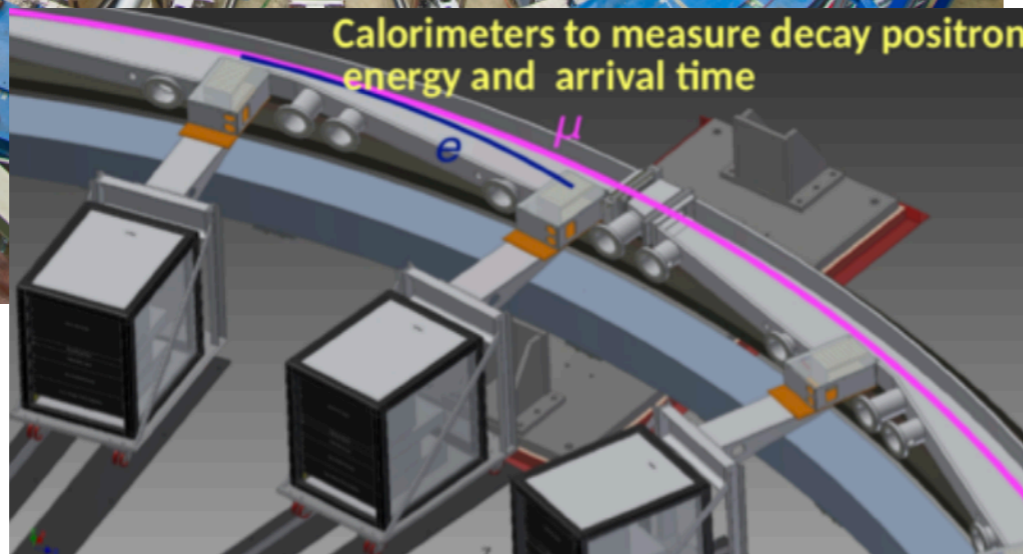
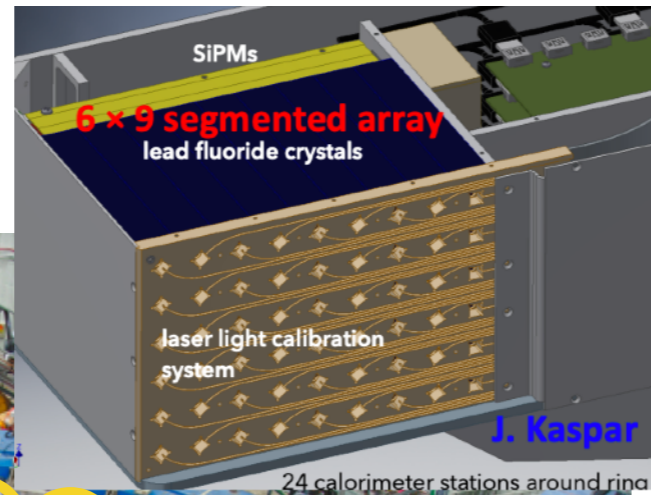


• Calorimeters

- 24 segmented PbF₂ crystal calorimeters stationed around the ring
- Detects energy and arrival time of e^+ decayed from muons: $\mu^+ \rightarrow e^+ \bar{\nu}_\mu \nu_e$

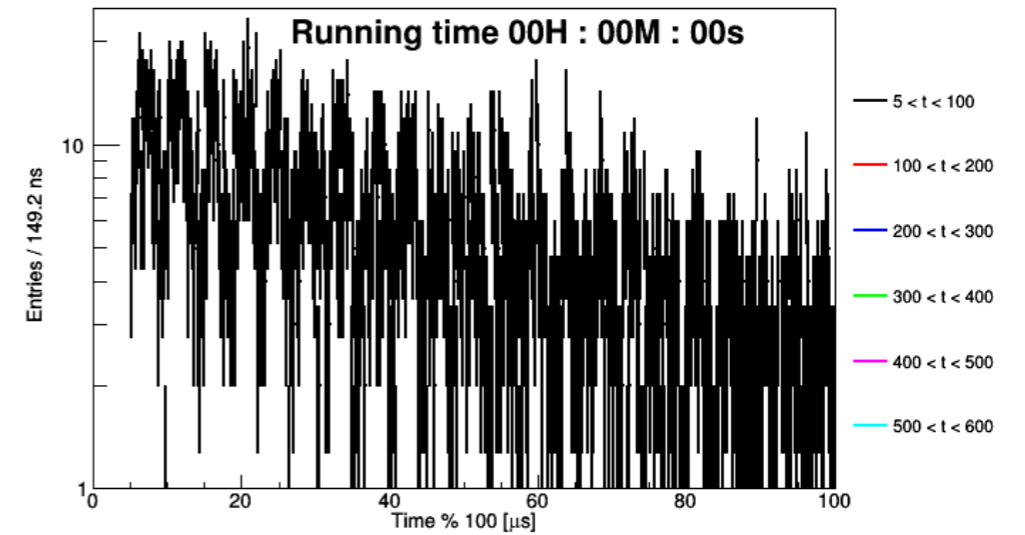


Detectors : Calorimeters

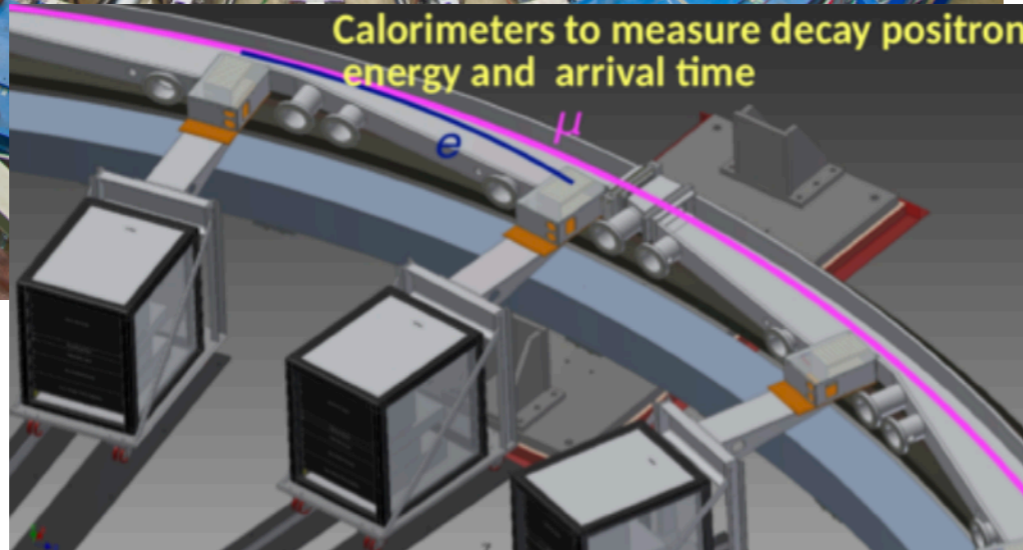
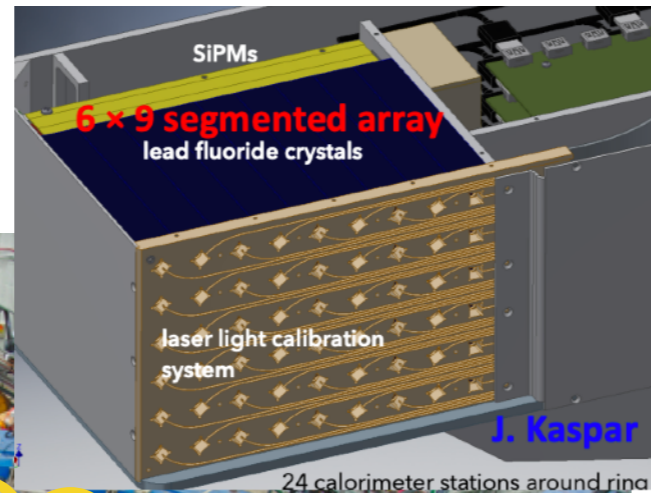


• Calorimeters

- 24 segmented PbF₂ crystal calorimeters stationed around the ring
- Detects energy and arrival time of e⁺ decayed from muons: $\mu^+ \rightarrow e^+ \bar{\nu}_\mu \nu_e$

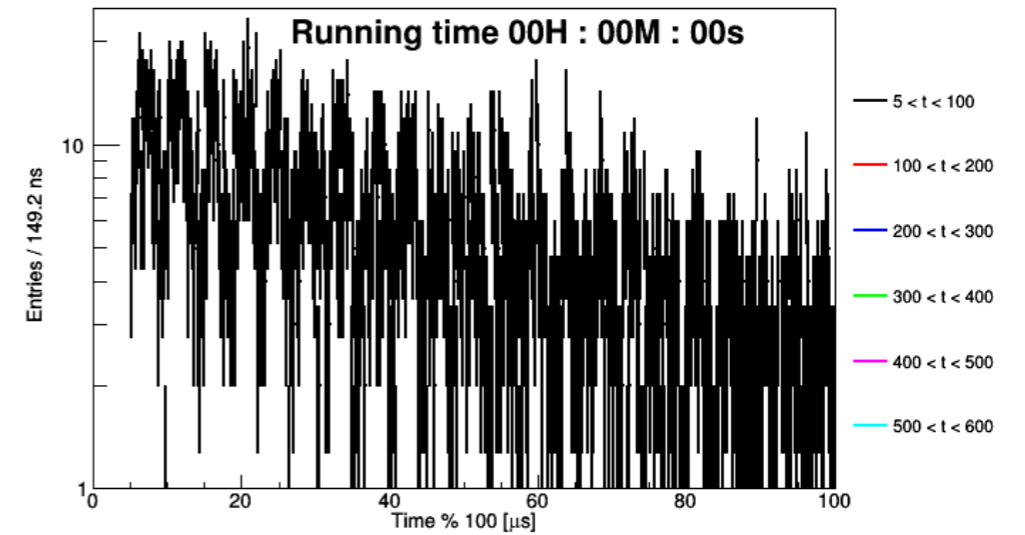


Detectors : Calorimeters



• Calorimeters

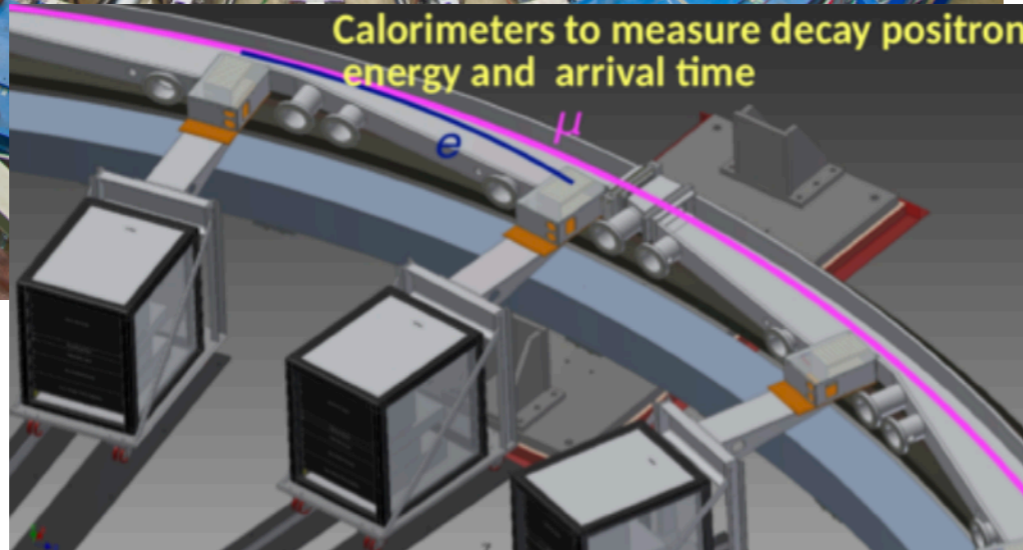
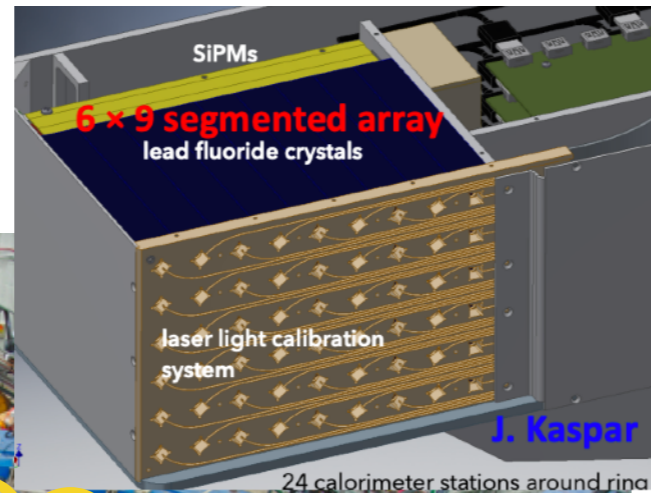
- 24 segmented PbF₂ crystal calorimeters stationed around the ring
- Detects energy and arrival time of e⁺ decayed from muons: $\mu^+ \rightarrow e^+ \bar{\nu}_\mu \nu_e$



$$N(t) = N_0 e^{-t/\tau} [1 + A \cos(\omega_a t + \phi)]$$

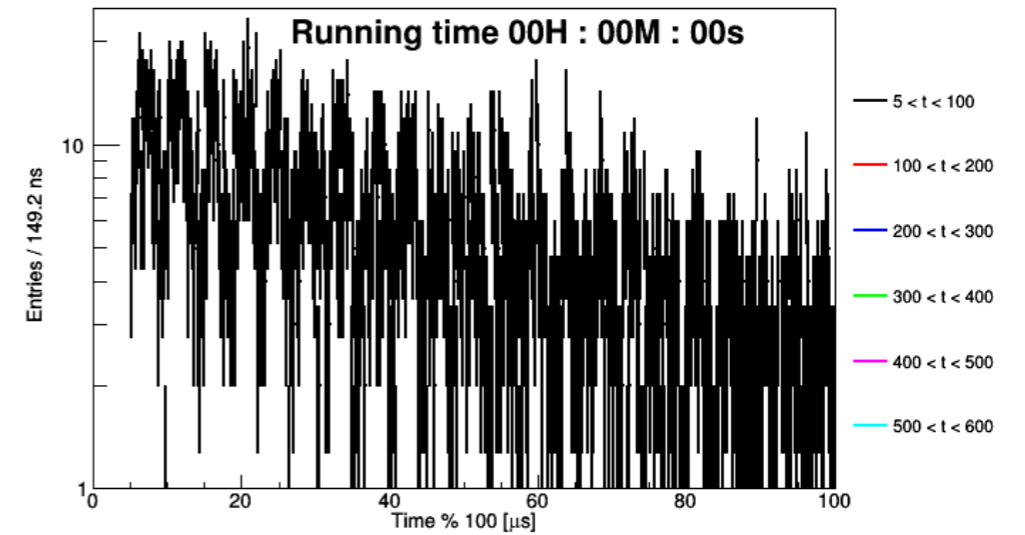
$$a_\mu = \left(\frac{g_e}{2} \right) \left(\frac{\omega_a}{\langle \omega_p \rangle} \right) \left(\frac{\mu_p}{\mu_e} \right) \left(\frac{m_\mu}{m_e} \right)$$

Detectors : Calorimeters



• Calorimeters

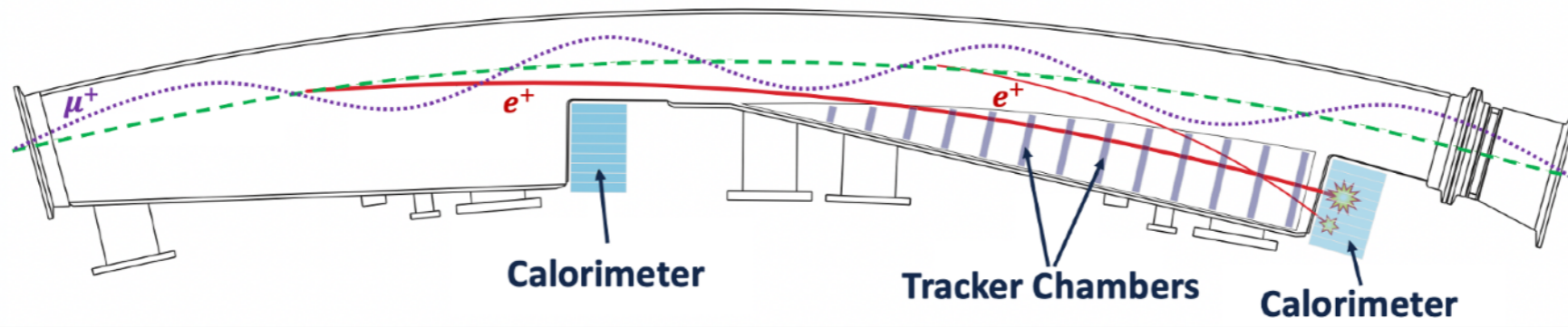
- 24 segmented PbF₂ crystal calorimeters stationed around the ring
- Detects energy and arrival time of e⁺ decayed from muons: $\mu^+ \rightarrow e^+ \bar{\nu}_\mu \nu_e$



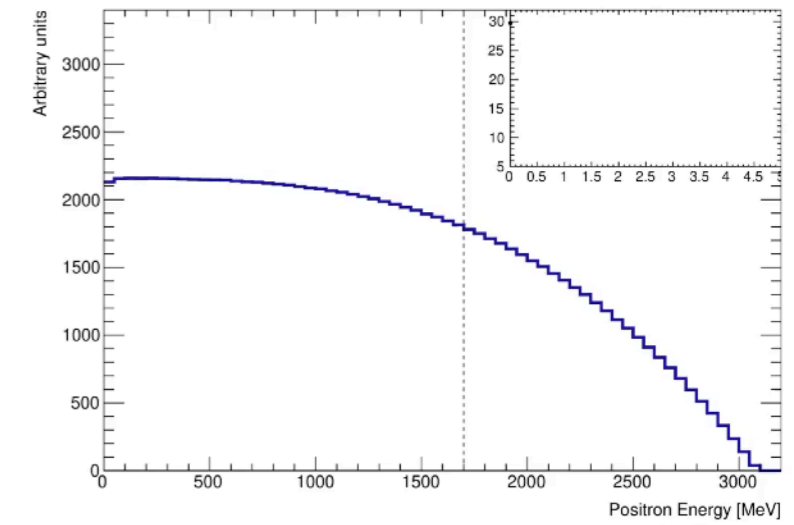
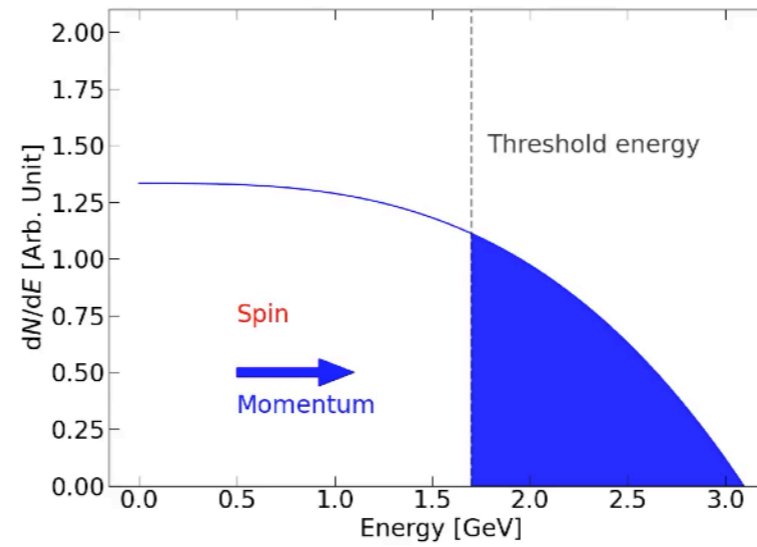
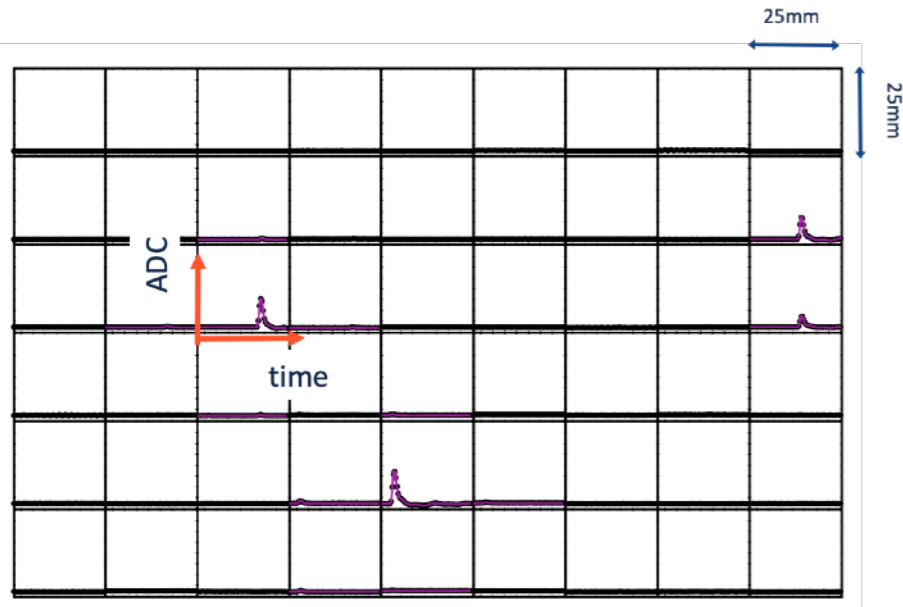
$$N(t) = N_0 e^{-t/\tau} [1 + A \cos(\omega_a t + \phi)]$$

$$a_\mu = \left(\frac{g_e}{2} \right) \left(\frac{\omega_a}{\langle \omega_p \rangle} \right) \left(\frac{\mu_p}{\mu_e} \right) \left(\frac{m_\mu}{m_e} \right)$$

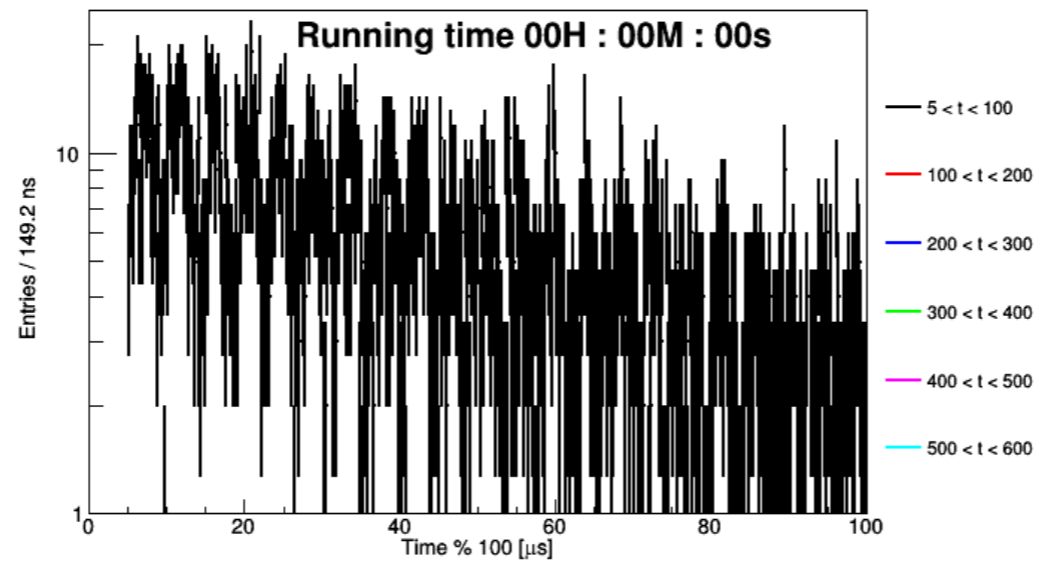
Calculating ω_a :



Energy distribution recorded in the calorimeter.

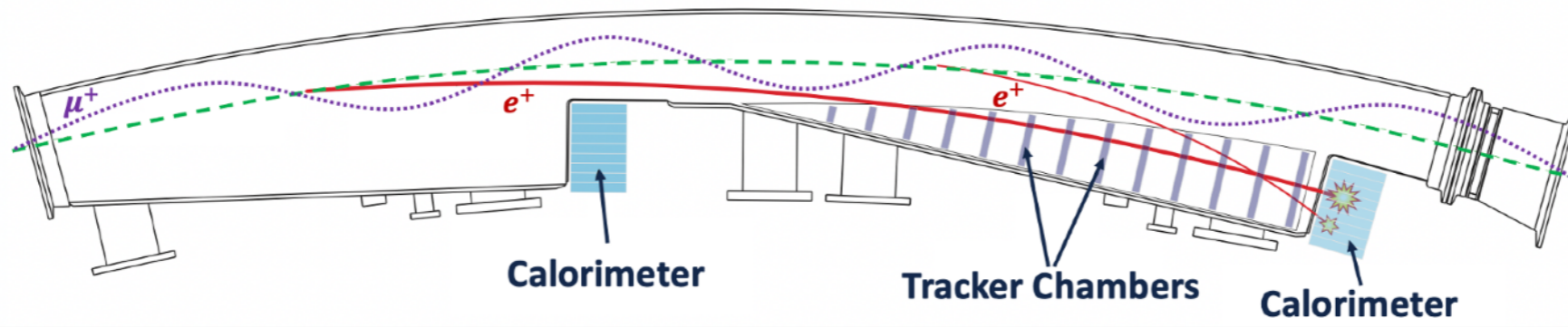


ω_a blinded by both hardware and software

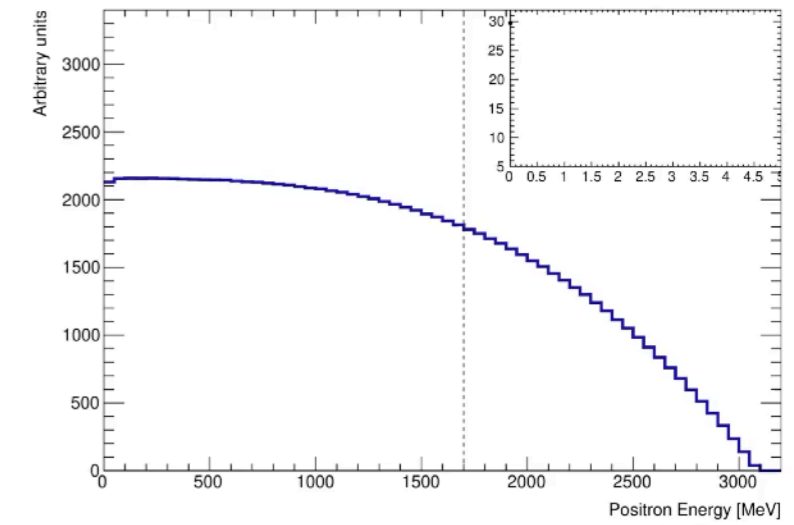
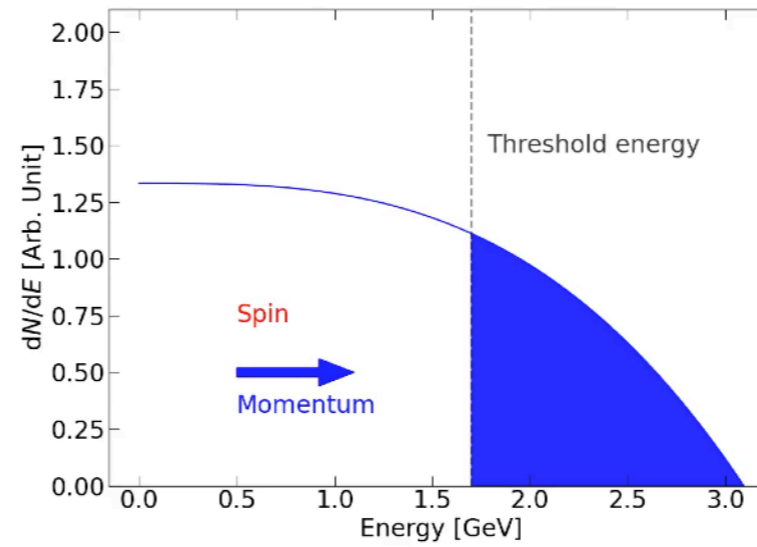
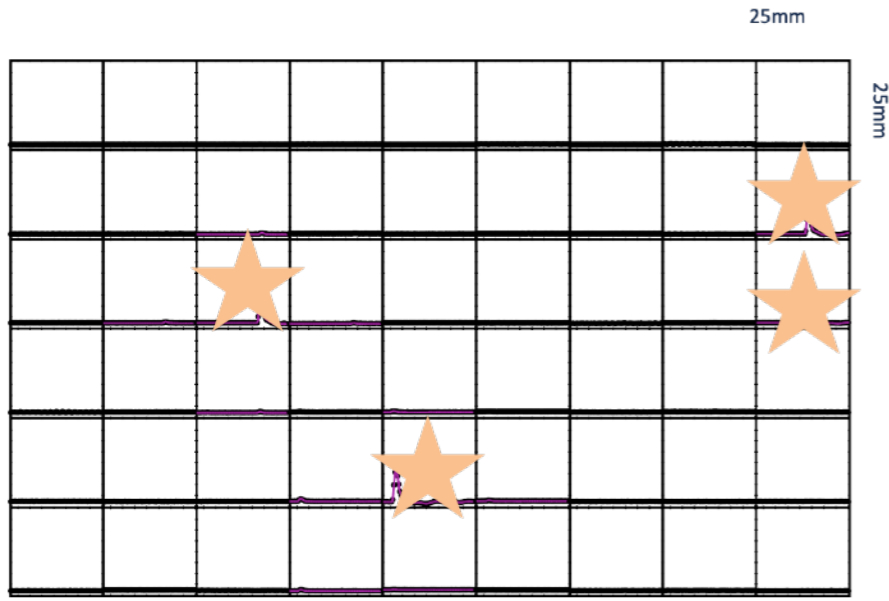


Wiggle plot

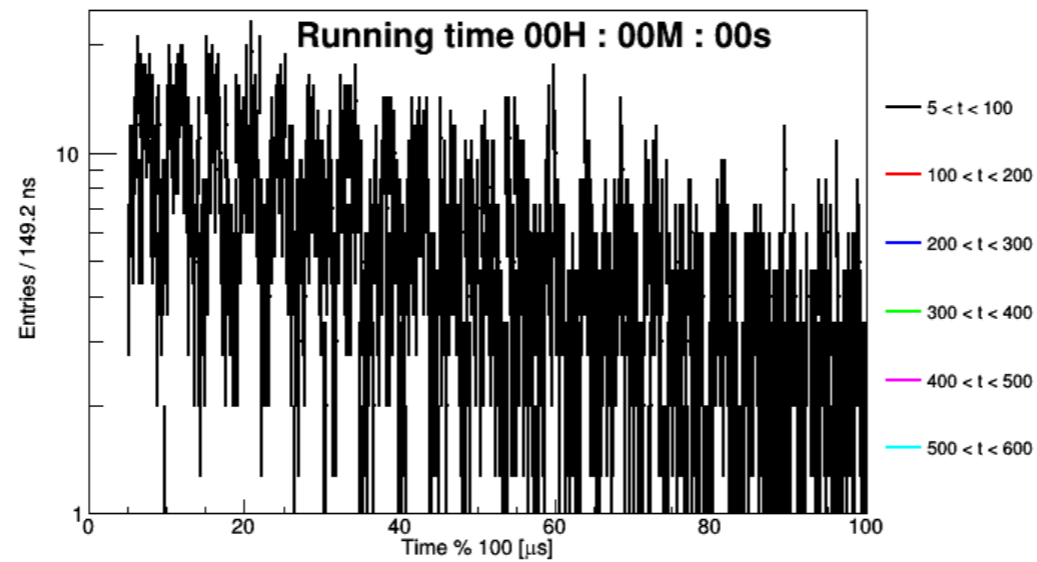
Calculating ω_a :



Energy distribution recorded in the calorimeter.

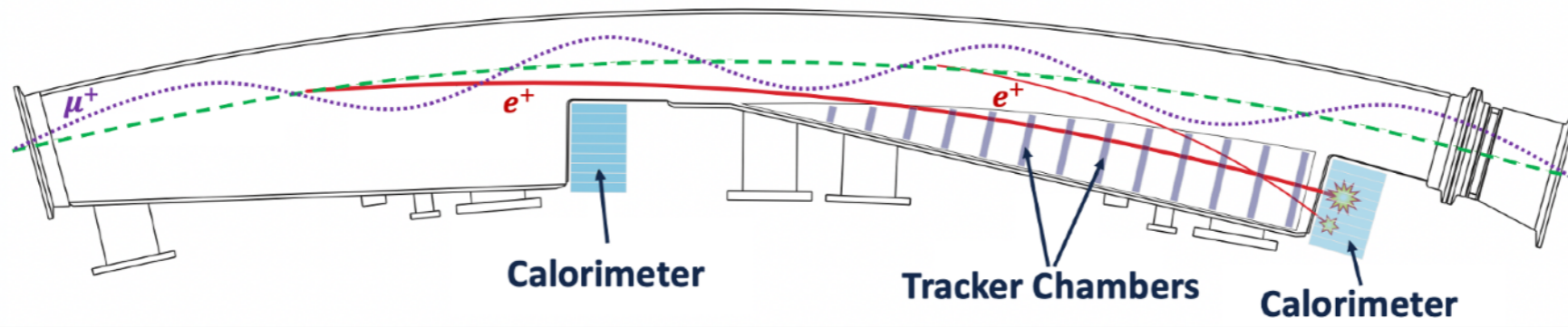


ω_a blinded by both hardware and software

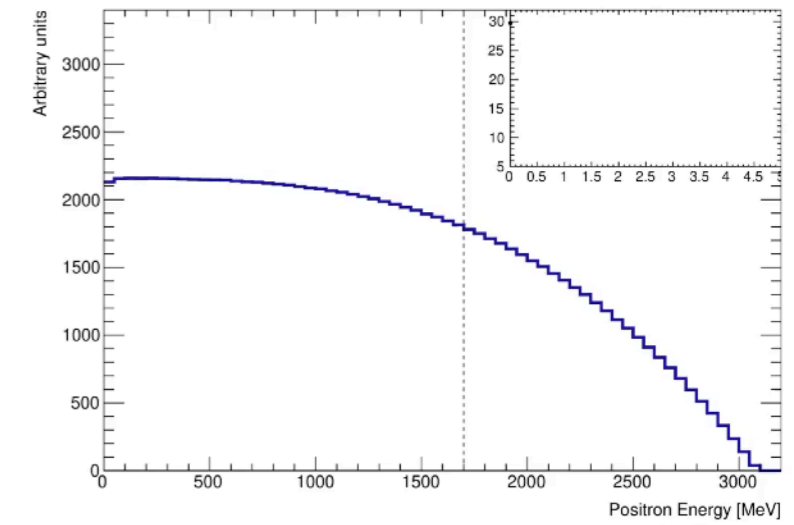
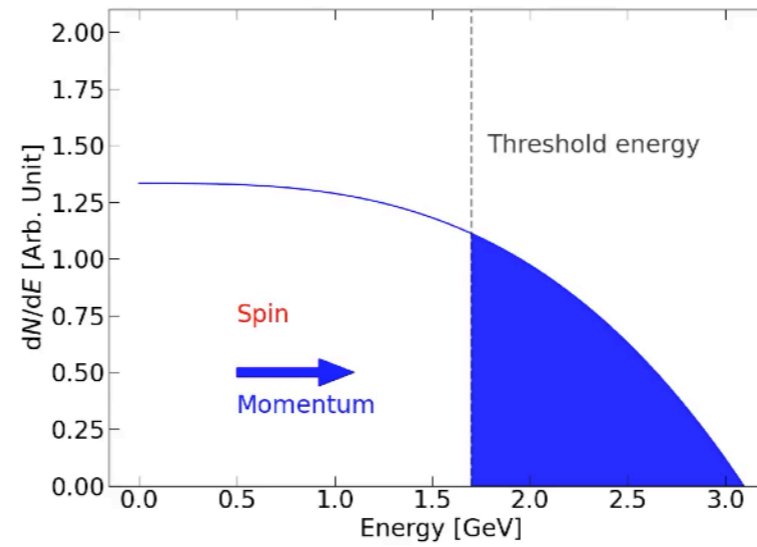
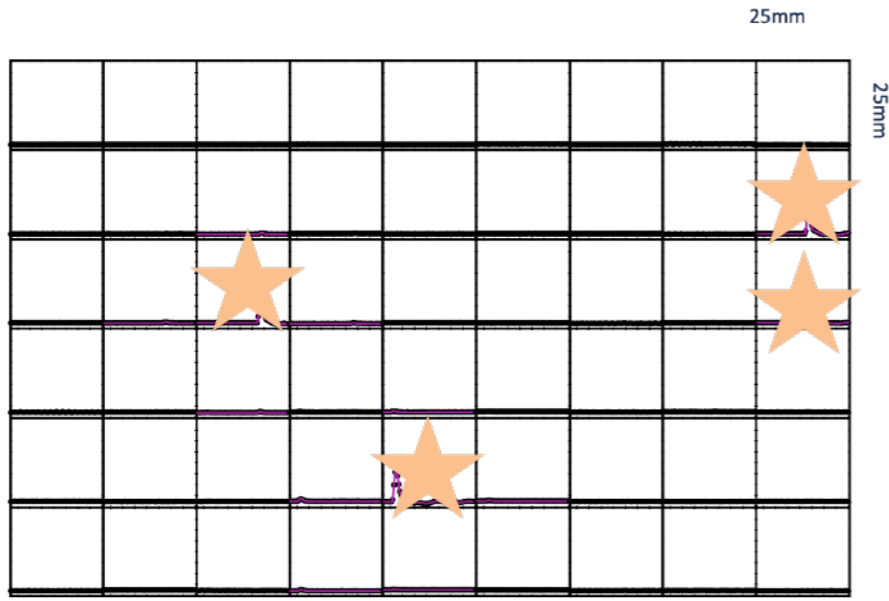


Wiggle plot

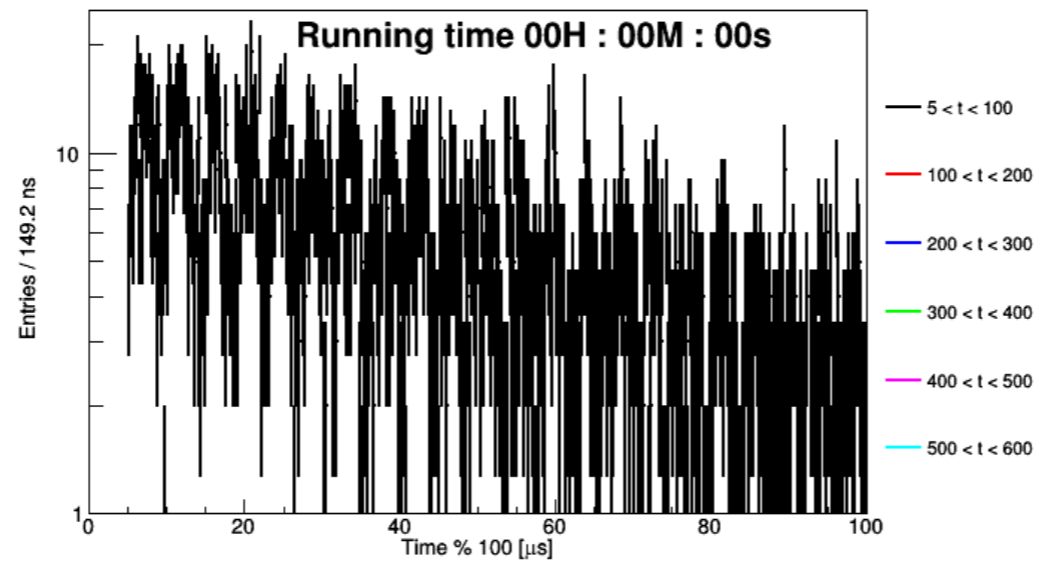
Calculating ω_a :



Energy distribution recorded in the calorimeter.

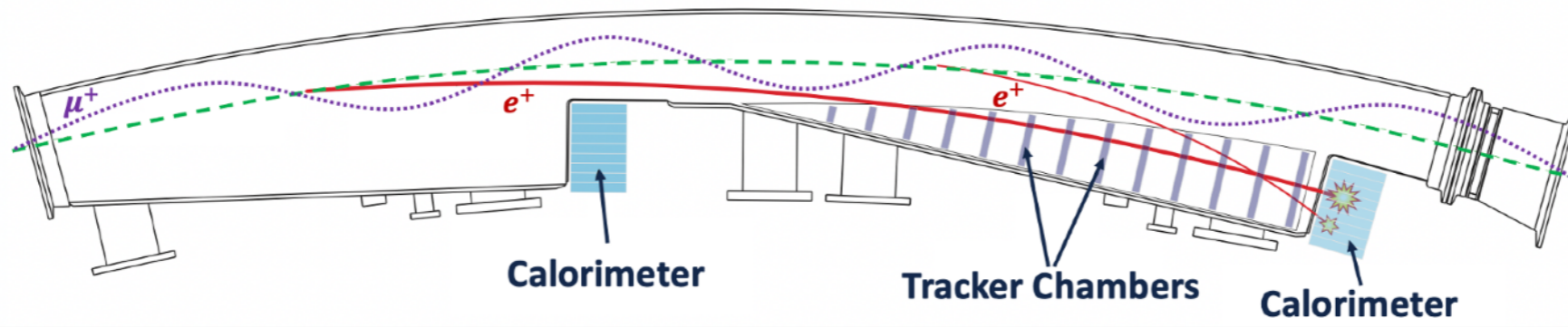


ω_a blinded by both hardware and software

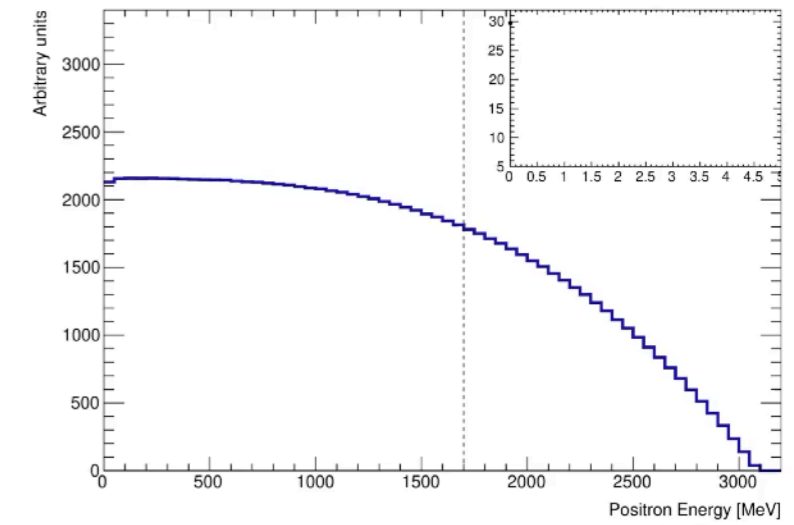
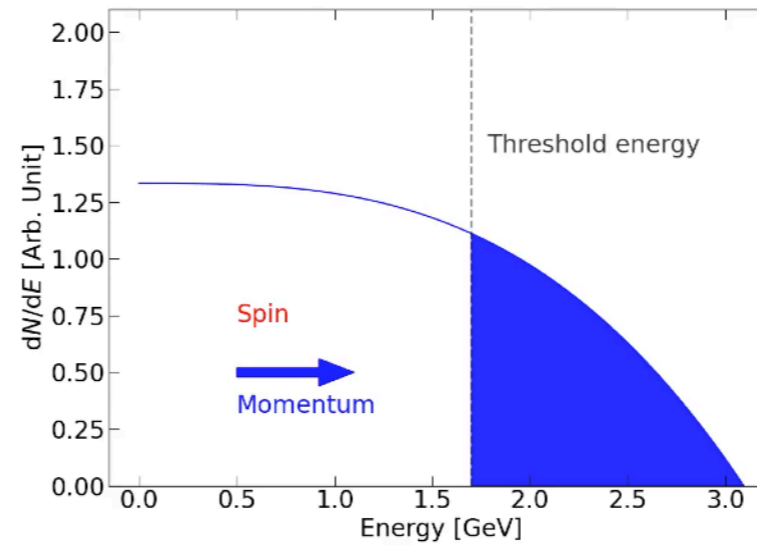
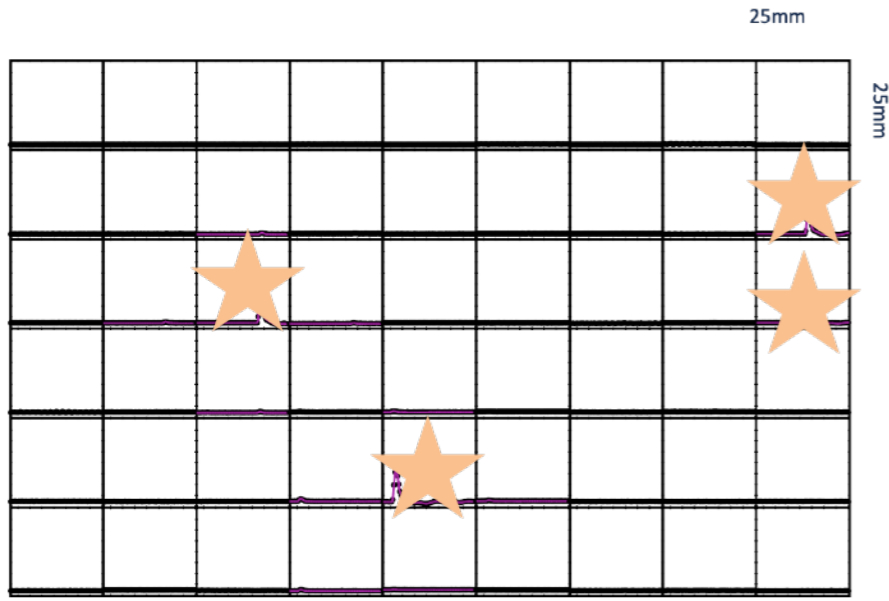


Wiggle plot

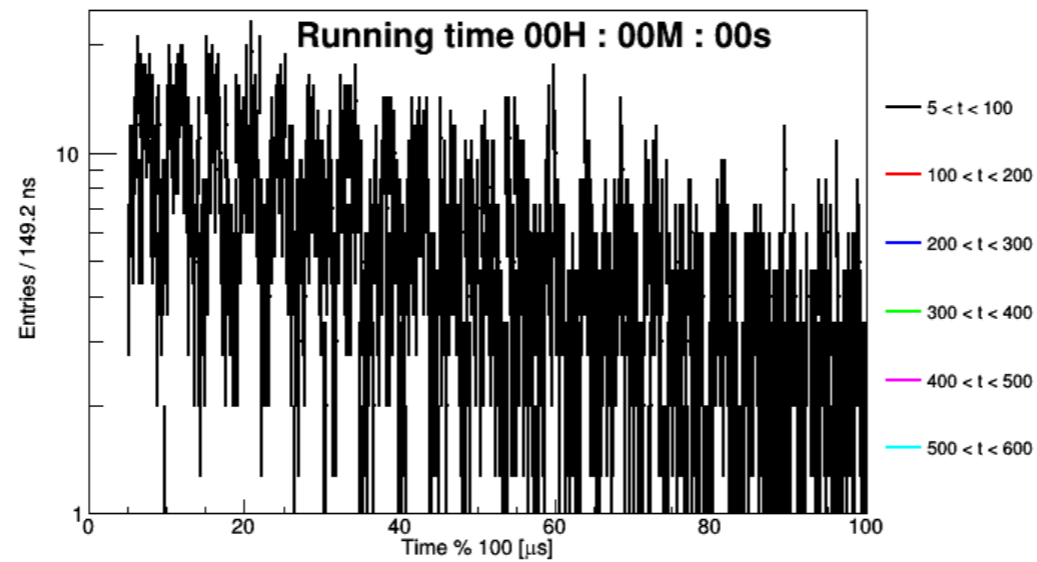
Calculating ω_a :



Energy distribution recorded in the calorimeter.



ω_a blinded by both hardware and software

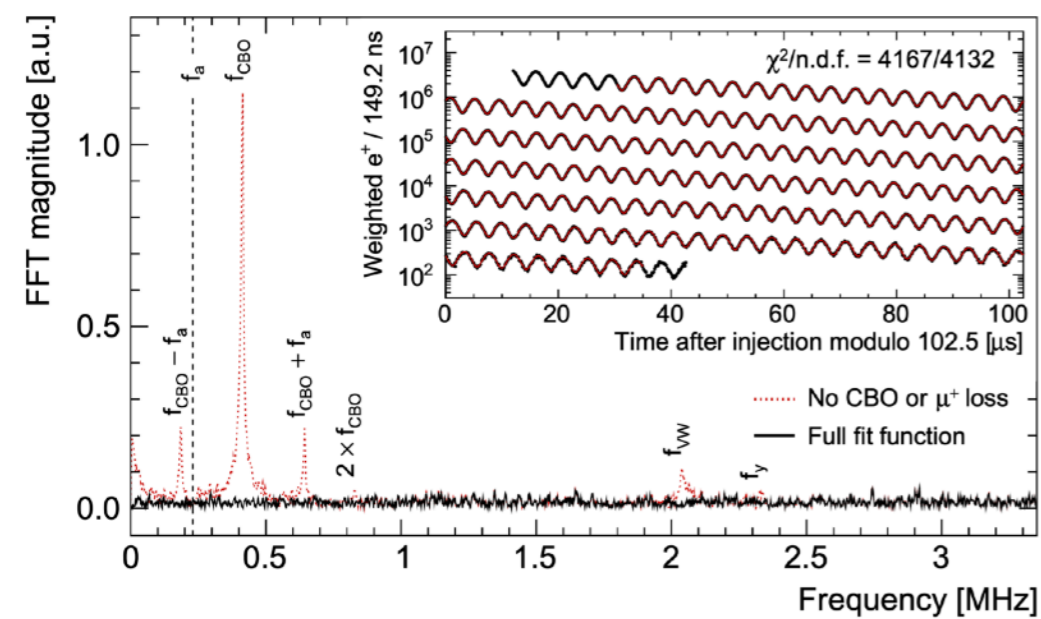


Wiggle plot

Calculating ω_a : Hidden information in the wiggle plot



FFT analysis of fit residuals



Calculating ω_a : Hidden information in the wiggle plot

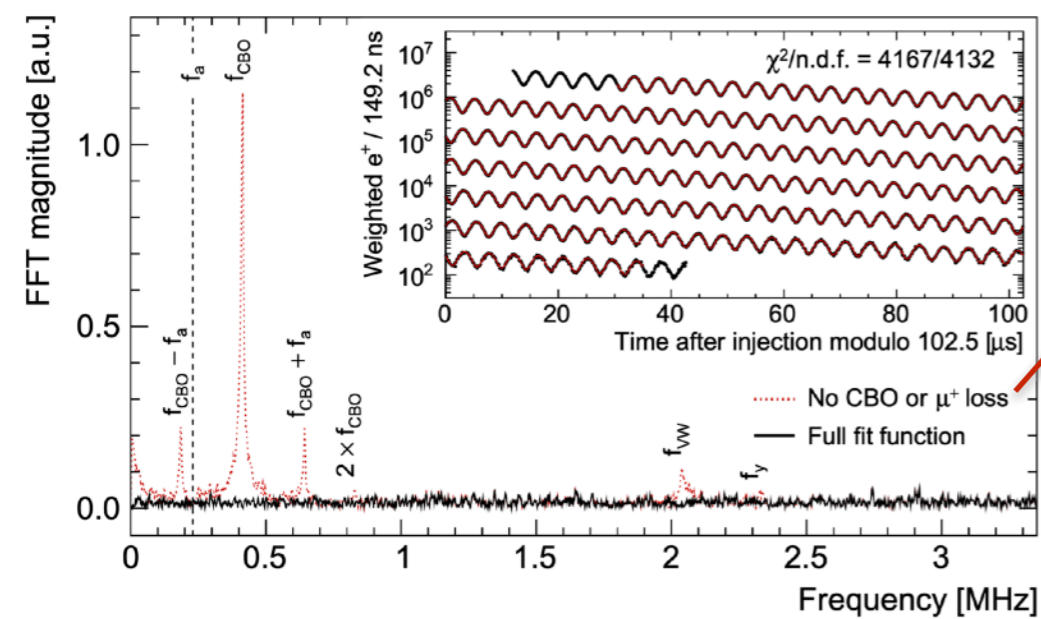


Underling Physics

5 parameter fit function

$$N(t) = N_0 e^{-t/\tau} [1 + A \cos(\omega_a t + \phi)]$$

FFT analysis of fit residuals



Calculating ω_a : Hidden information in the wiggle plot



Underling Physics

5 parameter fit function

$$N(t) = N_0 e^{-t/\tau} [1 + A \cos(\omega_a t + \phi)]$$

Systematic Effects

Including CBO, lost muon, other beam dynamics related parameters improve the fit results

$$N_0 e^{-\frac{t}{\tau}} (1 + A \cdot A_{BO}(t) \cos(\omega_a t + \phi \cdot \phi_{BO}(t))) \cdot N_{CBO}(t) \cdot N_{VW}(t) \cdot N_y(t) \cdot N_{2CBO}(t) \cdot J(t)$$

$$A_{BO}(t) = 1 + A_A \cos(\omega_{CBO}(t) + \phi_A) e^{-\frac{t}{\tau_{CBO}}}$$

$$\phi_{BO}(t) = 1 + A_\phi \cos(\omega_{CBO}(t) + \phi_\phi) e^{-\frac{t}{\tau_{CBO}}}$$

$$N_{CBO}(t) = 1 + A_{CBO} \cos(\omega_{CBO}(t) + \phi_{CBO}) e^{-\frac{t}{\tau_{CBO}}}$$

$$N_{2CBO}(t) = 1 + A_{2CBO} \cos(2\omega_{CBO}(t) + \phi_{2CBO}) e^{-\frac{t}{2\tau_{CBO}}}$$

$$N_{VW}(t) = 1 + A_{VW} \cos(\omega_{VW}(t)t + \phi_{VW}) e^{-\frac{t}{\tau_{VW}}}$$

$$N_y(t) = 1 + A_y \cos(\omega_y(t)t + \phi_y) e^{-\frac{t}{\tau_y}}$$

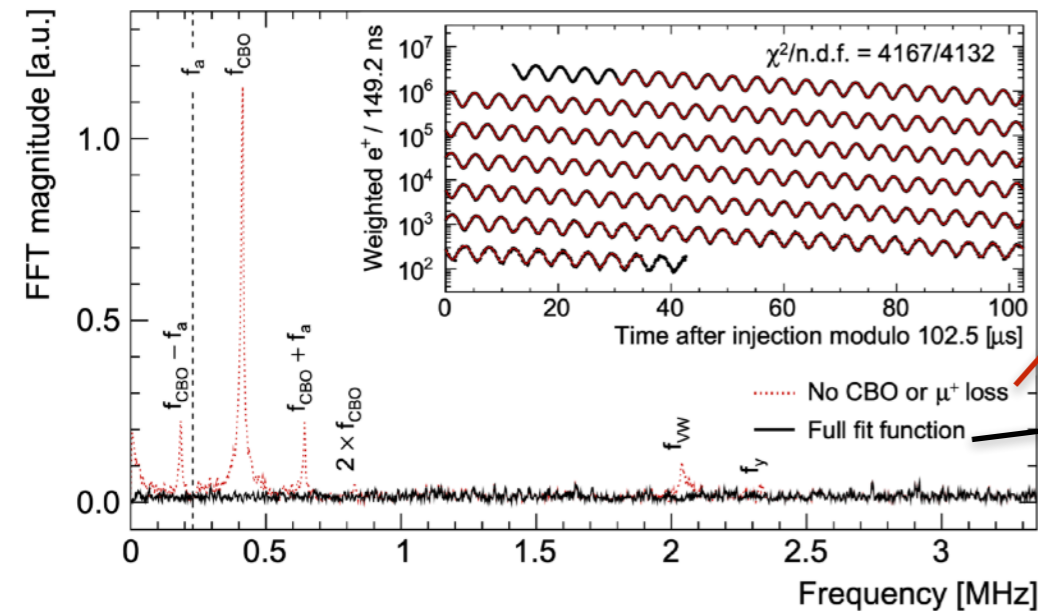
$$J(t) = 1 - k_{LM} \int_{t_0}^t \Lambda(t) dt$$

$$\omega_{CBO}(t) = \omega_0 t + A e^{-\frac{t}{\tau_A}} + B e^{-\frac{t}{\tau_B}}$$

$$\omega_y(t) = F \omega_{CBO}(t) \sqrt{2\omega_c / F \omega_{CBO}(t) - 1}$$

$$\omega_{VW}(t) = \omega_c - 2\omega_y(t)$$

FFT analysis of fit residuals



Calculating ω_a : Hidden information in the wiggle plot



Underling Physics

5 parameter fit function

$$N(t) = N_0 e^{-t/\tau} [1 + A \cos(\omega_a t + \phi)]$$

Systematic Effects

Including CBO, lost muon, other beam dynamics related parameters improve the fit results

$$N_0 e^{-\frac{t}{\tau}} (1 + A \cdot A_{BO}(t) \cos(\omega_a t + \phi \cdot \phi_{BO}(t))) \cdot N_{CBO}(t) \cdot N_{VW}(t) \cdot N_y(t) \cdot N_{2CBO}(t) \cdot J(t)$$

$$A_{BO}(t) = 1 + A_A \cos(\omega_{CBO}(t) + \phi_A) e^{-\frac{t}{\tau_{CBO}}}$$

$$\phi_{BO}(t) = 1 + A_\phi \cos(\omega_{CBO}(t) + \phi_\phi) e^{-\frac{t}{\tau_{CBO}}}$$

$$N_{CBO}(t) = 1 + A_{CBO} \cos(\omega_{CBO}(t) + \phi_{CBO}) e^{-\frac{t}{\tau_{CBO}}}$$

$$N_{2CBO}(t) = 1 + A_{2CBO} \cos(2\omega_{CBO}(t) + \phi_{2CBO}) e^{-\frac{t}{2\tau_{CBO}}}$$

$$N_{VW}(t) = 1 + A_{VW} \cos(\omega_{VW}(t)t + \phi_{VW}) e^{-\frac{t}{\tau_{VW}}}$$

$$N_y(t) = 1 + A_y \cos(\omega_y(t)t + \phi_y) e^{-\frac{t}{\tau_y}}$$

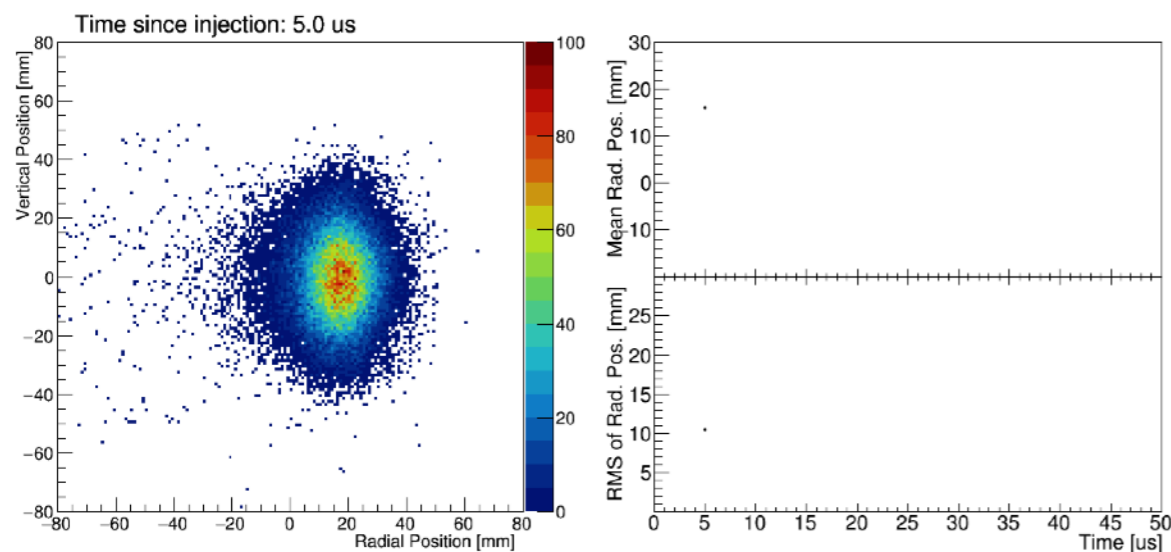
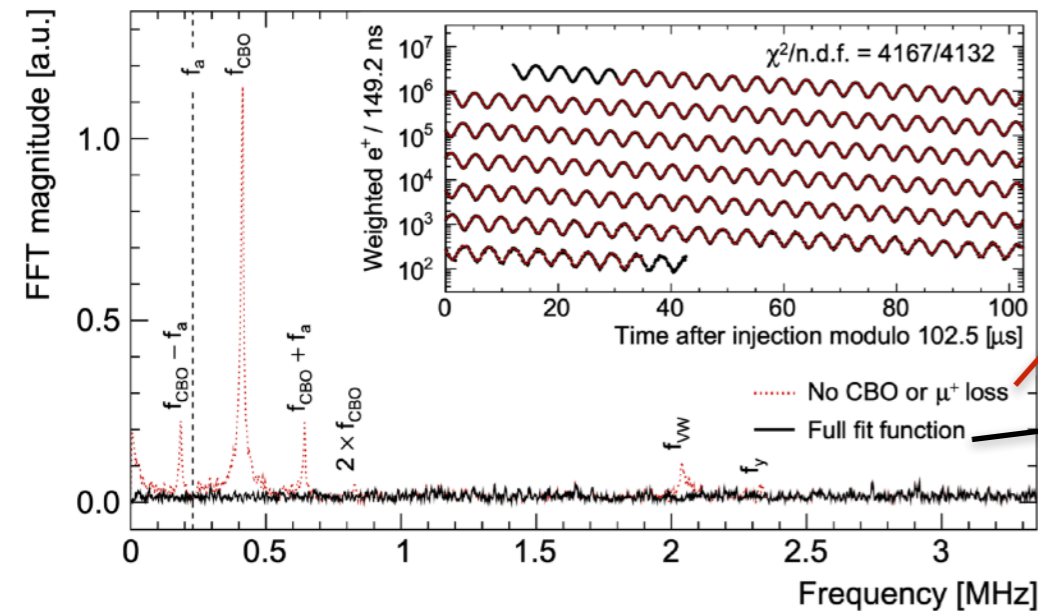
$$J(t) = 1 - k_{LM} \int_{t_0}^t \Lambda(t) dt$$

$$\omega_{CBO}(t) = \omega_0 t + A e^{-\frac{t}{\tau_A}} + B e^{-\frac{t}{\tau_B}}$$

$$\omega_y(t) = F \omega_{CBO}(t) \sqrt{2\omega_c / F \omega_{CBO}(t) - 1}$$

$$\omega_{VW}(t) = \omega_c - 2\omega_y(t)$$

FFT analysis of fit residuals



Calculating ω_a : Hidden information in the wiggle plot



Underling Physics

5 parameter fit function

$$N(t) = N_0 e^{-t/\tau} [1 + A \cos(\omega_a t + \phi)]$$

Systematic Effects

Including CBO, lost muon, other beam dynamics related parameters improve the fit results

$$N_0 e^{-\frac{t}{\tau}} (1 + A \cdot A_{BO}(t) \cos(\omega_a t + \phi \cdot \phi_{BO}(t))) \cdot N_{CBO}(t) \cdot N_{VW}(t) \cdot N_y(t) \cdot N_{2CBO}(t) \cdot J(t)$$

$$A_{BO}(t) = 1 + A_A \cos(\omega_{CBO}(t) + \phi_A) e^{-\frac{t}{\tau_{CBO}}}$$

$$\phi_{BO}(t) = 1 + A_\phi \cos(\omega_{CBO}(t) + \phi_\phi) e^{-\frac{t}{\tau_{CBO}}}$$

$$N_{CBO}(t) = 1 + A_{CBO} \cos(\omega_{CBO}(t) + \phi_{CBO}) e^{-\frac{t}{\tau_{CBO}}}$$

$$N_{2CBO}(t) = 1 + A_{2CBO} \cos(2\omega_{CBO}(t) + \phi_{2CBO}) e^{-\frac{t}{2\tau_{CBO}}}$$

$$N_{VW}(t) = 1 + A_{VW} \cos(\omega_{VW}(t)t + \phi_{VW}) e^{-\frac{t}{\tau_{VW}}}$$

$$N_y(t) = 1 + A_y \cos(\omega_y(t)t + \phi_y) e^{-\frac{t}{\tau_y}}$$

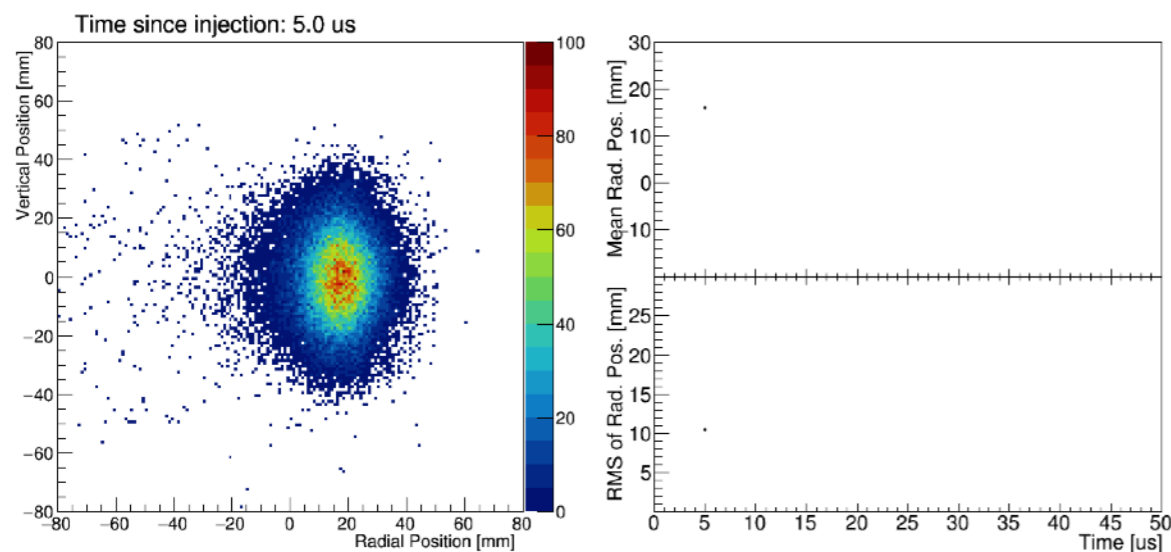
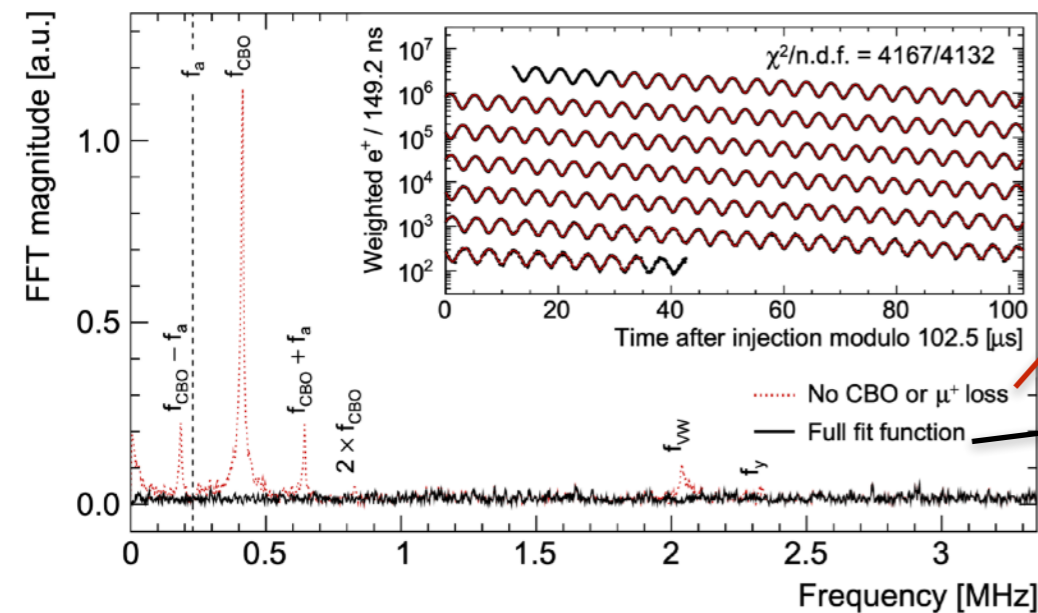
$$J(t) = 1 - k_{LM} \int_{t_0}^t \Lambda(t) dt$$

$$\omega_{CBO}(t) = \omega_0 t + A e^{-\frac{t}{\tau_A}} + B e^{-\frac{t}{\tau_B}}$$

$$\omega_y(t) = F \omega_{CBO}(t) \sqrt{2\omega_c / F \omega_{CBO}(t) - 1}$$

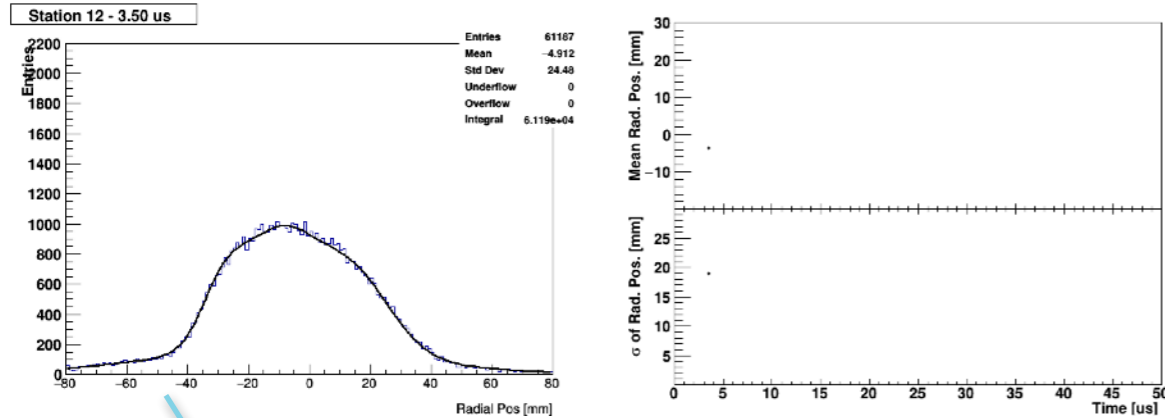
$$\omega_{VW}(t) = \omega_c - 2\omega_y(t)$$

FFT analysis of fit residuals

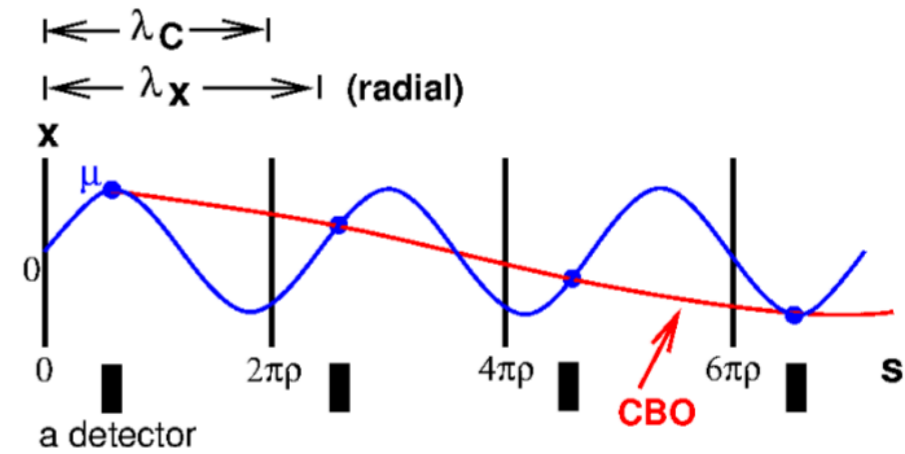
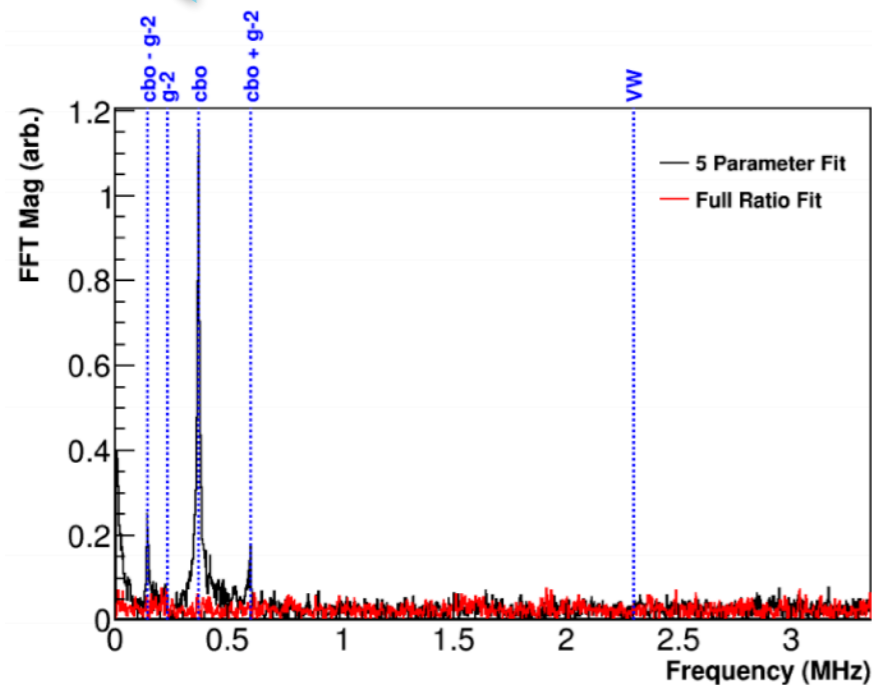


What is the beam doing after all these pulses and kicks

- CBO - Coherent Betatron Oscillation



Radial CBO movement



λ_x - radial wavelength

λ_c - cyclotron wavelength

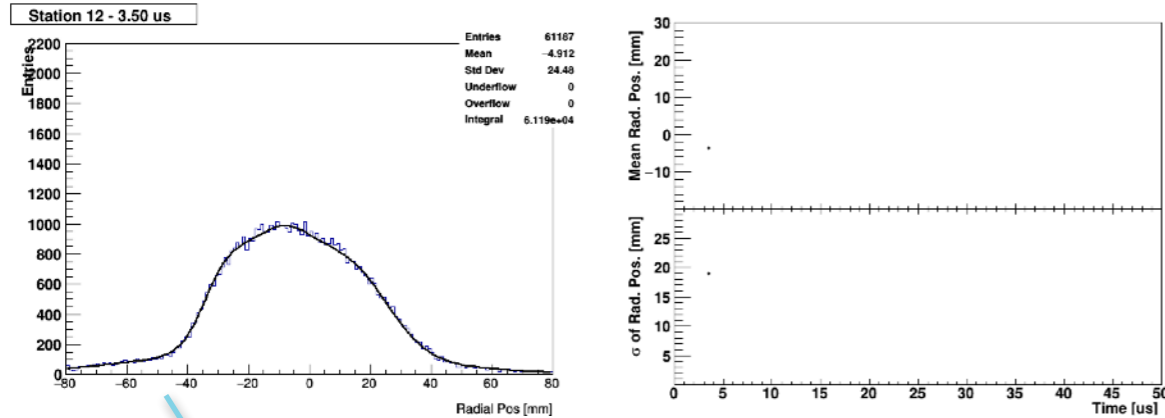
Frequency from detector point of view = $f_c - f_x$

$$x = x_e + A_x \cos(f_x t + \delta_x) \quad y = A_y \cos(f_y t + \delta_y)$$

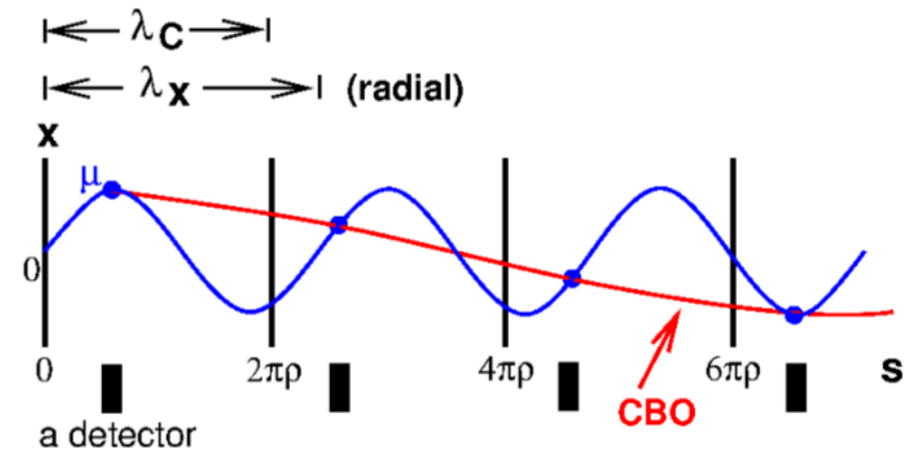
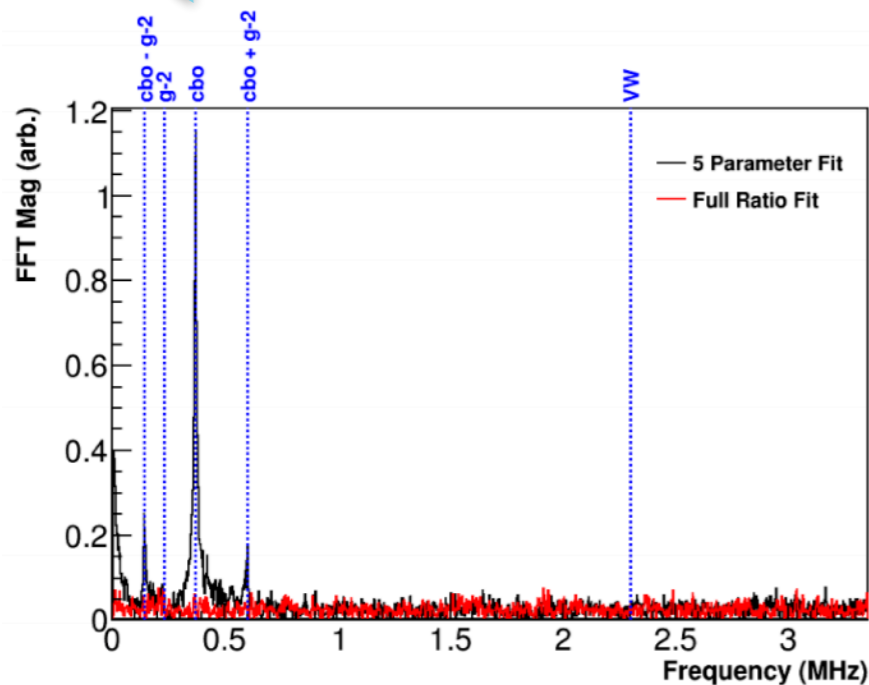
Simple Harmonic Motion

What is the beam doing after all these pulses and kicks

- CBO - Coherent Betatron Oscillation



Radial CBO movement



λ_x - radial wavelength

λ_c - cyclotron wavelength

Frequency from detector point of view = $f_c - f_x$

$$x = x_e + A_x \cos(f_x t + \delta_x) \quad y = A_y \cos(f_y t + \delta_y)$$

Simple Harmonic Motion

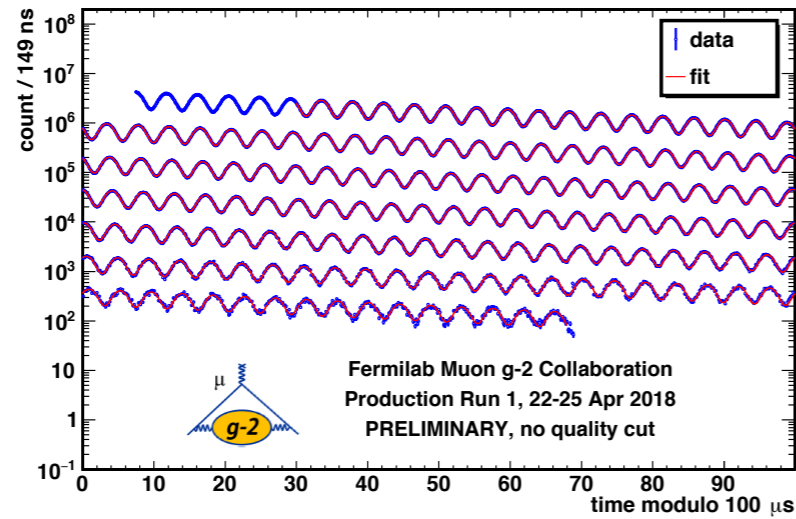
Gathered all the numbers!

$$a_{\mu} = \left(\frac{g_e}{2} \right) \left(\frac{\omega_a}{\langle \omega_p \rangle} \right) \left(\frac{\mu_p}{\mu_e} \right) \left(\frac{m_{\mu}}{m_e} \right)$$

0.26 ppt 3 ppb 22 ppb ⇒ 2017 CODATA

The diagram illustrates the components of the muon g-factor equation. Each term in the product is enclosed in a colored rounded rectangle: $\frac{g_e}{2}$ in green, $\frac{\omega_a}{\langle \omega_p \rangle}$ in orange, $\frac{\mu_p}{\mu_e}$ in blue, and $\frac{m_{\mu}}{m_e}$ in red. Colored arrows point from these boxes to a horizontal line below. Under the line, the uncertainties are listed: 0.26 ppt (green), 3 ppb (blue), and 22 ppb (red). To the right of the line, an arrow points to the text '2017 CODATA'.

Gathered all the numbers!



ω_a

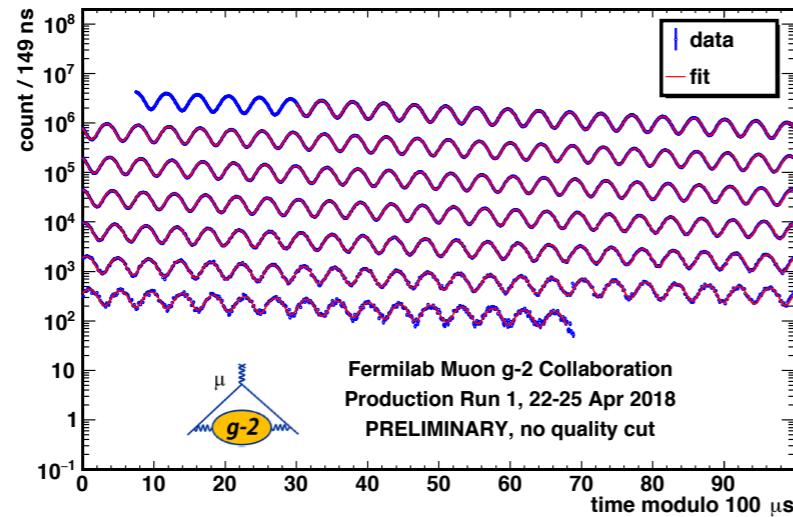
Extract from decay positron time spectra

$$N(t) = N_0 e^{-t/\tau_\mu} [1 + A \cos(\omega_a t + \phi)]$$

$$a_\mu = \left(\frac{g_e}{2} \right) \left(\frac{\omega_a}{\langle \omega_p \rangle} \right) \left(\frac{\mu_p}{\mu_e} \right) \left(\frac{m_\mu}{m_e} \right)$$

0.26 ppt
3 ppb
22 ppb
⇒ 2017 CODATA

Gathered all the numbers!

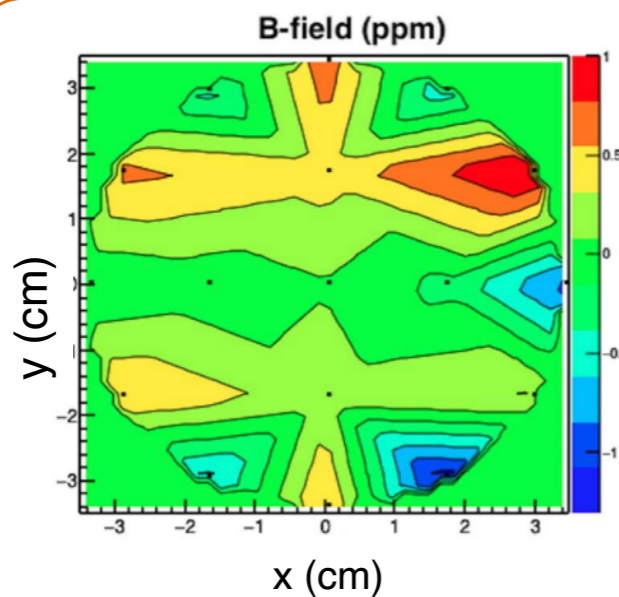


ω_a

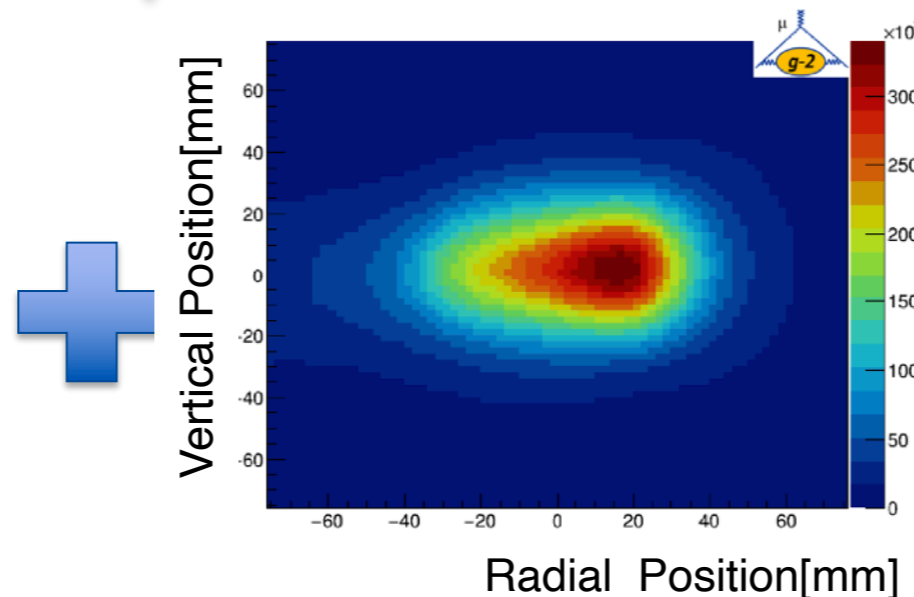
Extract from decay positron time spectra
 $N(t) = N_0 e^{-t/\tau_\mu} [1 + A \cos(\omega_a t + \phi)]$

$$a_\mu = \left(\frac{g_e}{2} \right) \left(\frac{\omega_a}{\langle \omega_p \rangle} \right) \left(\frac{\mu_p}{\mu_e} \right) \left(\frac{m_\mu}{m_e} \right)$$

0.26 ppt
3 ppb
22 ppb
⇒ 2017 CODATA



Map the magnetic field



Obtain muon distribution In the storage ring

$$\langle \omega_p \rangle \approx \omega_p \otimes \rho(r)$$

Average magnetic field weighted by muon distribution

ω_p : free proton precession frequency
 Using proton NMR $\hbar\omega_p = 2\mu_p B$

Systematics

$$a_{\mu} \propto \frac{f_{\text{clock}} \omega_a^m (1 + C_e + C_p + C_{ml} + C_{pa})}{f_{\text{calib}} \langle \omega'_p(x, y, \phi) \times M(x, y, \phi) \rangle (1 + B_k + B_q)}$$

f_{clock} •Blinded clock

ω_a^m •Measured precession frequency

C_e •Electric field correction

C_p •Pitch correction

C_{ml} •Muon loss correction

C_{pa} •Phase-acceptance correction

f_{calib} •Absolute magnetic field calibration

$\omega'_p(x, y, \phi)$ •Field tracking multipole distribution

$M(x, y, \phi)$ •Muon weighted multipole distributed

B_k •Transient field from the eddy current in kicker

B_q •Transient field from the quad charging

Phase Acceptance

$$a_{\mu} \propto \frac{f_{\text{clock}} \omega_a^m (1 + C_e + C_p + C_{ml} + C_{pa})}{f_{\text{calib}} \langle \omega'_p(x, y, \phi) \times M(x, y, \phi) \rangle (1 + B_k + B_q)}$$

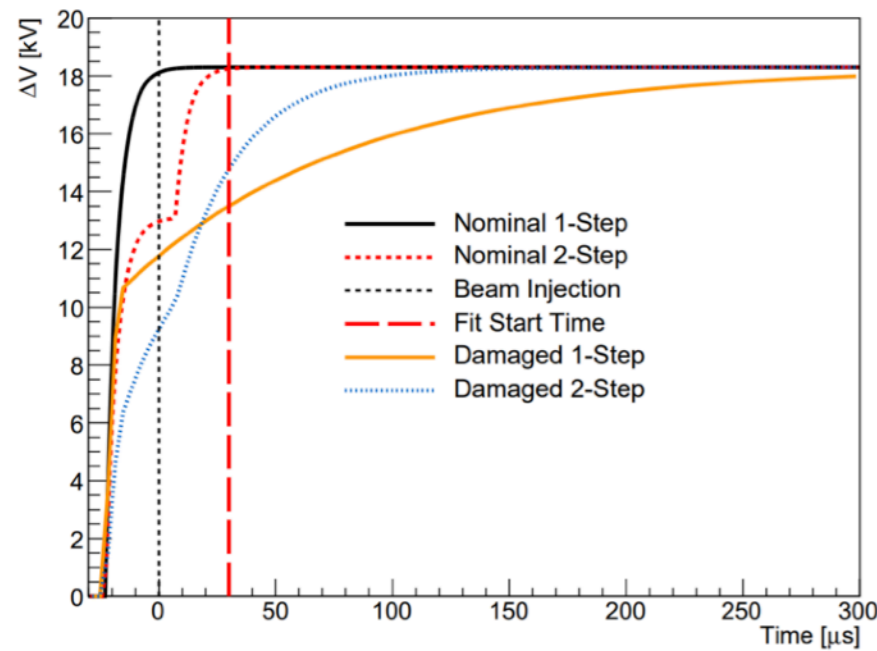
When there is a time dependent phase,

It shifts the ω_a !

Phase Acceptance

$$a_{\mu} \propto \frac{f_{\text{clock}} \omega_a^m (1 + C_e + C_p + C_{ml} + C_{pa})}{f_{\text{calib}} \langle \omega'_p(x, y, \phi) \times M(x, y, \phi) \rangle (1 + B_k + B_q)}$$

When there is a time dependent phase,
It shifts the ω_a !

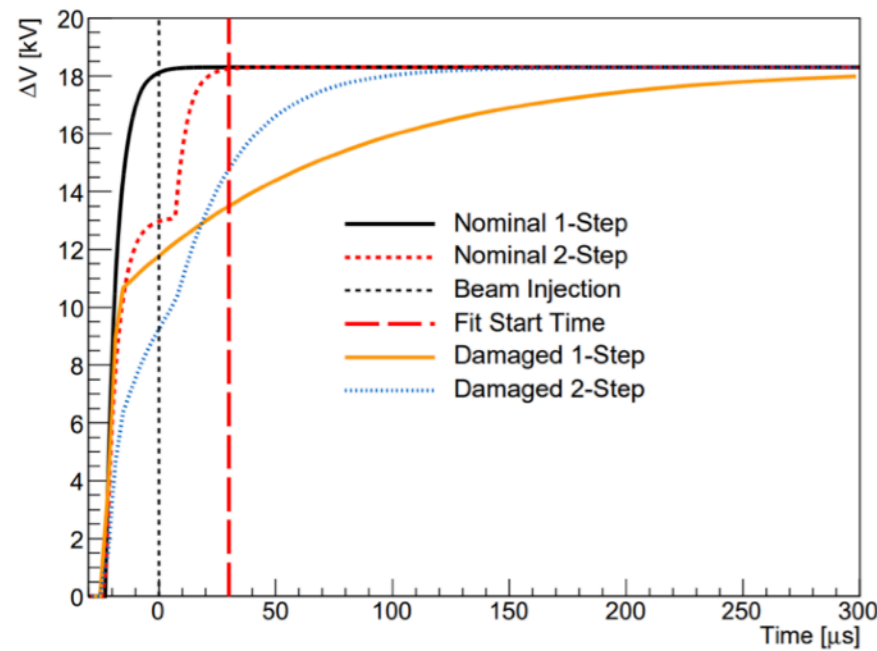


Due to damaged HV resistors; stored beam distribution was unstable.

Phase Acceptance

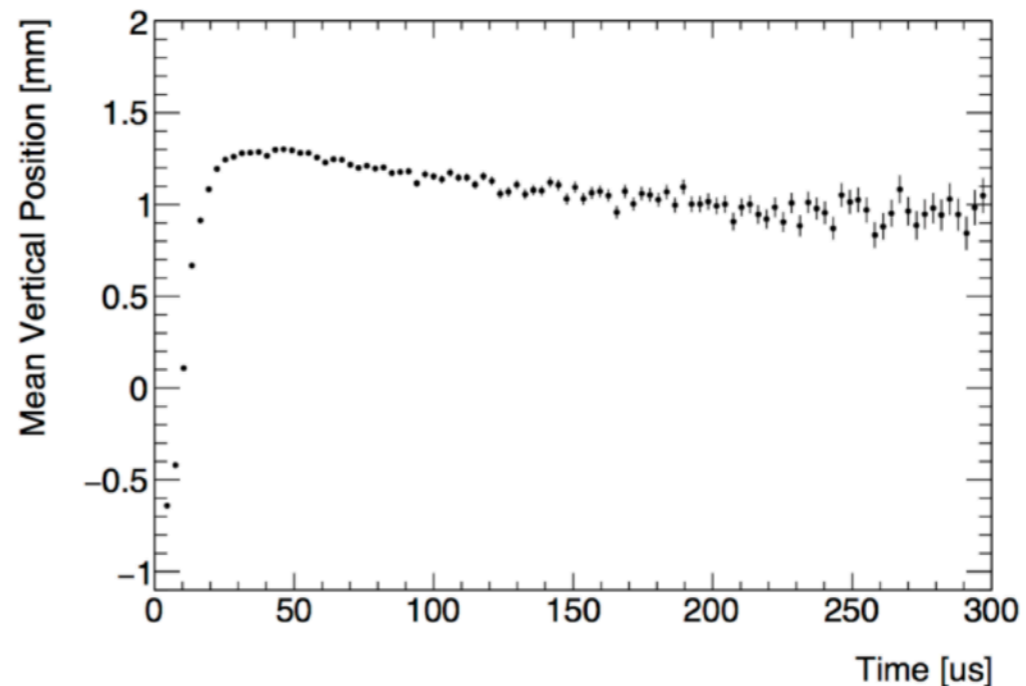
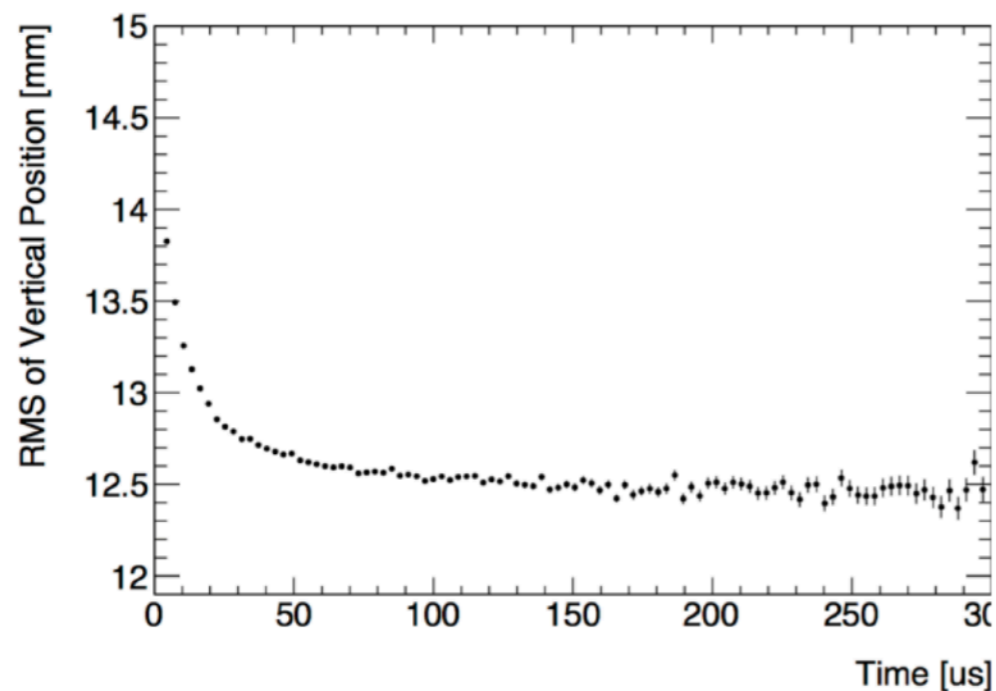
$$a_{\mu} \propto \frac{f_{\text{clock}} \omega_a^m (1 + C_e + C_p + C_{ml} + C_{pa})}{f_{\text{calib}} \langle \omega'_p(x, y, \phi) \times M(x, y, \phi) \rangle (1 + B_k + B_q)}$$

When there is a time dependent phase,
It shifts the ω_a !



Due to damaged HV resistors; stored beam distribution was unstable.

It caused a time dependent phase
Beam vertical mean and width changed



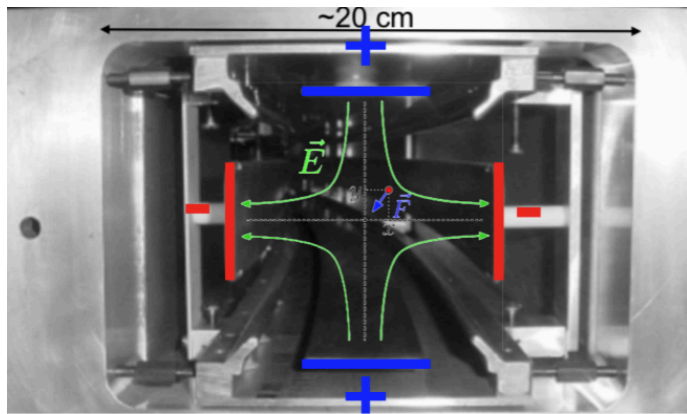
ESQ Transients

$$a_{\mu} \propto \frac{f_{\text{clock}} \omega_a^m (1 + C_e + C_p + C_{ml} + C_{pa})}{f_{\text{calib}} \langle \omega'_p(x, y, \phi) \times M(x, y, \phi) \rangle (1 + B_k + B_q)}$$

ESQ Transients

$$a_{\mu} \propto \frac{f_{\text{clock}} \omega_a^m (1 + C_e + C_p + C_{ml} + C_{pa})}{f_{\text{calib}} \langle \omega'_p(x, y, \phi) \times M(x, y, \phi) \rangle (1 + B_k + B_q)}$$

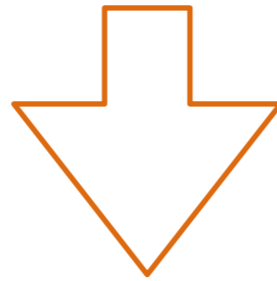
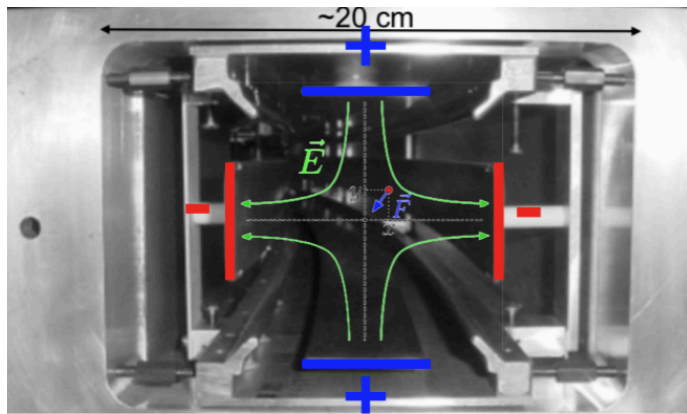
Quads charging and discharging cause mechanical vibration



ESQ Transients

$$a_{\mu} \propto \frac{f_{\text{clock}} \omega_a^m (1 + C_e + C_p + C_{ml} + C_{pa})}{f_{\text{calib}} \langle \omega'_p(x, y, \phi) \times M(x, y, \phi) \rangle (1 + B_k + B_q)}$$

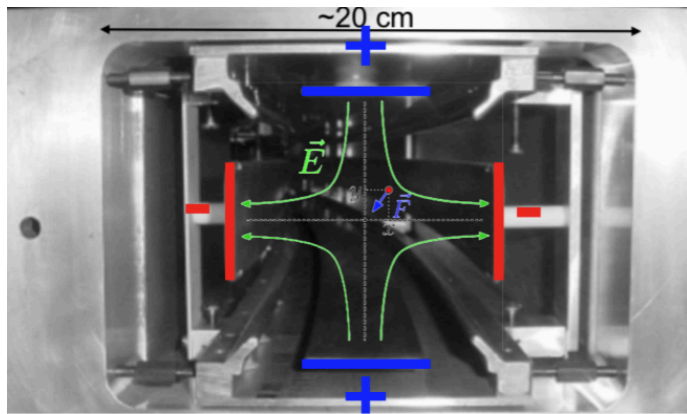
Quads charging and discharging cause mechanical vibration



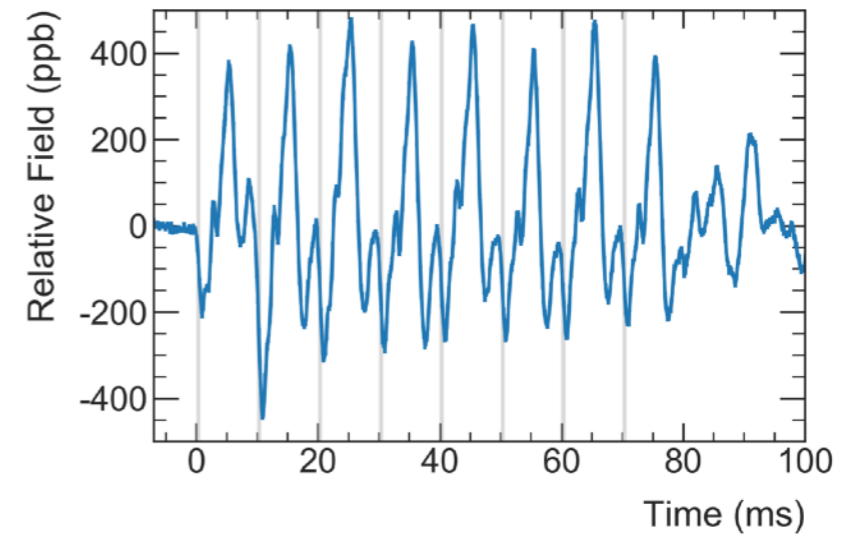
ESQ Transients

$$a_{\mu} \propto \frac{f_{\text{clock}} \omega_a^m (1 + C_e + C_p + C_{ml} + C_{pa})}{f_{\text{calib}} \langle \omega'_p(x, y, \phi) \times M(x, y, \phi) \rangle (1 + B_k + B_q)}$$

Quads charging and discharging cause mechanical vibration



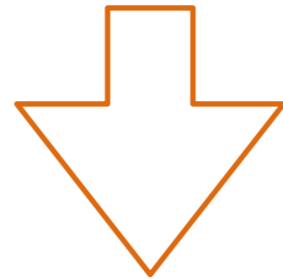
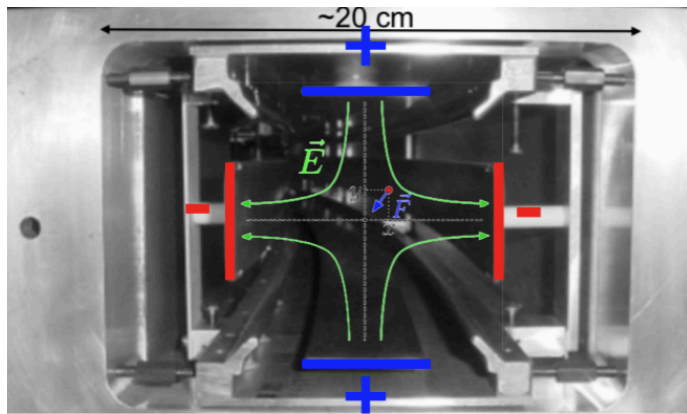
Field Perturbation



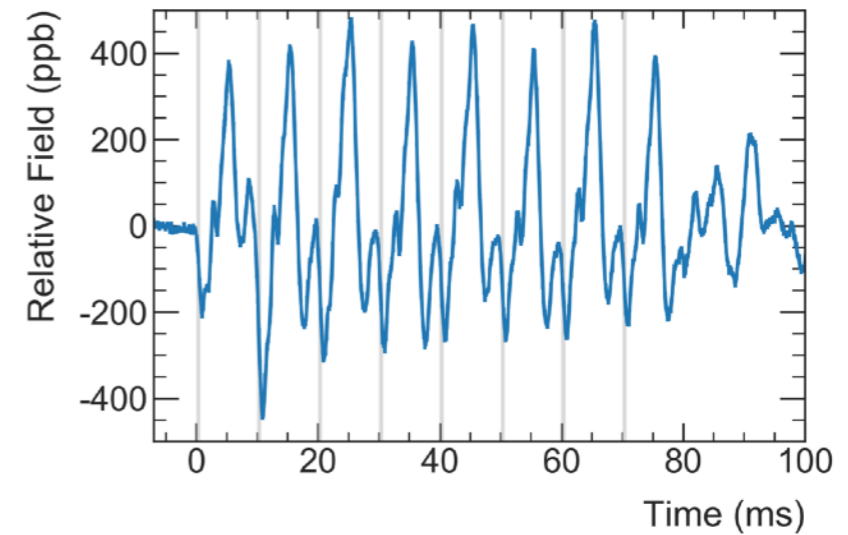
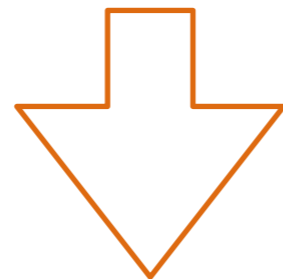
ESQ Transients

$$a_{\mu} \propto \frac{f_{\text{clock}} \omega_a^m (1 + C_e + C_p + C_{ml} + C_{pa})}{f_{\text{calib}} \langle \omega'_p(x, y, \phi) \times M(x, y, \phi) \rangle (1 + B_k + B_q)}$$

Quads charging and discharging cause mechanical vibration



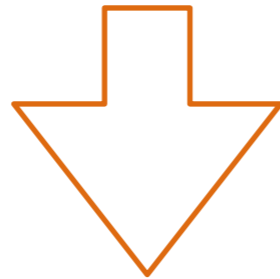
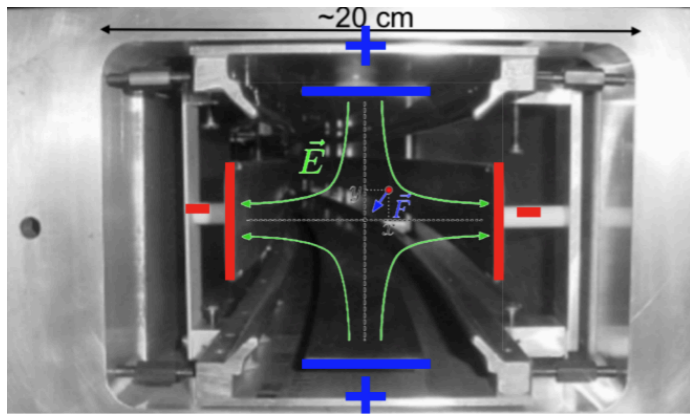
Field Perturbation



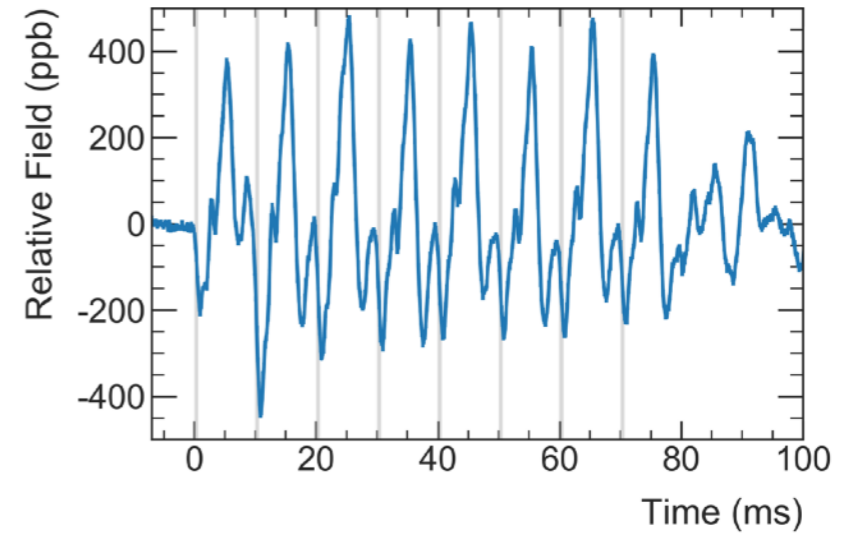
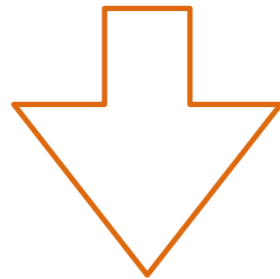
ESQ Transients

$$a_{\mu} \propto \frac{f_{\text{clock}} \omega_a^m (1 + C_e + C_p + C_{ml} + C_{pa})}{f_{\text{calib}} \langle \omega'_p(x, y, \phi) \times M(x, y, \phi) \rangle (1 + B_k + B_q)}$$

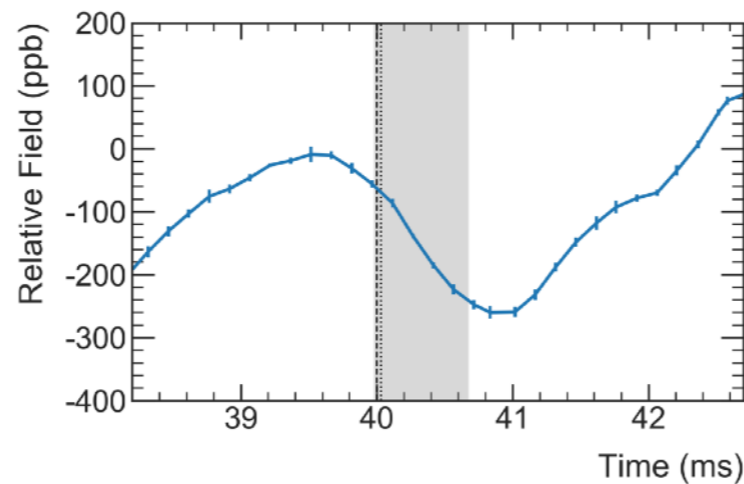
Quads charging and discharging cause mechanical vibration



Field Perturbation



Measure the field with special NMR probes and map the effect!



E-field and Pitch Correction

$$a_\mu \propto \frac{f_{\text{clock}} \omega_a^m (1 + C_e + C_p + C_{ml} + C_{pa})}{f_{\text{calib}} \langle \omega'_p(x, y, \phi) \times M(x, y, \phi) \rangle (1 + B_k + B_q)}$$

$$\vec{\omega}_a = \frac{e}{m} \left[a_\mu \vec{B} - a_\mu \frac{\gamma}{\gamma+1} (\vec{\beta} \cdot \vec{B}) \vec{\beta} - \left(a_\mu - \frac{1}{\gamma^2-1} \right) \vec{\beta} \times \vec{E} \right]$$

E-field and Pitch Correction

$$a_\mu \propto \frac{f_{\text{clock}} \omega_a^m (1 + C_e + C_p + C_{ml} + C_{pa})}{f_{\text{calib}} \langle \omega'_p(x, y, \phi) \times M(x, y, \phi) \rangle (1 + B_k + B_q)}$$

Not all of the muons are at magic momentum!

There is a 0.5% momentum acceptance

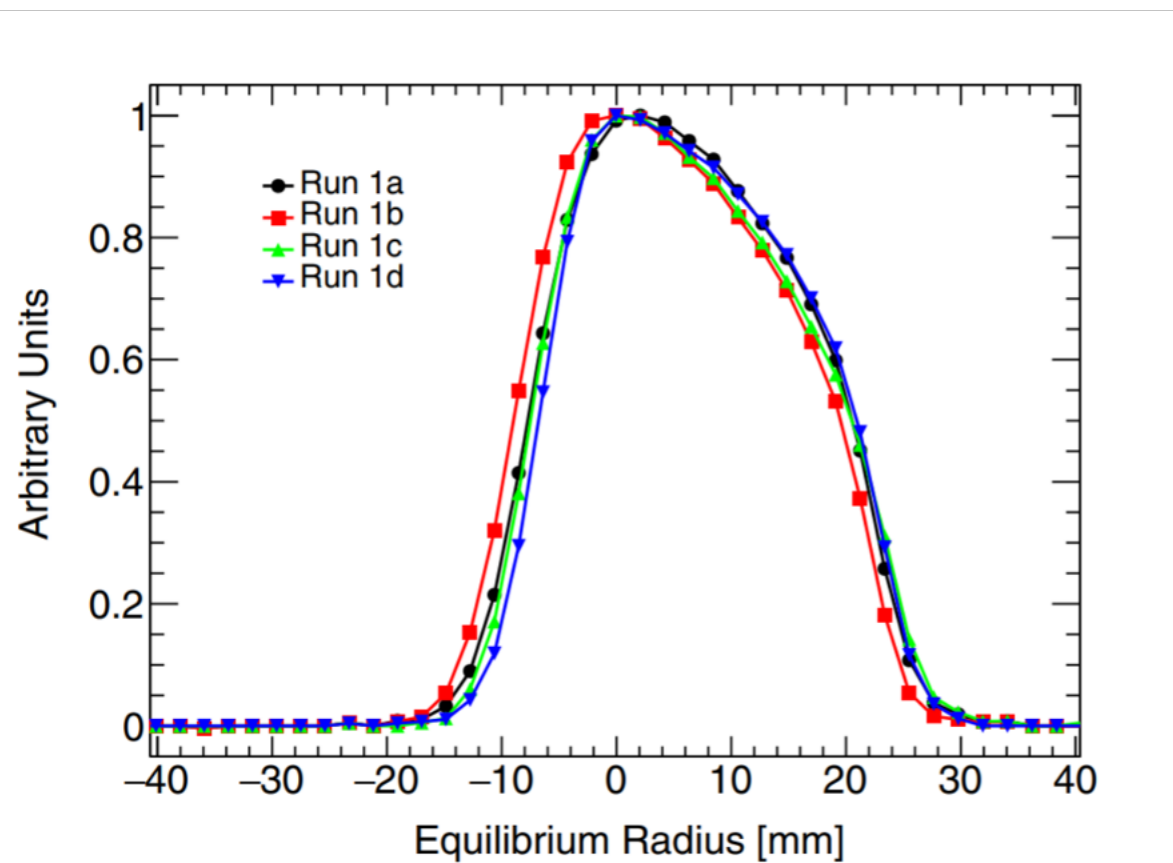
$$\vec{\omega}_a = \frac{e}{m} \left[a_\mu \vec{B} - a_\mu \frac{\gamma}{\gamma+1} (\vec{\beta} \cdot \vec{B}) \vec{\beta} - \left(a_\mu - \frac{1}{\gamma^2-1} \right) \vec{\beta} \times \vec{E} \right]$$

E-field and Pitch Correction

$$a_\mu \propto \frac{f_{\text{clock}} \omega_a^m (1 + C_e + C_p + C_{ml} + C_{pa})}{f_{\text{calib}} \langle \omega'_p(x, y, \phi) \times M(x, y, \phi) \rangle (1 + B_k + B_q)}$$

Not all of the muons are at magic momentum!
There is a 0.5% momentum acceptance

$$\vec{\omega}_a = \frac{e}{m} \left[a_\mu \vec{B} - a_\mu \frac{\gamma}{\gamma+1} (\vec{\beta} \cdot \vec{B}) \vec{\beta} - \left(a_\mu - \frac{1}{\gamma^2-1} \right) \vec{\beta} \times \vec{E} \right]$$

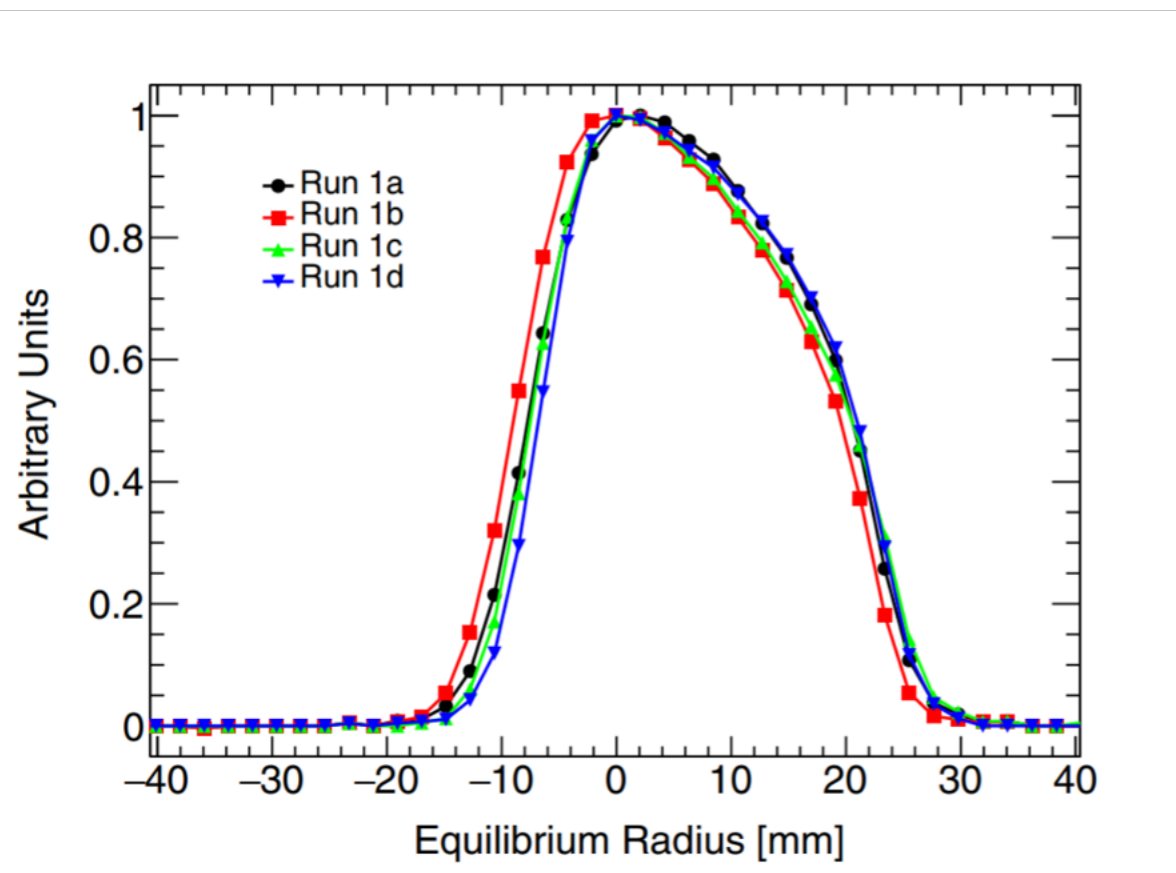


E-field and Pitch Correction

$$a_\mu \propto \frac{f_{\text{clock}} \omega_a^m (1 + C_e + C_p + C_{ml} + C_{pa})}{f_{\text{calib}} \langle \omega'_p(x, y, \phi) \times M(x, y, \phi) \rangle (1 + B_k + B_q)}$$

Not all of the muons are at magic momentum!
There is a 0.5% momentum acceptance

~~$$\vec{\omega}_a = \frac{e}{m} \left[a_\mu \vec{B} - a_\mu \frac{\gamma}{\gamma+1} (\vec{\beta} \cdot \vec{B}) \vec{\beta} - \left(a_\mu - \frac{1}{\gamma^2-1} \right) \vec{\beta} \times \vec{E} \right]$$~~



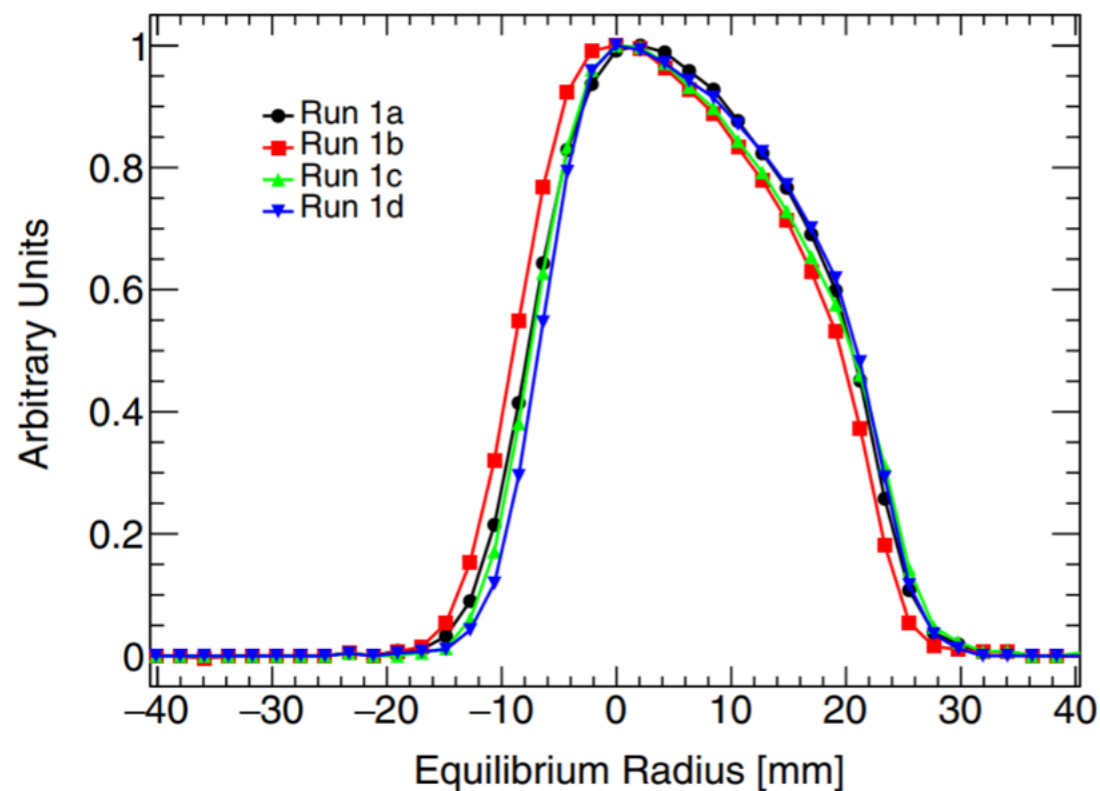
Vertical betatron oscillations cause non-zero average value for $\vec{\beta} \cdot \vec{B}$

E-field and Pitch Correction

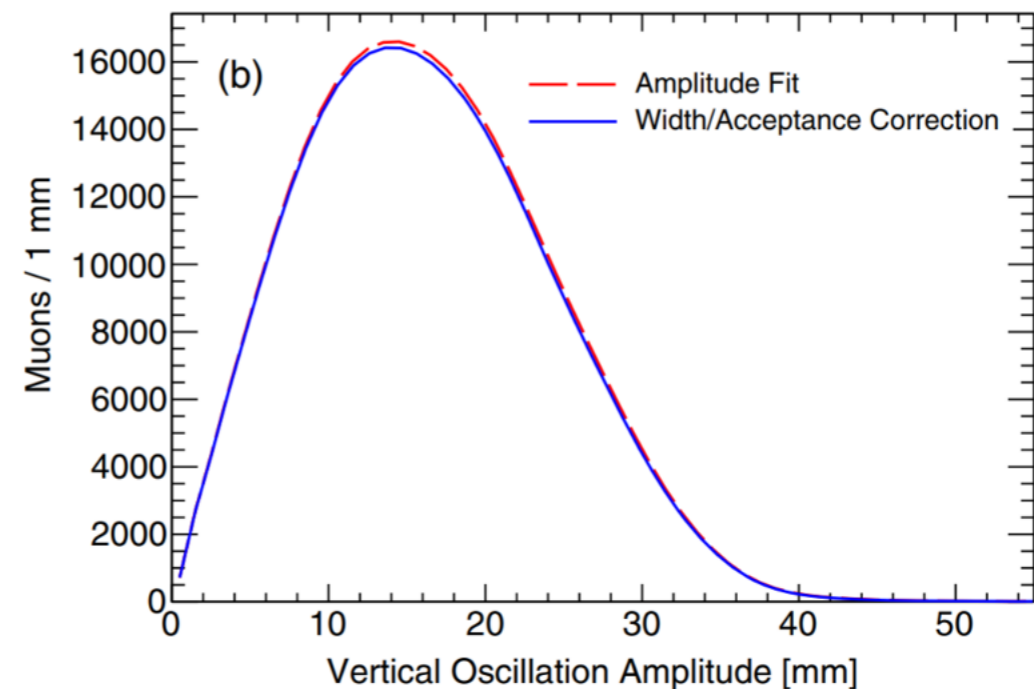
$$a_\mu \propto \frac{f_{\text{clock}} \omega_a^m (1 + C_e + C_p + C_{ml} + C_{pa})}{f_{\text{calib}} \langle \omega'_p(x, y, \phi) \times M(x, y, \phi) \rangle (1 + B_k + B_q)}$$

Not all of the muons are at magic momentum!
There is a 0.5% momentum acceptance

~~$$\vec{\omega}_a = \frac{e}{m} \left[a_\mu \vec{B} - a_\mu \frac{\gamma}{\gamma+1} (\vec{\beta} \cdot \vec{B}) \vec{\beta} - \left(a_\mu - \frac{1}{\gamma^2-1} \right) \vec{\beta} \times \vec{E} \right]$$~~



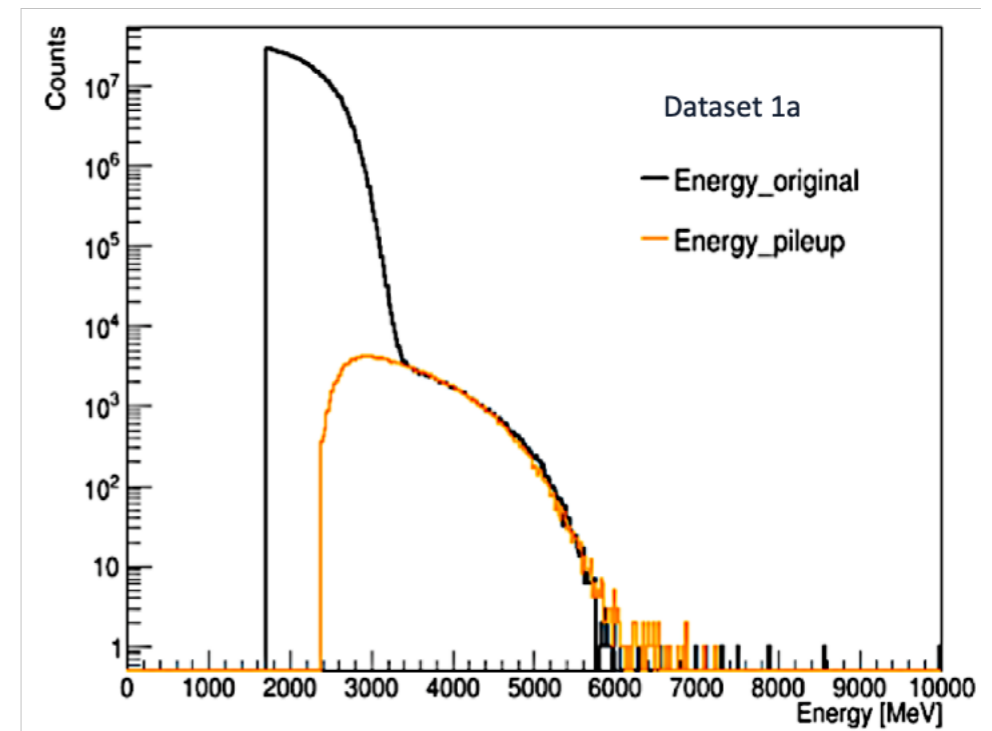
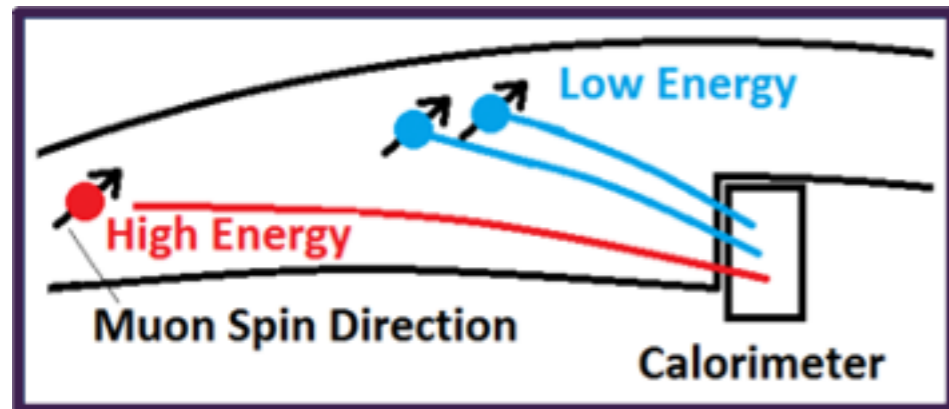
Vertical betatron oscillations cause non-zero average value for $\vec{\beta} \cdot \vec{B}$



Pileup

$$a_{\mu} \propto \frac{f_{\text{clock}} \omega_a^m (1 + C_e + C_p + C_{ml} + C_{pa})}{f_{\text{calib}} \langle \omega'_p(x, y, \phi) \times M(x, y, \phi) \rangle (1 + B_k + B_q)}$$

- Pileup is one of the systematics that modulated precession frequency.
- When more than two positrons hit the detector at the same time and place, they could be treated as a single pulse.
- That distorts the time and energy spectrum!

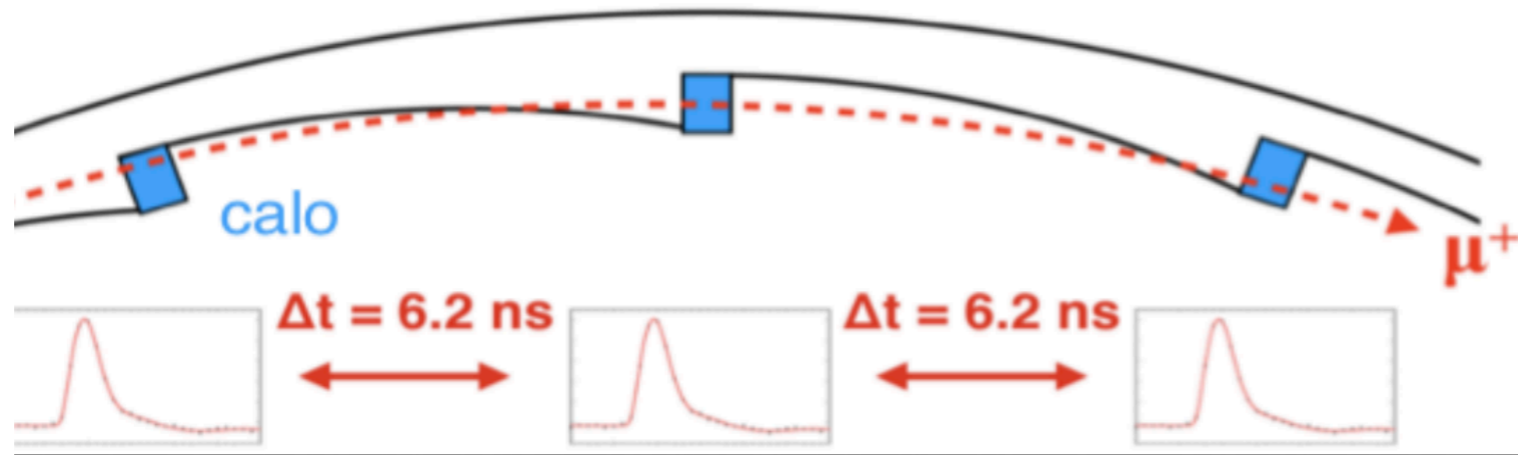


Muon Loss

$$a_{\mu} \propto \frac{f_{\text{clock}} \omega_a^m (1 + C_e + C_p + C_{ml} + C_{pa})}{f_{\text{calib}} \langle \omega'_p(x, y, \phi) \times M(x, y, \phi) \rangle (1 + B_k + B_q)}$$

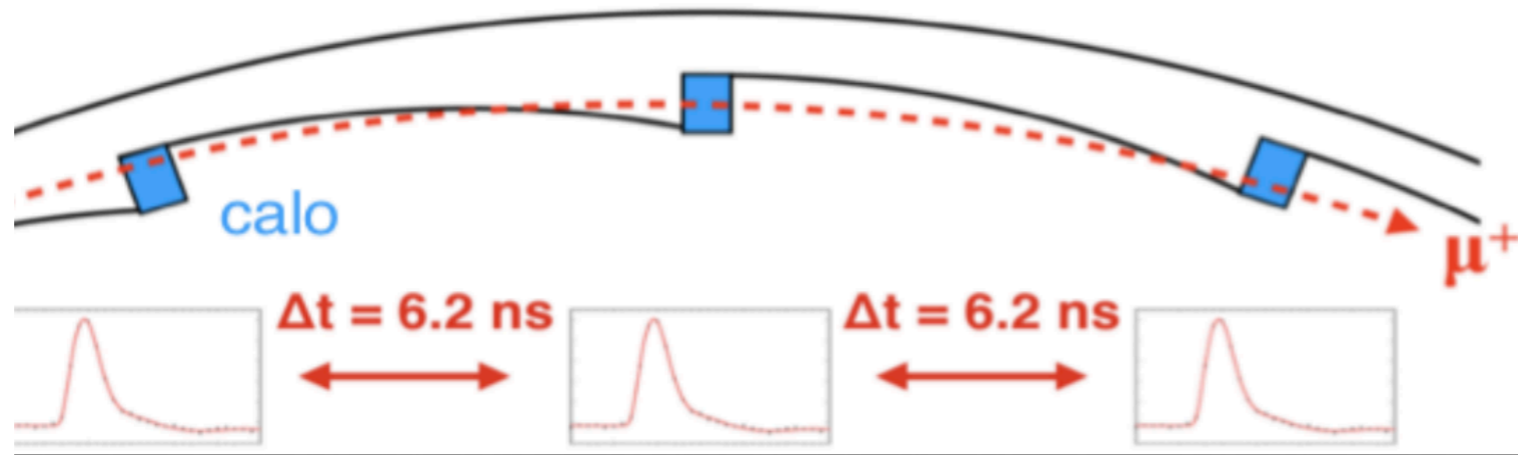
Muon Loss

$$a_{\mu} \propto \frac{f_{\text{clock}} \omega_a^m (1 + C_e + C_p + C_{ml} + C_{pa})}{f_{\text{calib}} \langle \omega'_p(x, y, \phi) \times M(x, y, \phi) \rangle (1 + B_k + B_q)}$$



Muon Loss

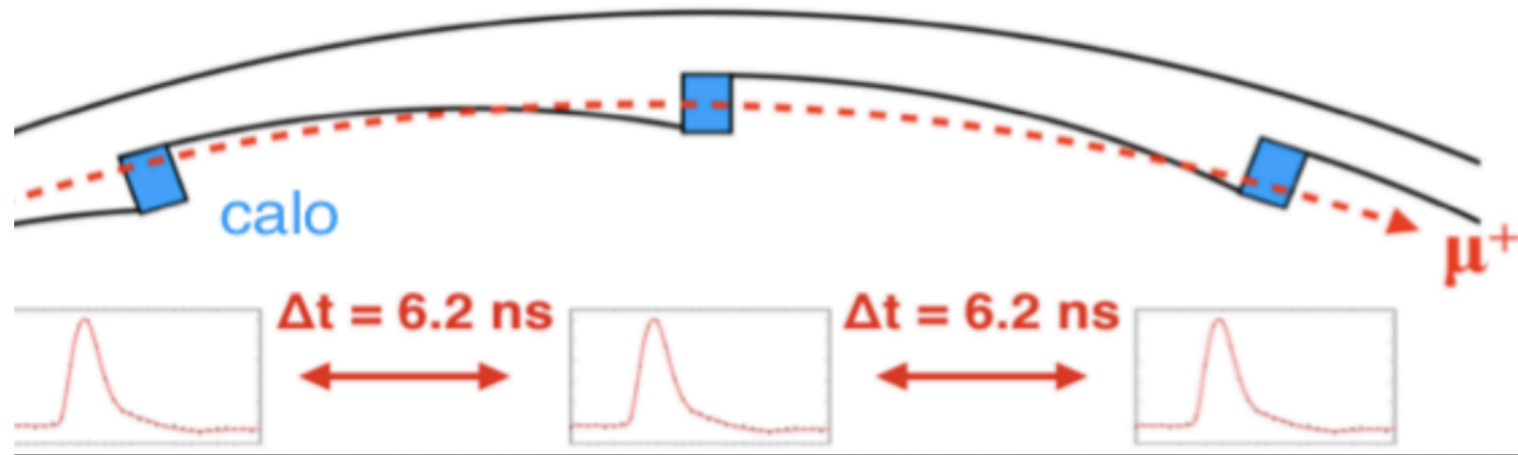
$$a_{\mu} \propto \frac{f_{\text{clock}} \omega_a^m (1 + C_e + C_p + C_{ml} + C_{pa})}{f_{\text{calib}} \langle \omega'_p(x, y, \phi) \times M(x, y, \phi) \rangle (1 + B_k + B_q)}$$



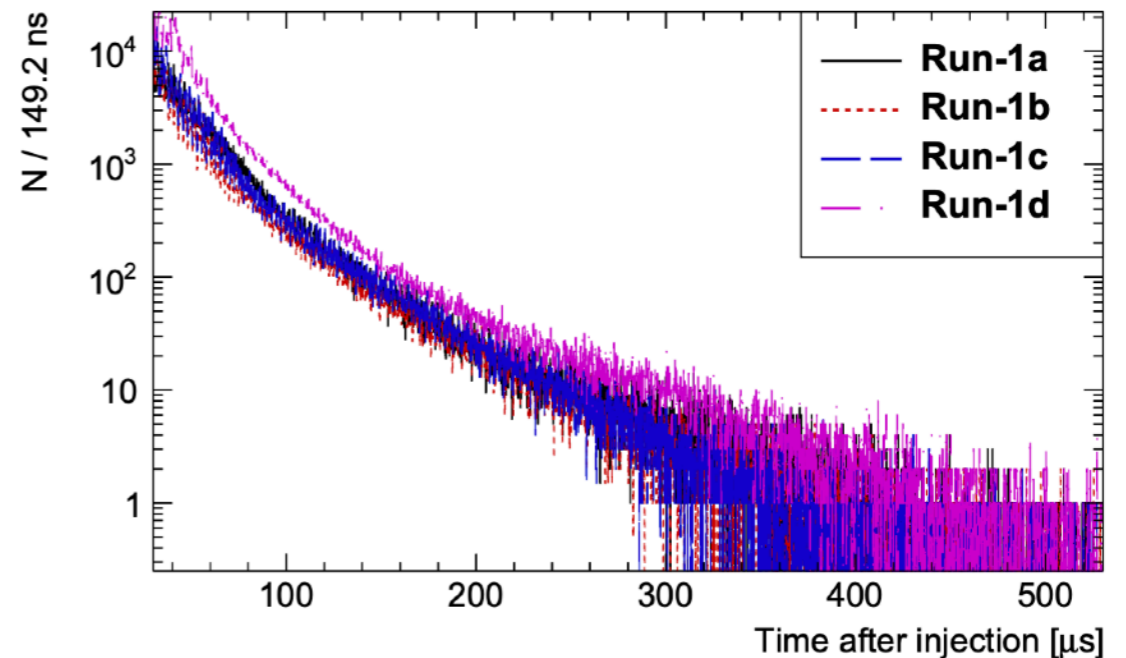
- Muons that were scattered from different materials before decaying and then punch through multiple calorimeters.
- They have different phase than stored muons so they modulate ω_a , producing a systematic error.
- We need to identify them in the data!

Muon Loss

$$a_{\mu} \propto \frac{f_{\text{clock}} \omega_a^m (1 + C_e + C_p + C_{ml} + C_{pa})}{f_{\text{calib}} \langle \omega'_p(x, y, \phi) \times M(x, y, \phi) \rangle (1 + B_k + B_q)}$$



- Muons that were scattered from different materials before decaying and then punch through multiple calorimeters.
- They have different phase than stored muons so they modulate ω_a , producing a systematic error.
- We need to identify them in the data!



Crunching the numbers...

| Quantity | Correction Terms (ppb) | Uncertainty (ppb) |
|---|---------------------------|----------------------|
| ω_a (statistical) | – | 434 |
| ω_a (systematic) | – | 56 |
| C_e | 489 | 53 |
| C_p | 180 | 13 |
| C_{ml} | -11 | 5 |
| C_{pa} | -158 | 75 |
| $f_{\text{calib}} \langle \omega'_p(x, y, \phi) \times M(x, y, \phi) \rangle$ | – | 56 |
| B_k | -27 | 37 |
| B_q | -17 | 92 |
| $\mu'_p(34.7^\circ)/\mu_e$ | – | 10 |
| m_μ/m_e | – | 22 |
| $g_e/2$ | – | 0 |
| Total systematic | – | 157 |
| Total fundamental factors | – | 25 |
| Totals | 544 | 462 |

Dominated by statistical uncertainty

Crunching the numbers...

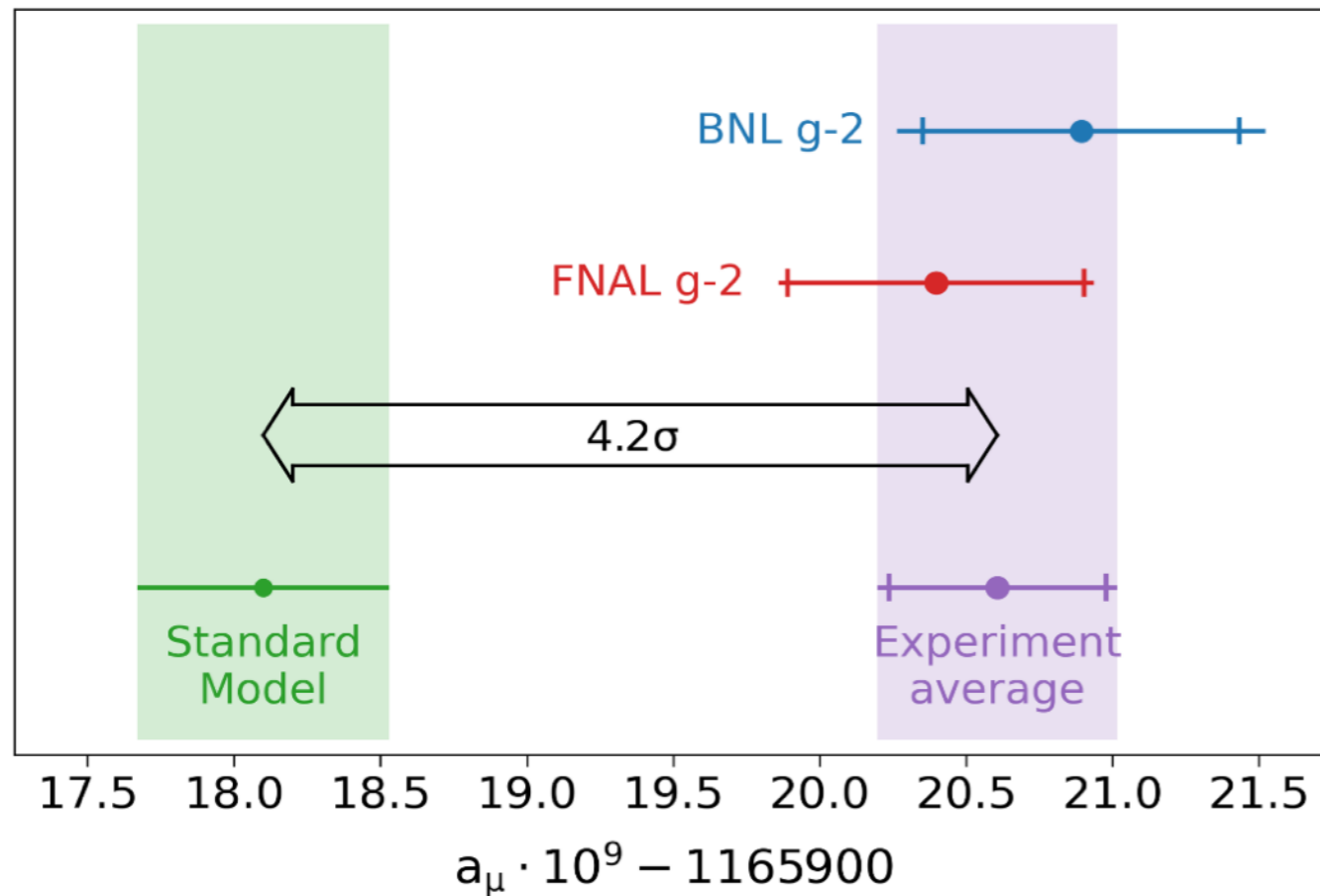
| Quantity | Correction Terms (ppb) | Uncertainty (ppb) | |
|---|---------------------------|----------------------|---|
| ω_a (statistical) | – | 434 | |
| ω_a (systematic) | – | 56 | |
| C_e | 489 | 53 | |
| C_p | 180 | 13 | |
| C_{ml} | -11 | 5 | |
| C_{pa} | -158 | 75 | ← Systematics dominated by |
| $f_{\text{calib}} \langle \omega'_p(x, y, \phi) \times M(x, y, \phi) \rangle$ | – | 56 | |
| B_k | -27 | 37 | |
| B_q | -17 | 92 | ← PA and Field Transients |
| $\mu'_p(34.7^\circ)/\mu_e$ | – | 10 | |
| m_μ/m_e | – | 22 | |
| $g_e/2$ | – | 0 | |
| Total systematic | – | 157 | *Nearly half of BNL |
| Total fundamental factors | – | 25 | *Will be even better for Run-2 and beyond |
| Totals | 544 | 462 | |

Crunching the numbers...

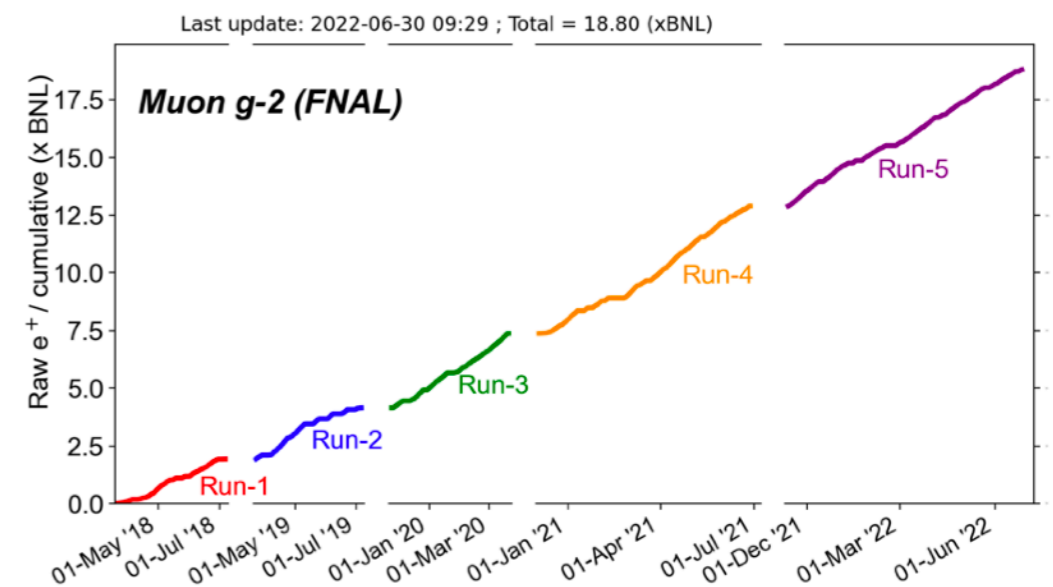
| Quantity | Correction Terms (ppb) | Uncertainty (ppb) |
|---|---------------------------|----------------------|
| ω_a (statistical) | – | 434 |
| ω_a (systematic) | – | 56 |
| C_e | 489 | 53 |
| C_p | 180 | 13 |
| C_{ml} | -11 | 5 |
| C_{pa} | -158 | 75 |
| $f_{\text{calib}} \langle \omega'_p(x, y, \phi) \times M(x, y, \phi) \rangle$ | – | 56 |
| B_k | -27 | 37 |
| B_q | -17 | 92 |
| $\mu'_p(34.7^\circ)/\mu_e$ | – | 10 |
| m_μ/m_e | – | 22 |
| $g_e/2$ | – | 0 |
| Total systematic | – | 157 |
| Total fundamental factors | – | 25 |
| Totals | 544 | 462 |

Enormous effort to evaluate every number !

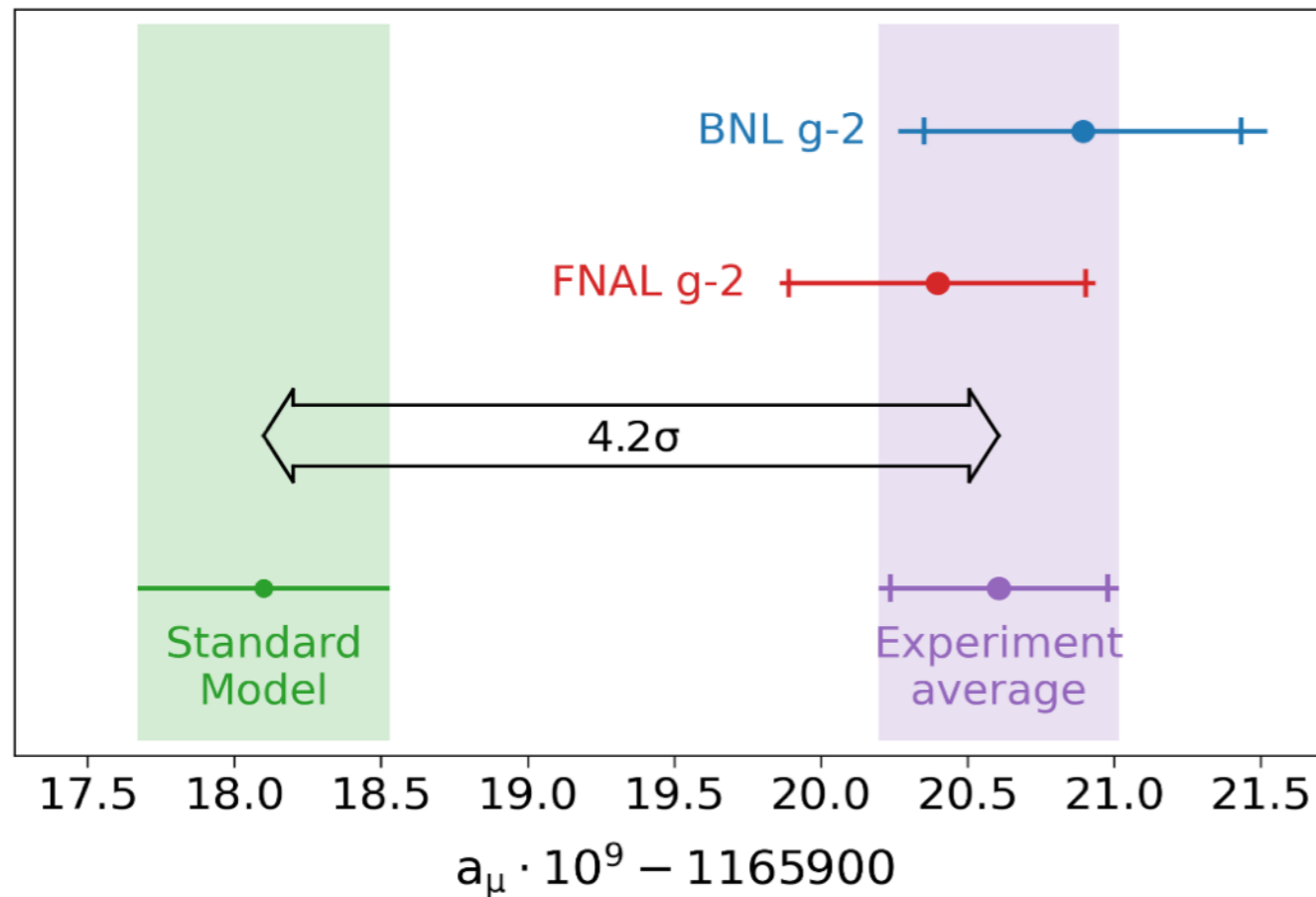
Experimental Result and the Comparison



- ✓ FNAL determined anomaly with 460 ppb precision
- ✓ Nothing was found that indicated contradiction with BNL results
- ✓ 15% smaller error
- ✓ Good agreement

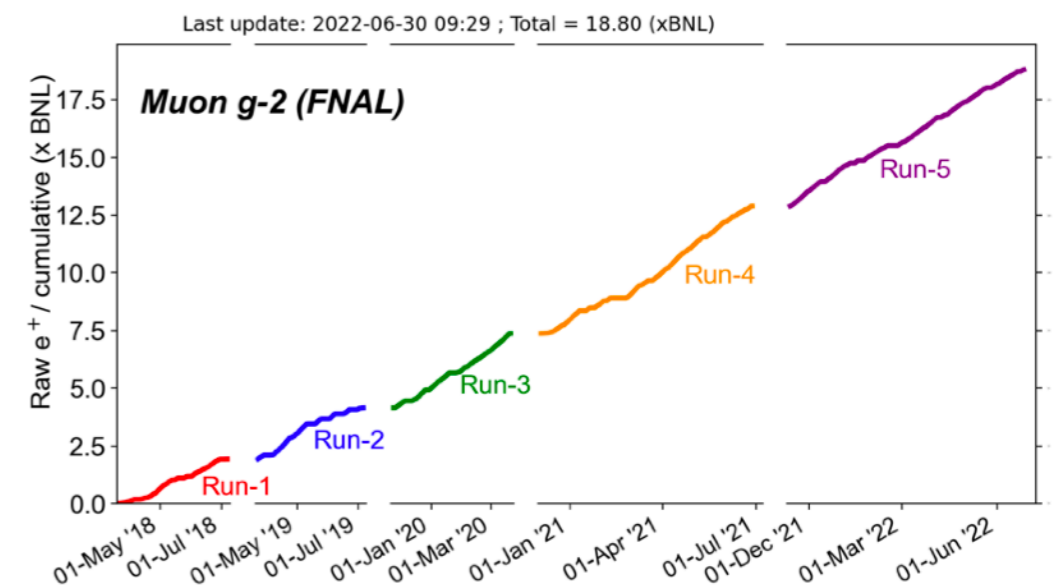


Experimental Result and the Comparison

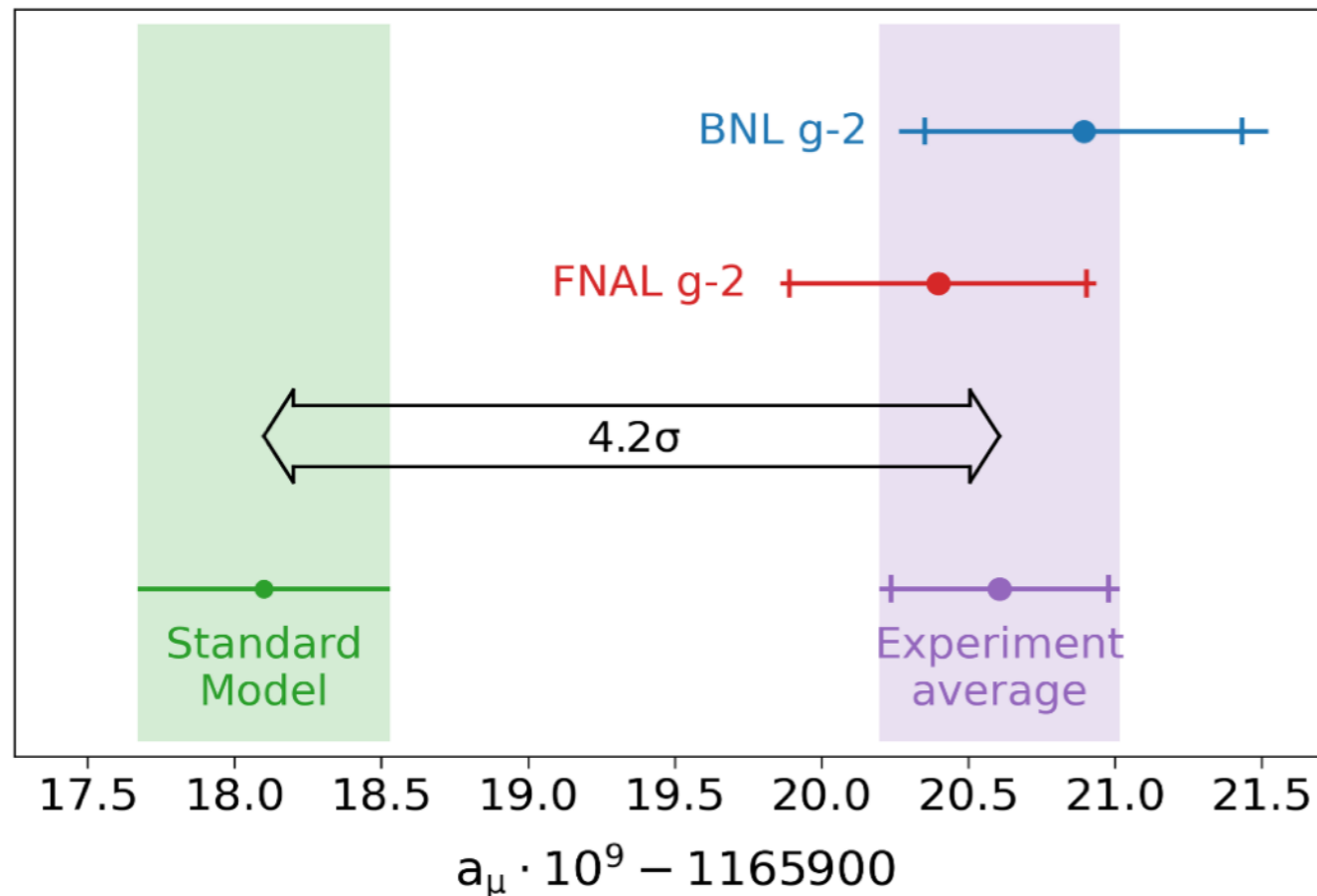


$$a_{\mu} \text{ (BNL)} = 116\,592\,089(63) \times 10^{-11} \text{ (540 ppb)}$$

- ✓ FNAL determined anomaly with 460 ppb precision
- ✓ Nothing was found that indicated contradiction with BNL results
- ✓ 15% smaller error
- ✓ Good agreement



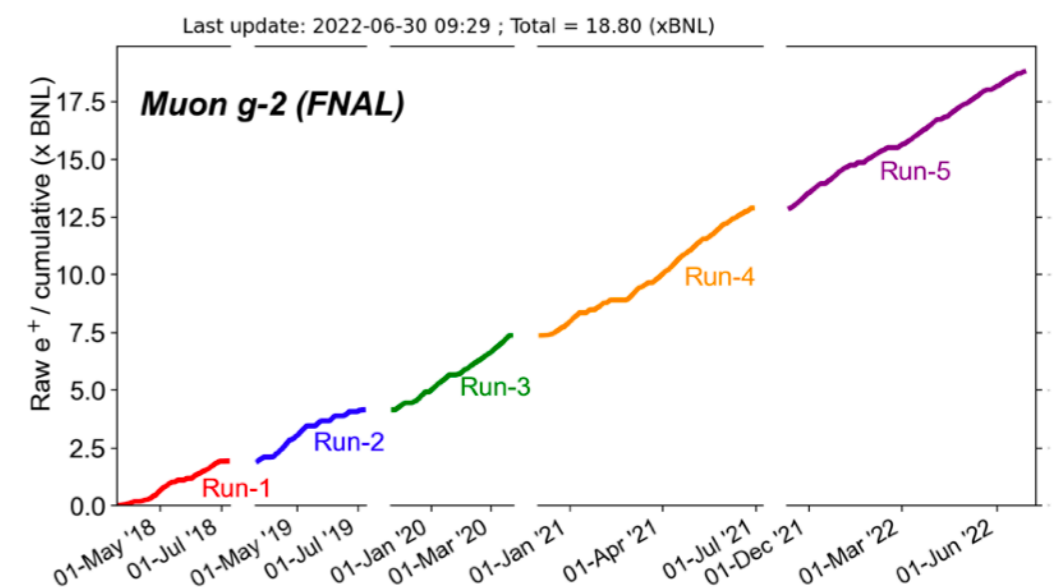
Experimental Result and the Comparison



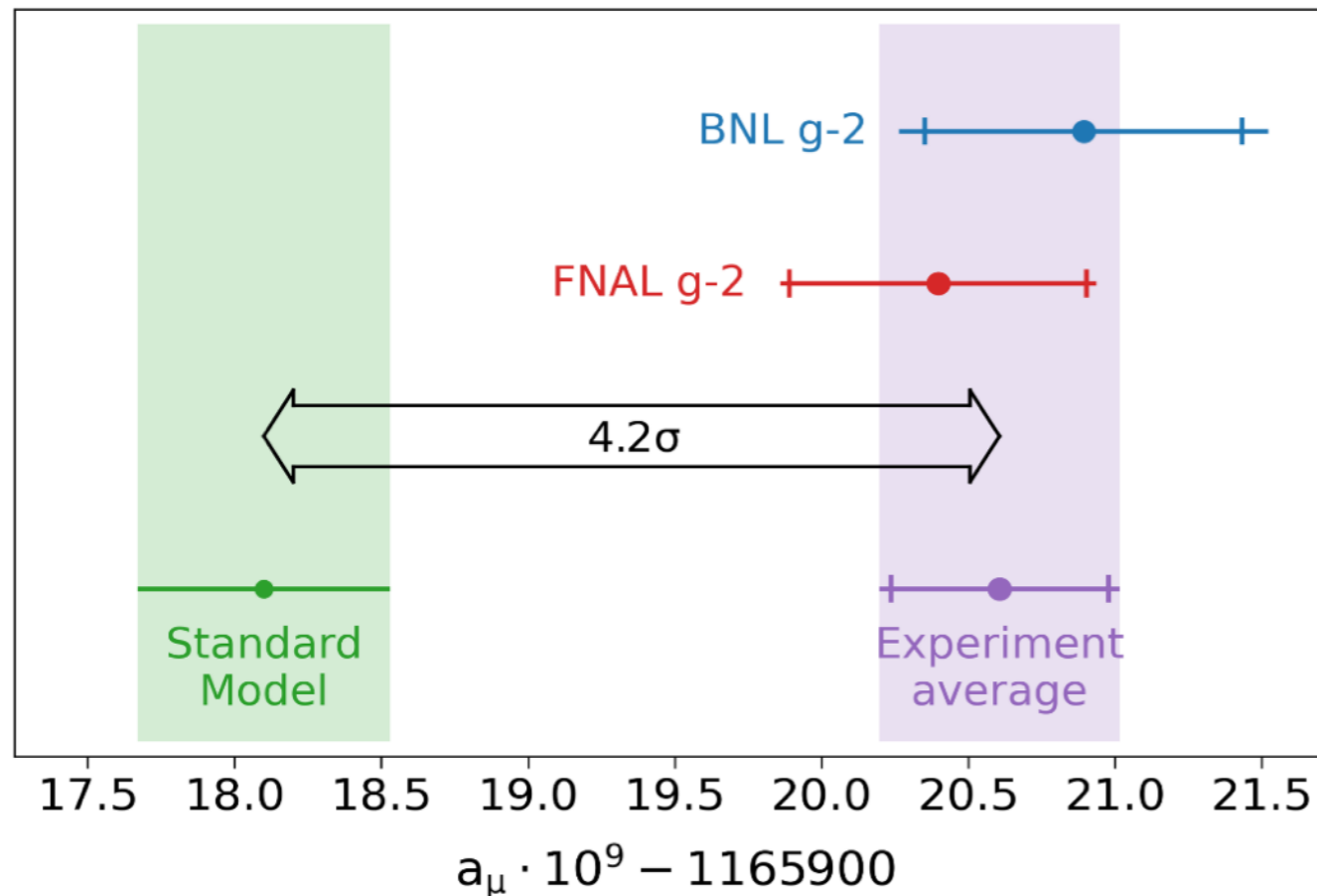
$$a_{\mu} \text{ (BNL)} = 116\,592\,089(63) \times 10^{-11} \text{ (540 ppb)}$$

$$a_{\mu} \text{ (FNAL)} = 116\,592\,040(54) \times 10^{-11} \text{ (460 ppb)}$$

- ✓ FNAL determined anomaly with 460 ppb precision
- ✓ Nothing was found that indicated contradiction with BNL results
- ✓ 15% smaller error
- ✓ Good agreement



Experimental Result and the Comparison

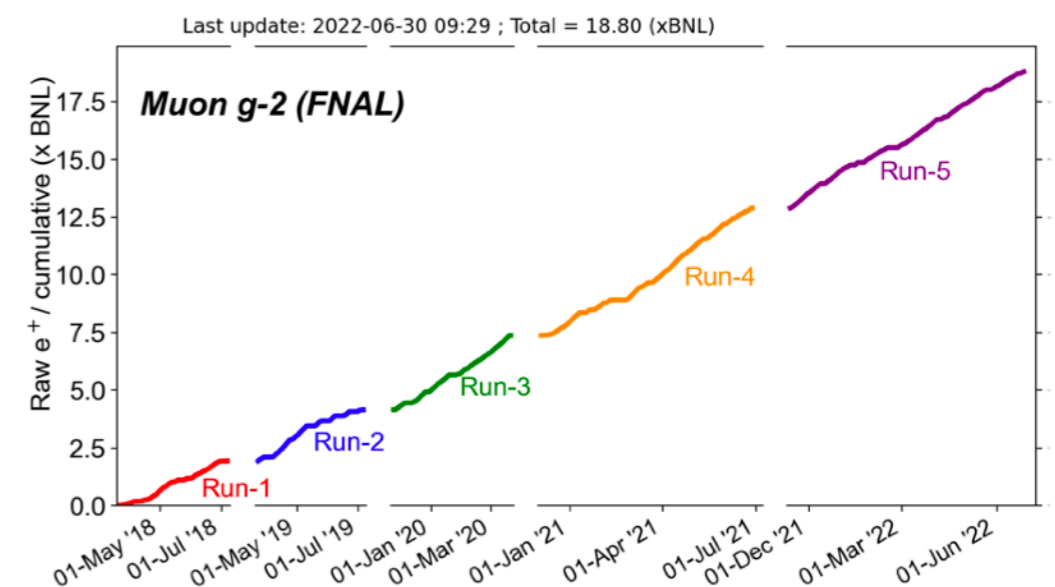


$$a_\mu (\text{BNL}) = 116\,592\,089(63) \times 10^{-11} \text{ (540 ppb)}$$

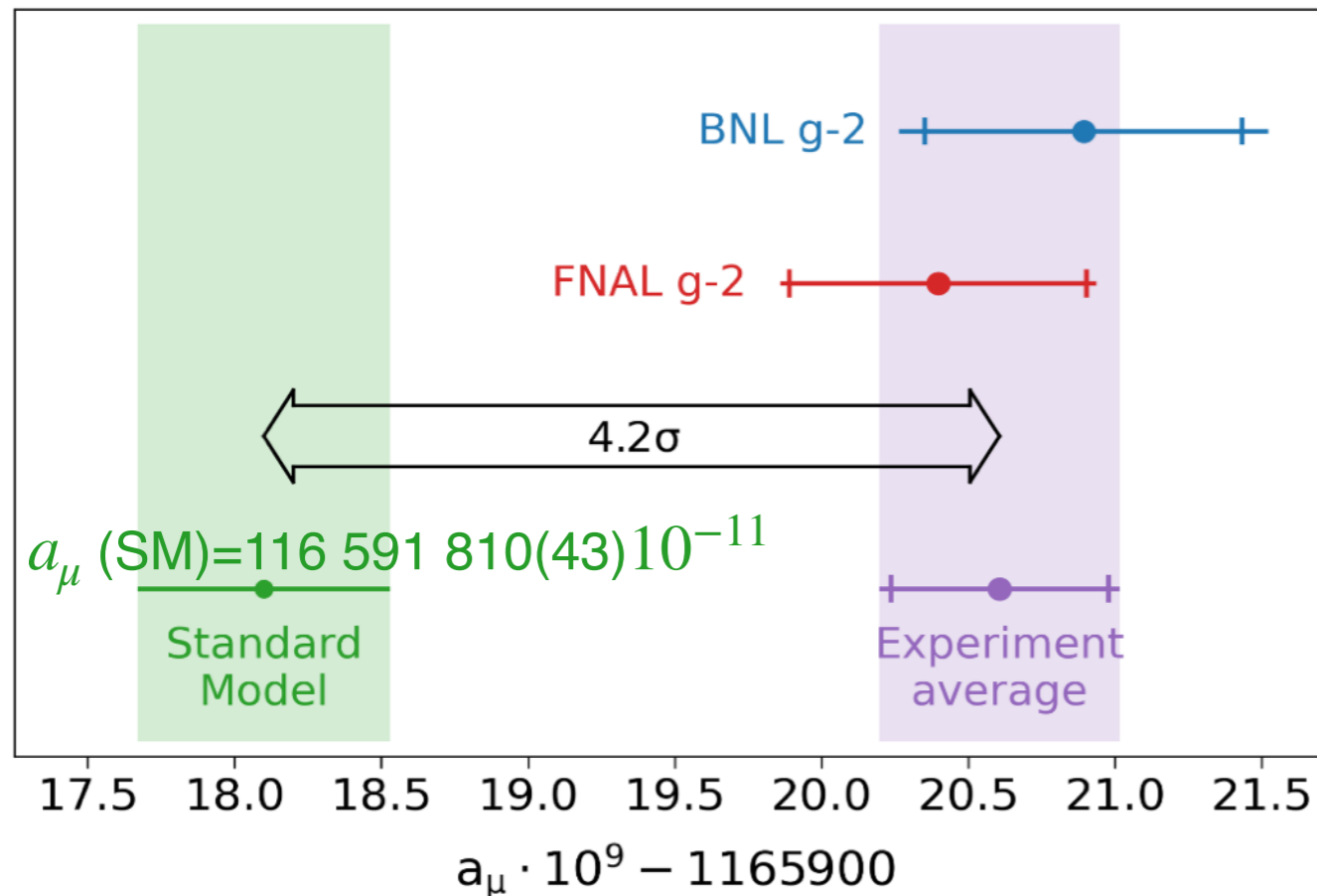
$$a_\mu (\text{FNAL}) = 116\,592\,040(54) \times 10^{-11} \text{ (460 ppb)}$$

$$a_\mu (\text{Exp}) = 116\,592\,061(41) \times 10^{-11} \text{ (350 ppb)}$$

- ✓ FNAL determined anomaly with 460 ppb precision
- ✓ Nothing was found that indicated contradiction with BNL results
- ✓ 15% smaller error
- ✓ Good agreement



Experimental Result and the Comparison

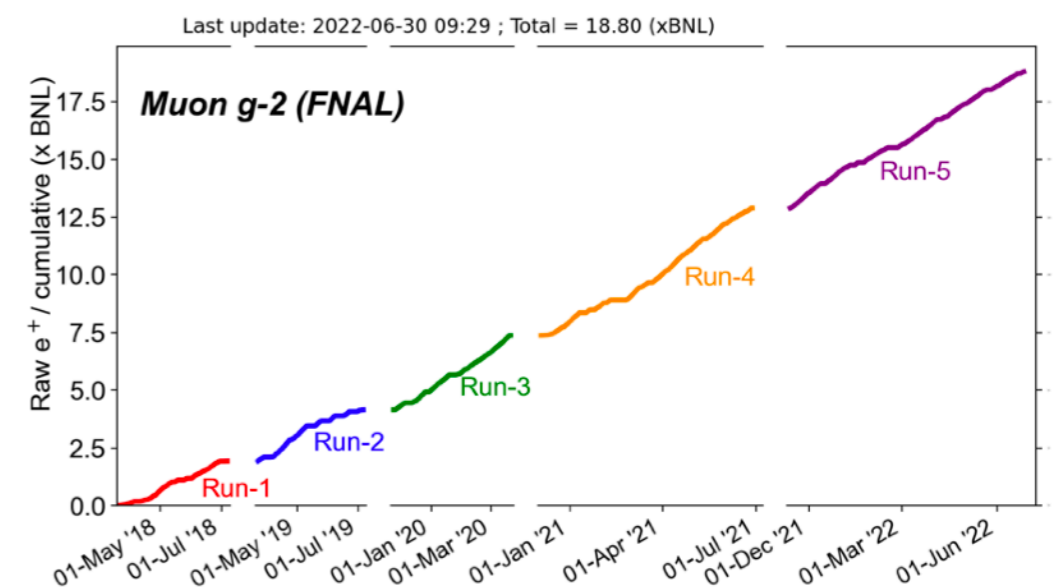


$$a_\mu \text{ (BNL)} = 116\,592\,089(63) \times 10^{-11} \text{ (540 ppb)}$$

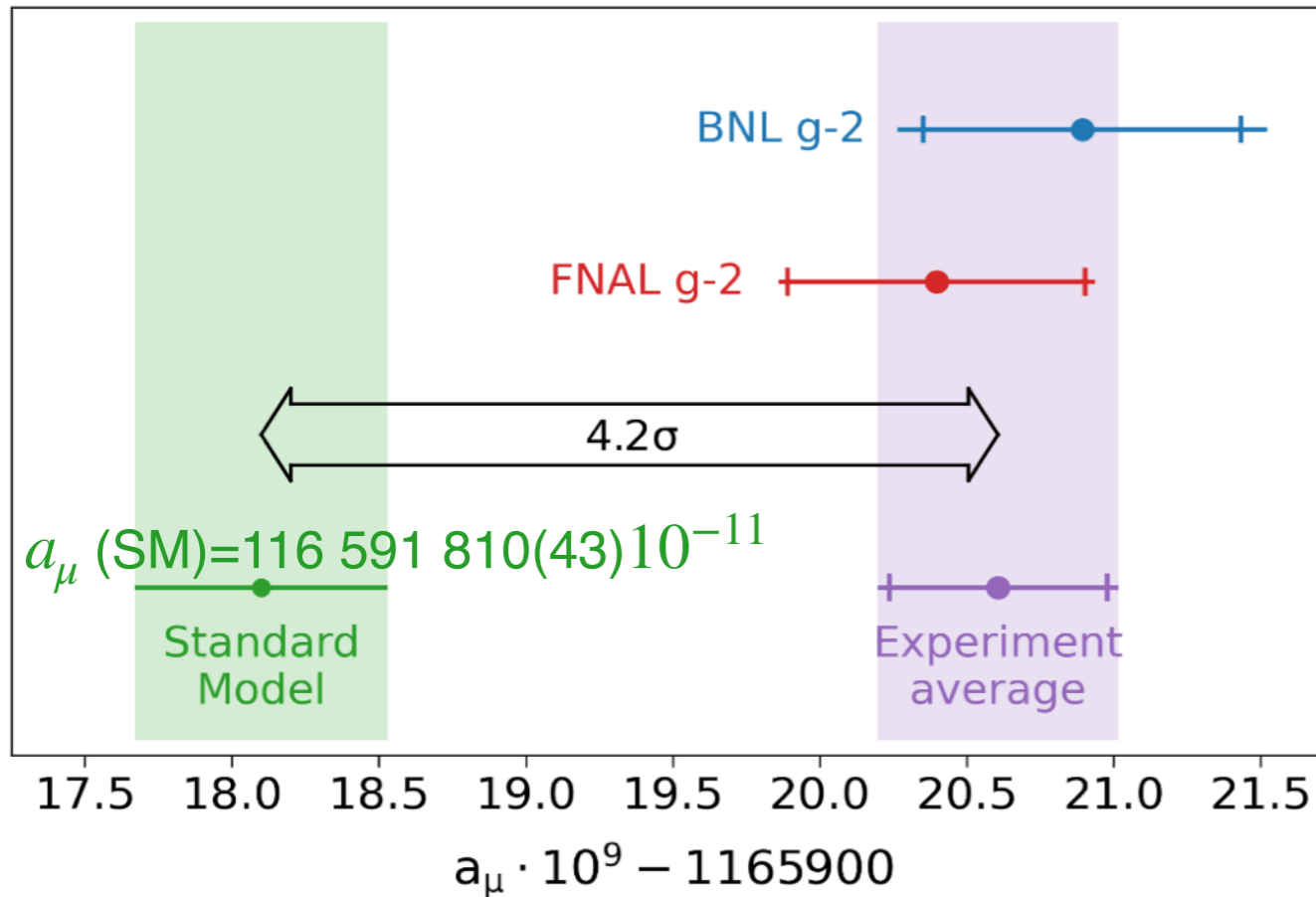
$$a_\mu \text{ (FNAL)} = 116\,592\,040(54) \times 10^{-11} \text{ (460 ppb)}$$

$$a_\mu \text{ (Exp)} = 116\,592\,061(41) \times 10^{-11} \text{ (350 ppb)}$$

- ✓ FNAL determined anomaly with 460 ppb precision
- ✓ Nothing was found that indicated contradiction with BNL results
- ✓ 15% smaller error
- ✓ Good agreement



Experimental Result and the Comparison



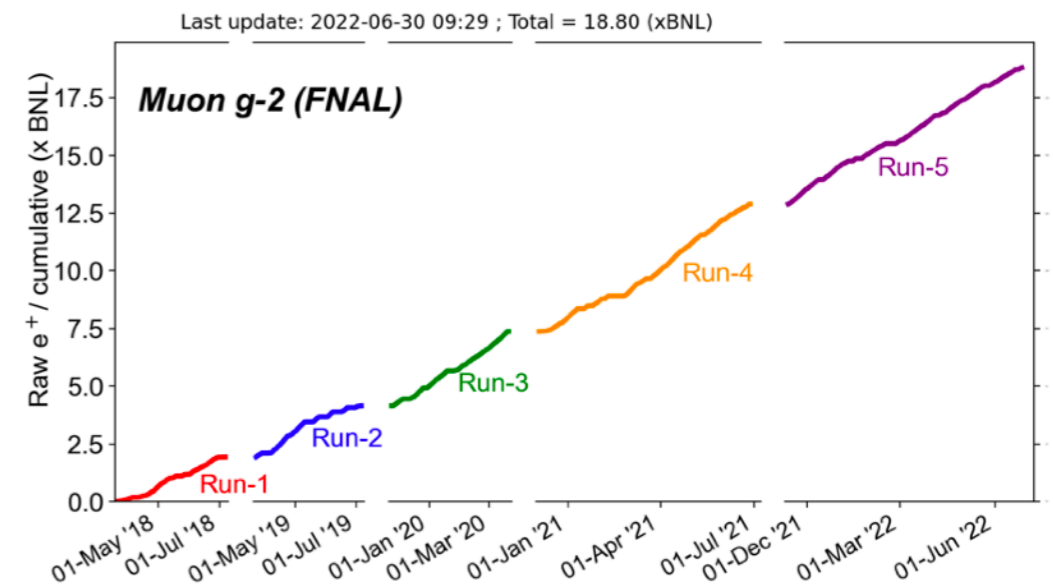
$$a_\mu (\text{BNL}) = 116\,592\,089(63) \times 10^{-11} \text{ (540 ppb)}$$

$$a_\mu (\text{FNAL}) = 116\,592\,040(54) \times 10^{-11} \text{ (460 ppb)}$$

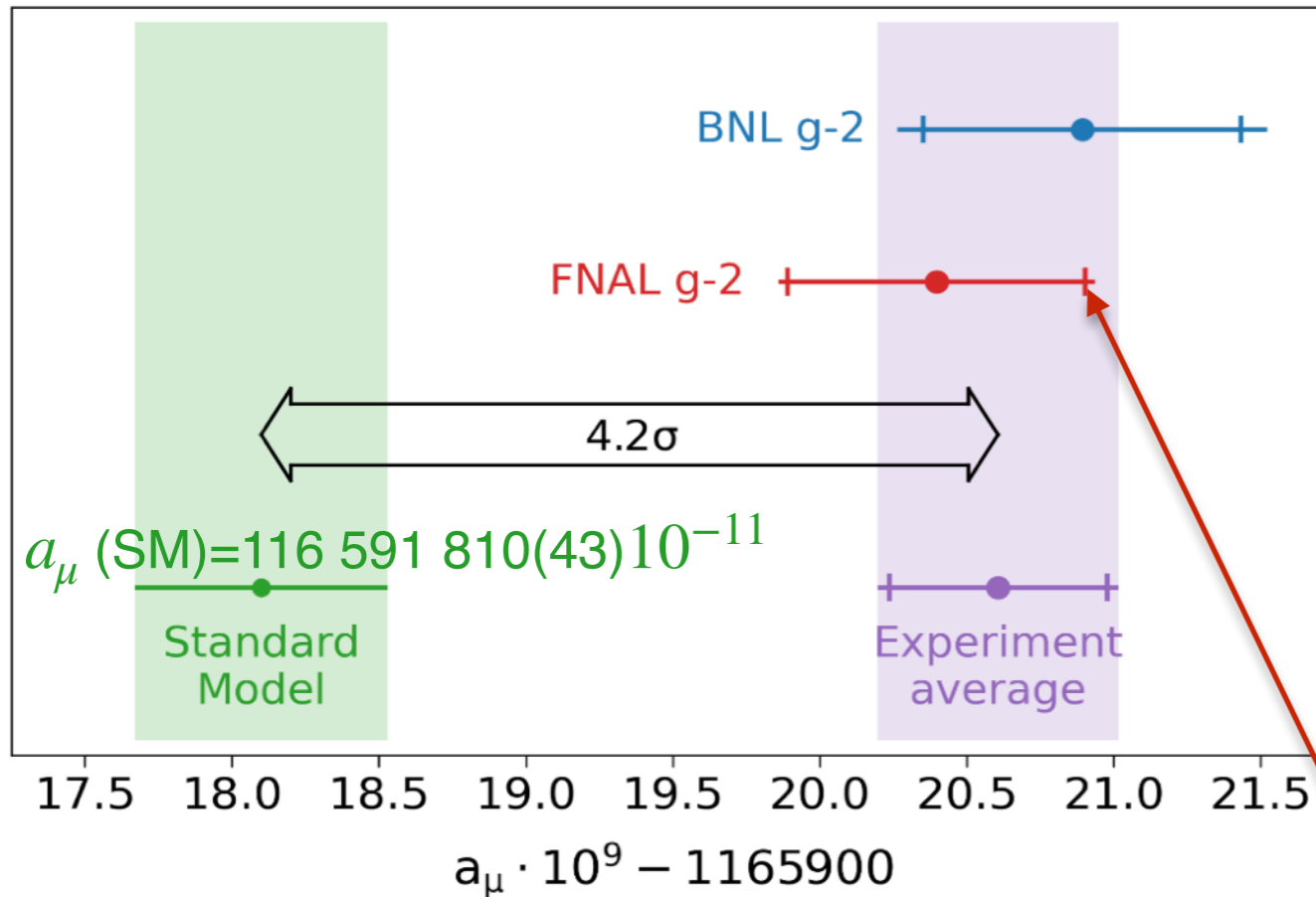
$$a_\mu (\text{Exp-SM}) = 251(59) \times 10^{-11} \rightarrow 4.2\sigma$$

$$a_\mu (\text{Exp}) = 116\,592\,061(41) \times 10^{-11} \text{ (350 ppb)}$$

- ✓ FNAL determined anomaly with 460 ppb precision
- ✓ Nothing was found that indicated contradiction with BNL results
- ✓ 15% smaller error
- ✓ Good agreement



Experimental Result and the Comparison



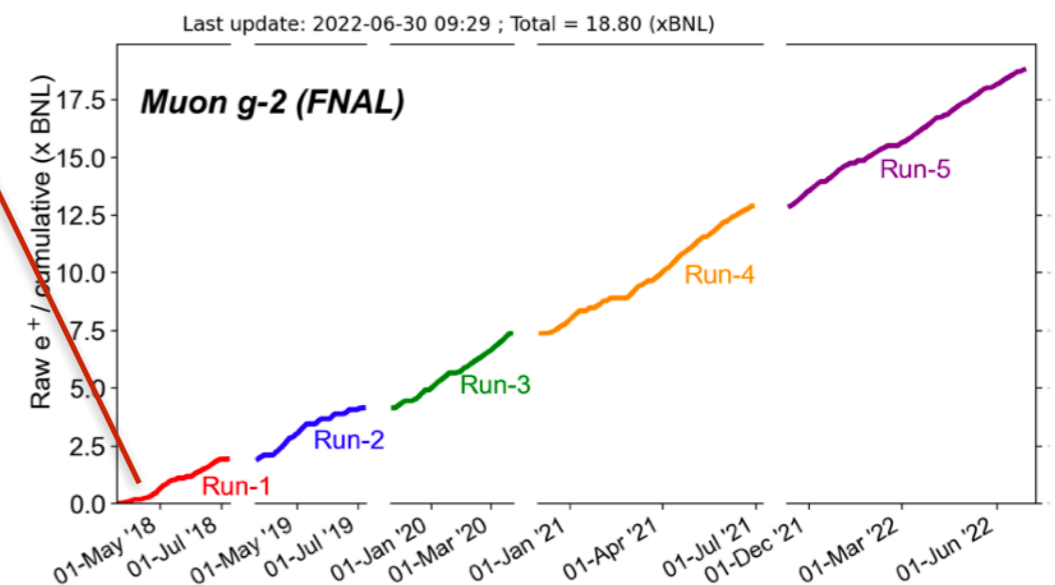
$$a_\mu (\text{BNL}) = 116\,592\,089(63) \times 10^{-11} \text{ (540 ppb)}$$

$$a_\mu (\text{FNAL}) = 116\,592\,040(54) \times 10^{-11} \text{ (460 ppb)}$$

$$a_\mu (\text{Exp-SM}) = 251(59) \times 10^{-11} \rightarrow 4.2\sigma$$

$$a_\mu (\text{Exp}) = 116\,592\,061(41) \times 10^{-11} \text{ (350 ppb)}$$

- ✓ FNAL determined anomaly with 460 ppb precision
- ✓ Nothing was found that indicated contradiction with BNL results
- ✓ 15% smaller error
- ✓ Good agreement



SM Theory Calculations

Lattice

Data-based Dispersive

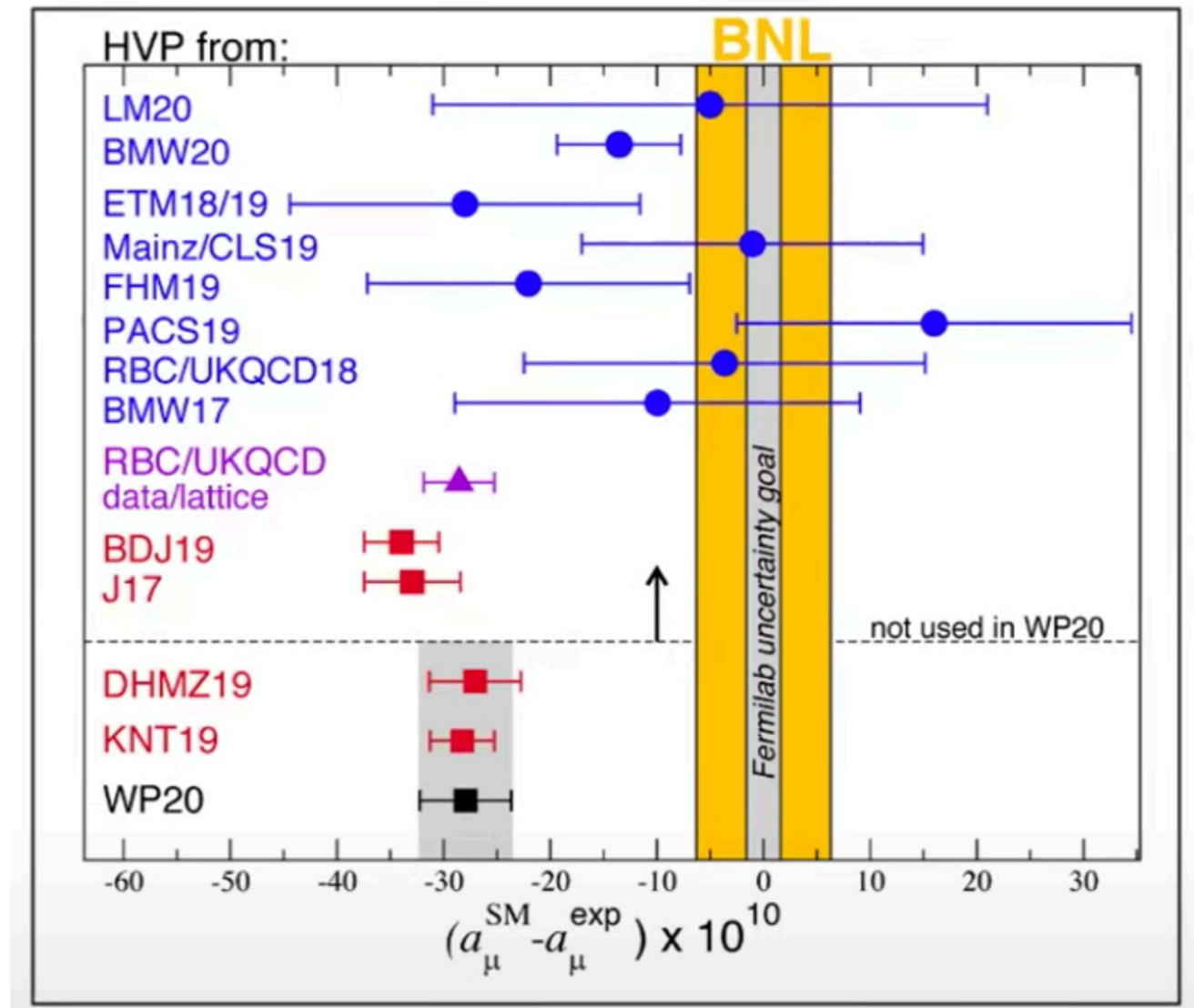
Lattice and Data

Official WP20

The anomalous magnetic moment of the muon in the Standard Model

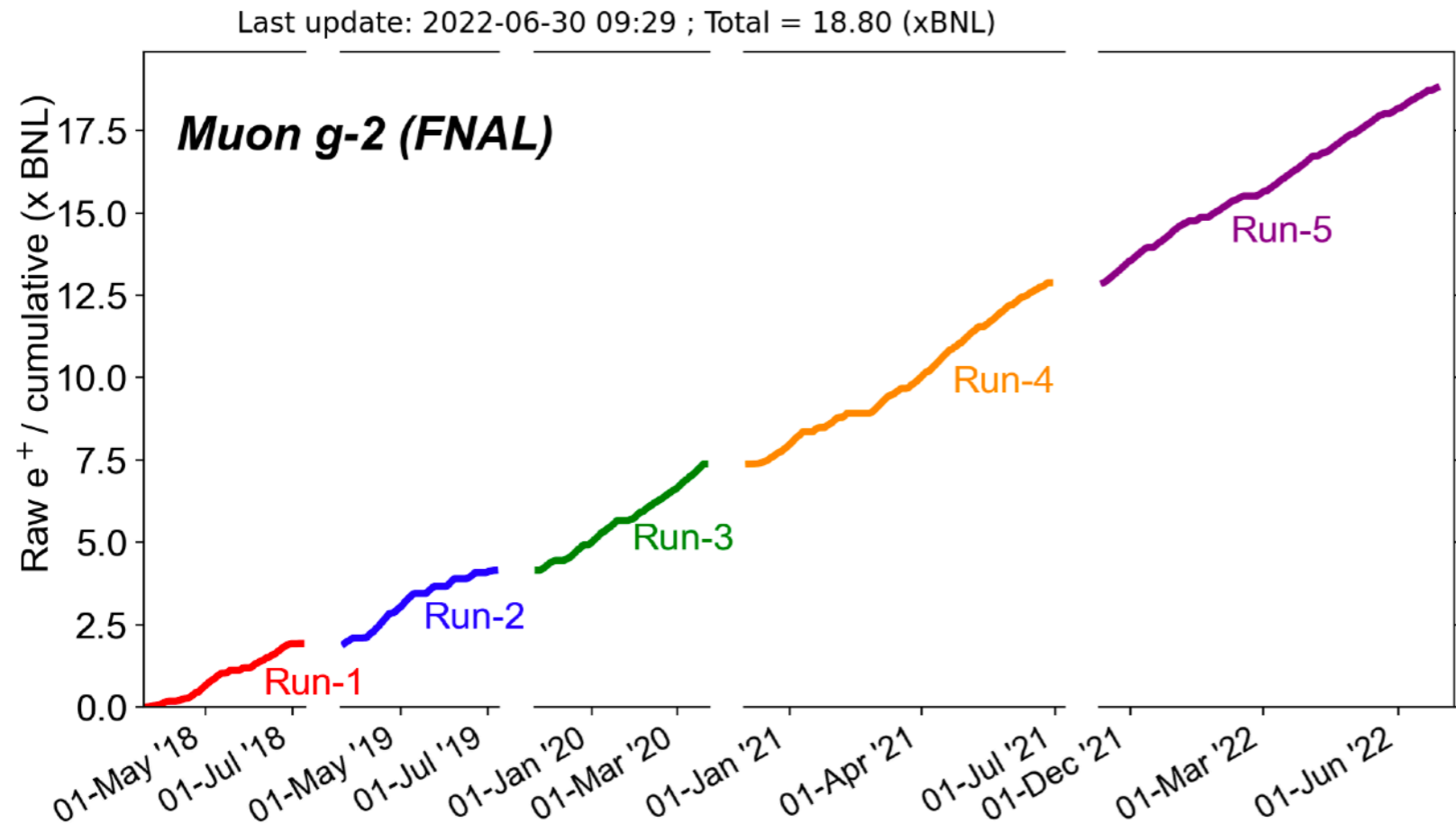
T. Aoyama^{1,2,3}, N. Asmussen⁴, M. Benayoun⁵, J. Bijnens⁶, T. Blum^{7,8}, M. Bruno⁹, I. Caprini¹⁰,
 C. M. Carloni Calame¹¹, M. Cè^{9,12,13}, G. Colangelo^{7,14}, F. Curciarello^{15,16}, H. Czyz¹⁷, I. Danilkin¹², M. Davier¹⁸,
 C. T. H. Davies¹⁹, M. Della Morte²⁰, S. I. Eidelman^{12,21}, A. X. El-Khadra^{7,23,24}, A. Gérardin²⁵, D. Giusti^{26,27},
 M. Golterman²⁸, Steven Gottlieb²⁹, V. Gülpers³⁰, F. Hagelstein¹⁴, M. Hayakawa^{31,2}, G. Herdoíza³², D. W. Hertzog³³,
 A. Hoecker³⁴, M. Hoferichter^{14,35}, B.-L. Hoid³⁶, R. J. Hudspith^{12,13}, F. Ignatov²¹, T. Izubuchi^{37,8}, F. Jegerlehner³⁸,
 L. Jin^{7,8}, A. Keshavarzi³⁹, T. Kinoshita^{40,41}, B. Kubis³⁶, A. Kupich²¹, A. Kupś^{42,43}, L. Laub¹⁴, C. Lehner^{126,37},
 L. Lellouch²⁵, I. Logashenko²¹, B. Malaescu⁵, K. Maltman^{44,45}, M. K. Marinković^{46,47}, P. Masjuan^{48,49},
 A. S. Meyer³⁷, H. B. Meyer^{12,13}, T. Mibe¹¹, K. Miura^{12,13,3}, S. E. Müller⁵⁰, M. Nio^{2,51}, D. Nomura^{52,53},
 A. Nyffeler^{7,12}, V. Pascalutsa¹², M. Passera⁵⁴, E. Perez del Rio⁵⁵, S. Peris^{48,49}, A. Portelli³⁰, M. Procura⁵⁶,
 C. F. Redmer¹², B. L. Roberts⁵⁷, P. Sánchez-Puertas⁴⁹, S. Serednyakov²¹, B. Shwartz²¹, S. Simula²⁷,
 D. Stöckinger⁵⁸, H. Stöckinger-Kim⁵⁸, P. Stoffer⁵⁹, T. Teubner⁶⁰, R. Van de Water²⁴, M. Vanderhaeghen^{12,13},
 G. Venanzoni⁶¹, G. von Hippel¹², H. Wittig^{12,13}, Z. Zhang¹⁸,
 M. N. Achasov²¹, A. Bashir⁶², N. Cardoso⁴⁷, B. Chakraborty⁶³, E.-H. Chao¹², J. Charles²⁵, A. Crivellin^{64,65},
 O. Deineka¹², A. Denig^{12,13}, C. DeTar⁶⁶, C. A. Dominguez⁶⁷, A. E. Dorokhov⁶⁸, V. P. Druzhinin²¹, G. Eichmann^{69,47},
 M. Fael⁷⁰, C. S. Fischer⁷¹, E. Gámiz⁷², Z. Gelzer²³, J. R. Green⁹, S. Guellati-Khelifa⁷³, D. Hatton¹⁹,
 N. Hermansson-Truedsson¹⁴, S. Holz³⁶, B. Hörz⁷⁴, M. Knecht²⁵, J. Koponen¹, A. S. Kronfeld²⁴, J. Laiho⁷⁵,
 S. Leupold⁴², P. B. Mackenzie²⁴, W. J. Marciano³⁷, C. McNeile²⁶, D. Mohler^{12,13}, J. Monnard¹⁴, E. T. Neil⁷⁷,
 A. V. Nesterenko⁶⁸, K. Ottnad¹², V. Pauk¹², A. E. Radzhabov⁷⁸, E. de Rafael²⁵, K. Raya⁷⁹, A. Risch¹²,
 A. Rodríguez-Sánchez⁶, P. Roig⁸⁰, T. San José^{12,13}, E. P. Solodov²¹, R. Sugar⁸¹, K. Yu. Todyshev²¹, A. Vainshtein⁸²,
 A. Vaquero Avilés-Casco⁶⁶, E. Weil⁷¹, J. Wilhelm¹², R. Williams⁷¹, A. S. Zhevlakov⁷⁸

04822v2 [hep-ph] 13 Nov 2020



- BMW20 is also in tension with data-based dispersive result.
- Will be interested to see how it evolves in future but lattice QCD calculations requires a huge amount of computing resource. All groups are working on defining intermediate results (simpler way to compare things)
- By 2025, both hadronic calculations (HVP and HLbL) will give both data-driven and lattice results which will match the experiment precision

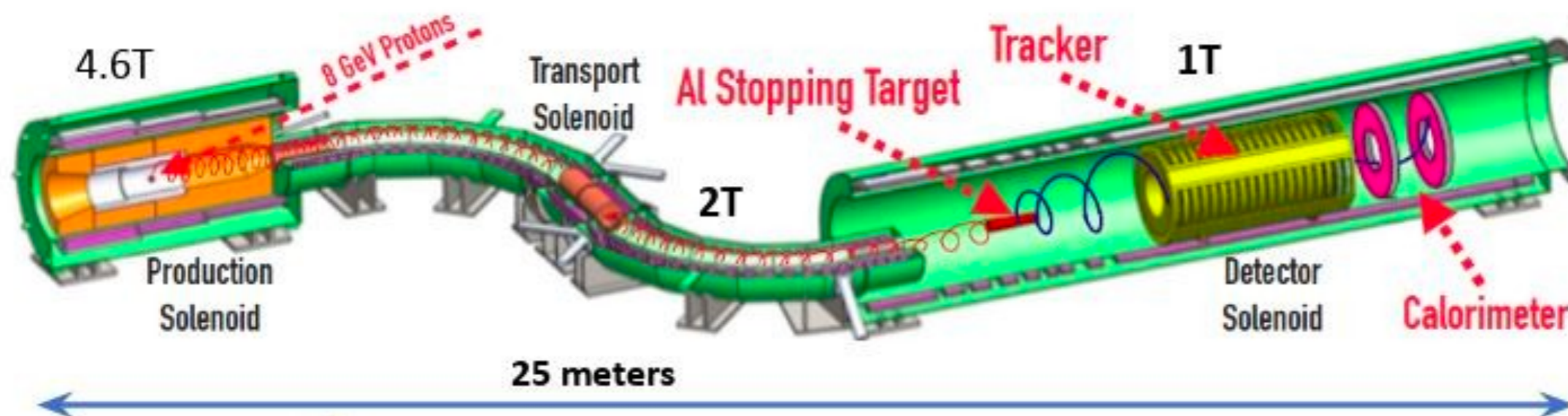
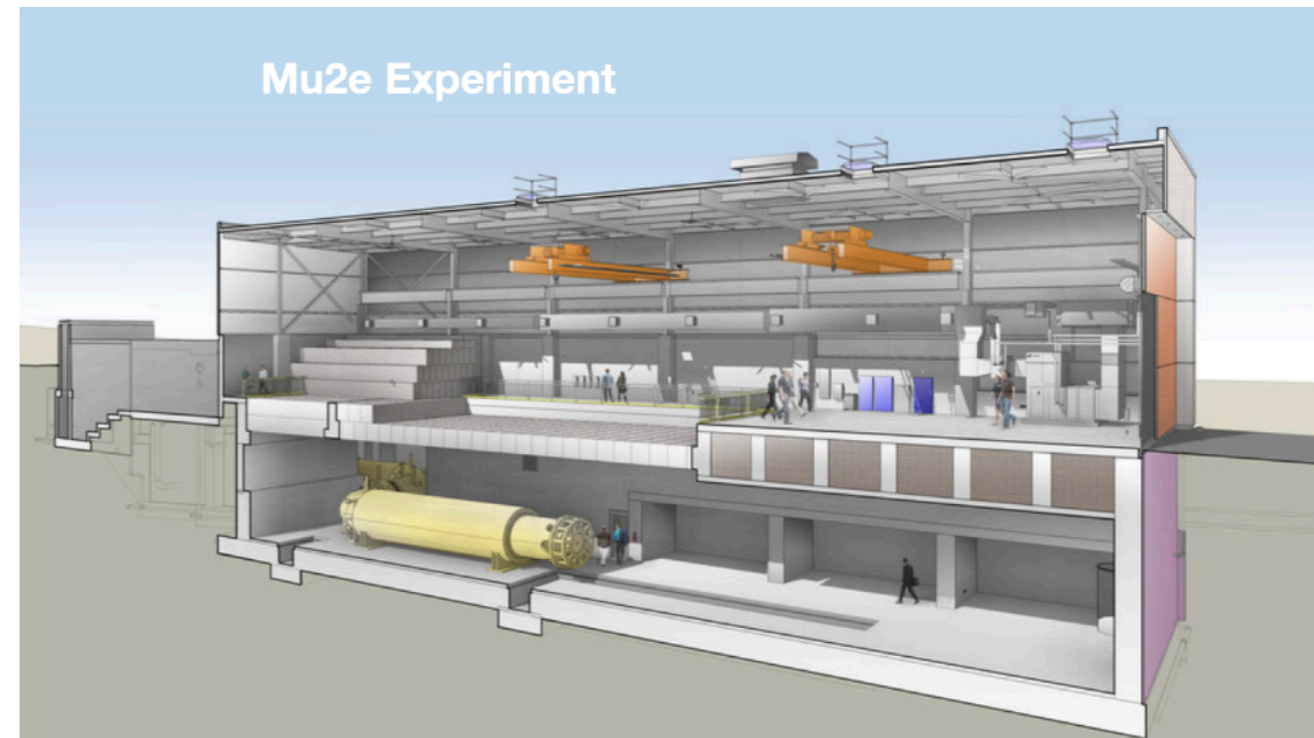
Experiment Status



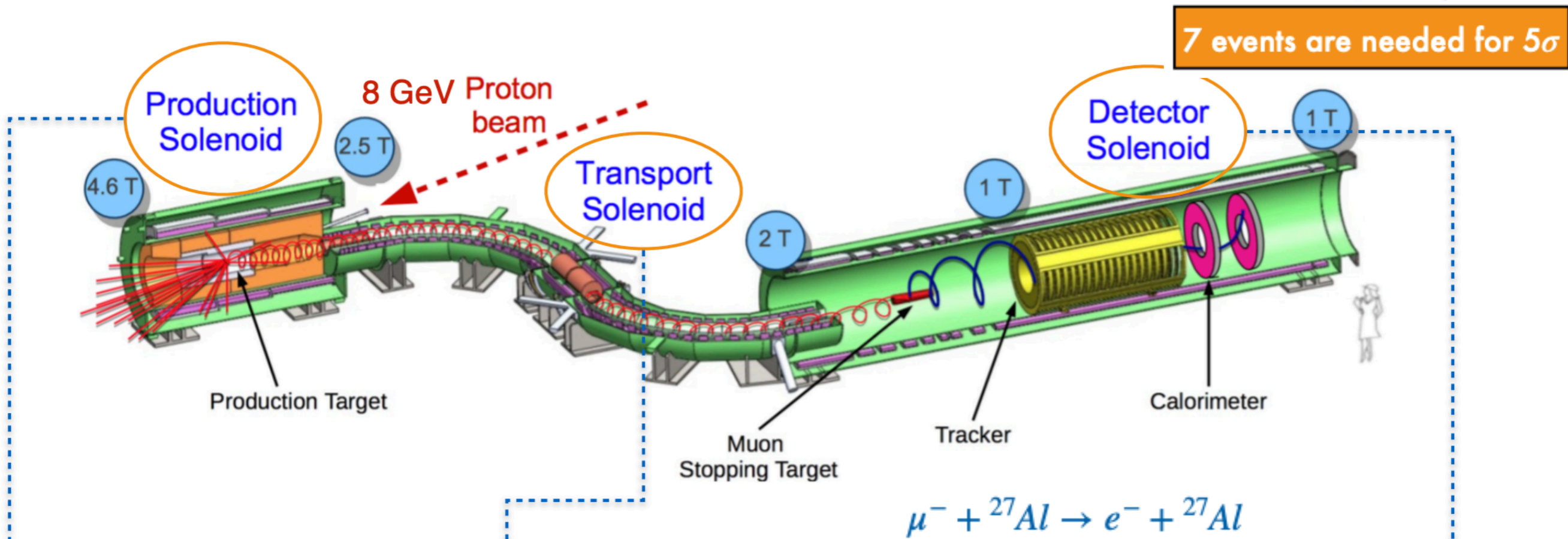
- Run-2 and Run-3 analysis are ongoing -> reduce combined exp. error by 2 times
- Run-5 will end in July-> Run-4 and beyond will reduce the statistical uncertainties down to **100 ppb** in total.
- Run-6 will be the last year to collect data

Next muon project at Fermilab: Mu2e Experiment

- Mu2e will start right after muon g-2 stops taking data
- Potential Experiments after PIP-II
 - Mu2e-II and Potential Storage ring experiments are being discussed



Mu2e Basics



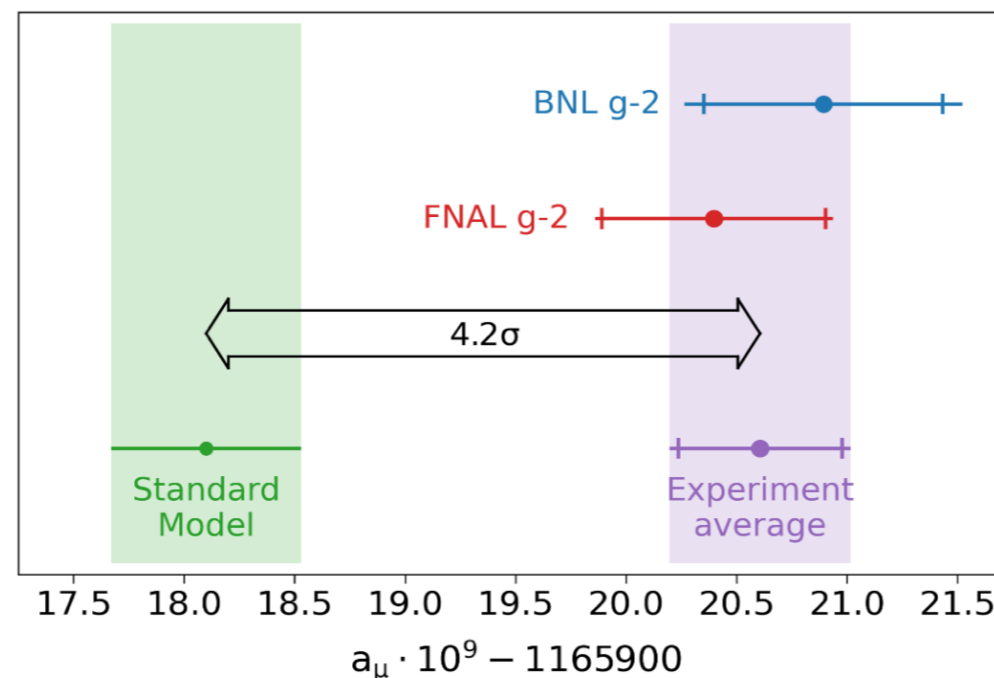
- Direct low momentum pions/muons to transport solenoid.

- S-shaped geometry with collimators select low momentum and negatively charged particles.

- Houses muon stopping target, tracker & calorimeter.

Summary and Outlook

- Fermilab g-2 experiment published first result with 460 ppb precision
- Experiment combination increased the tension with theory to 4.2σ level
- Rest of the data will take the statistical uncertainty to 100 ppb
- Systematic uncertainty will hit the 100 ppb goal
- Next result will be published in the beginning of 2023
- Mu2e experiment will begin after g-2 to focus on neutrino-less conversion of the muon in the presence of Al nucleus
- Mu2e is expected to start commissioning in 2023 and start taking data in 2026 until Fermilab accelerator shutdown, will continue later to collect more data

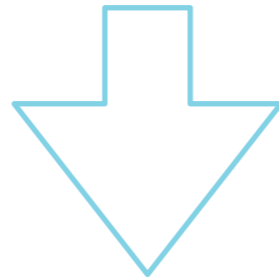


Thanks!

Back-up

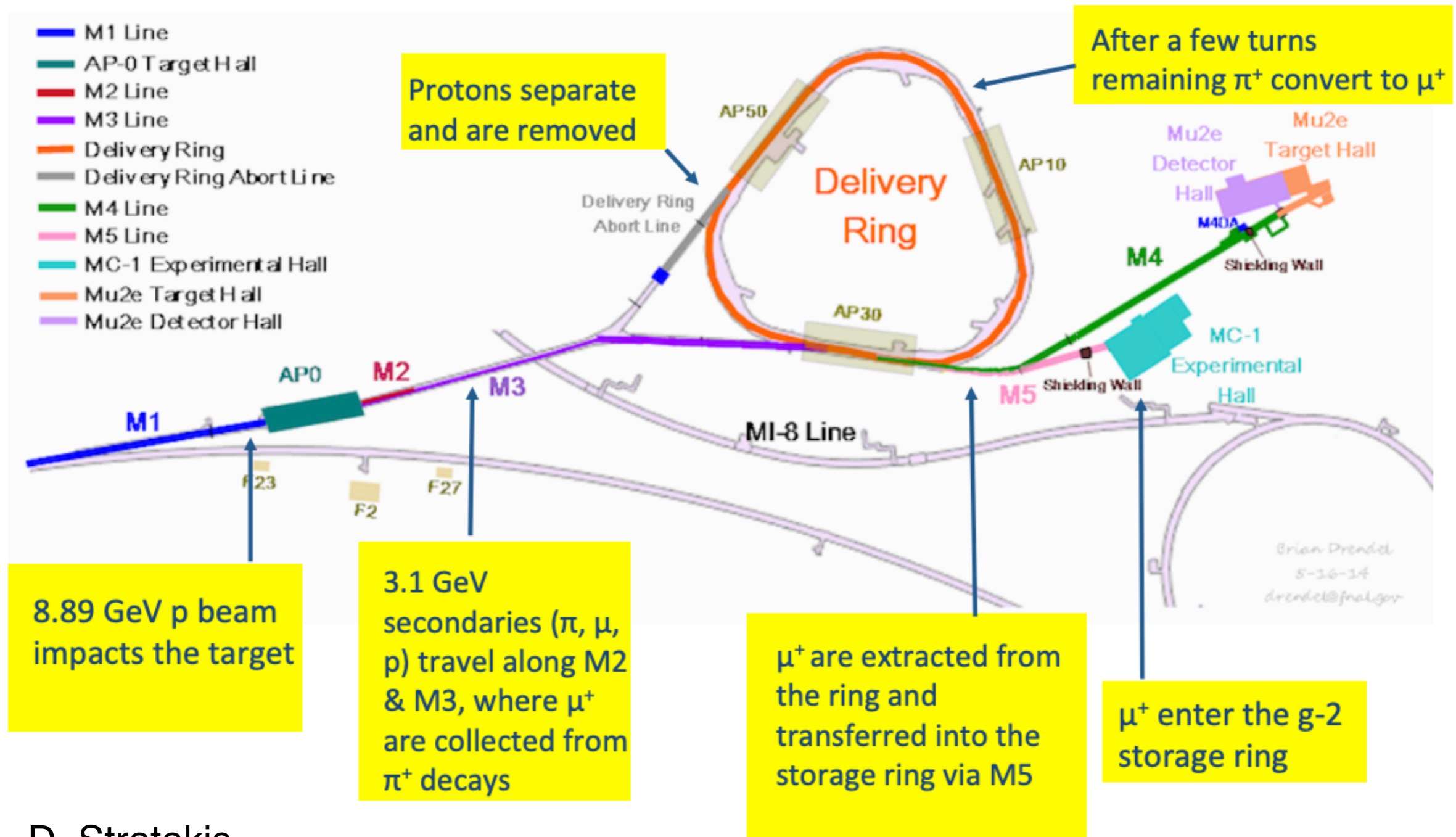
Most promising models to explain the discrepancy

- Muon $g-2$ can indicate if there is a CP-conserving, lepton-flavor conserving or BSM chirality-flipping interaction but can't tell which one is the most promising.
- Possible explanations:
 - SUSY models (while evading LHC limits)
 - Leptoquark models (if leptoquark masses are above all LHC limits)
 - 2-Higgs doublet models



Establishing a $g-2$ discrepancy from SM would place a strict limit on BSM scenarios

Muon Beamline at Fermilab



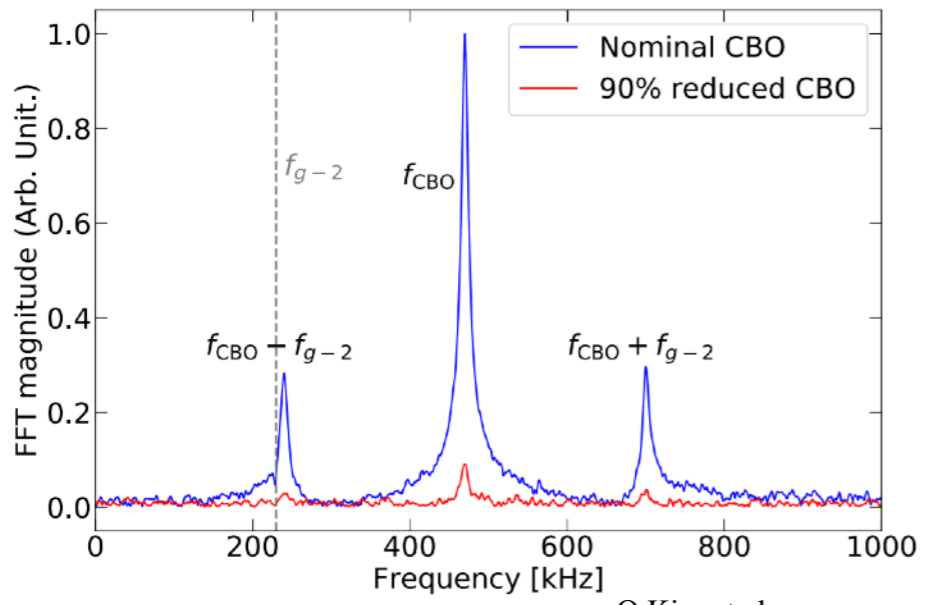
D. Stratakis

Improvements since Run-1: Quad-RF System

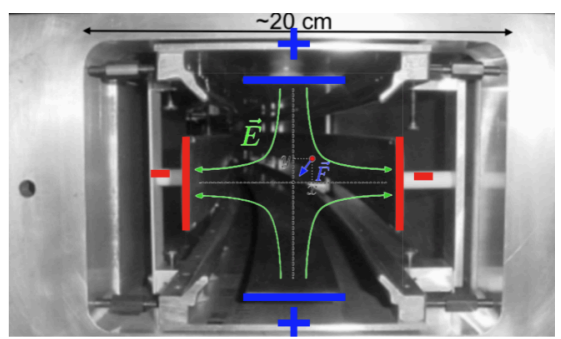
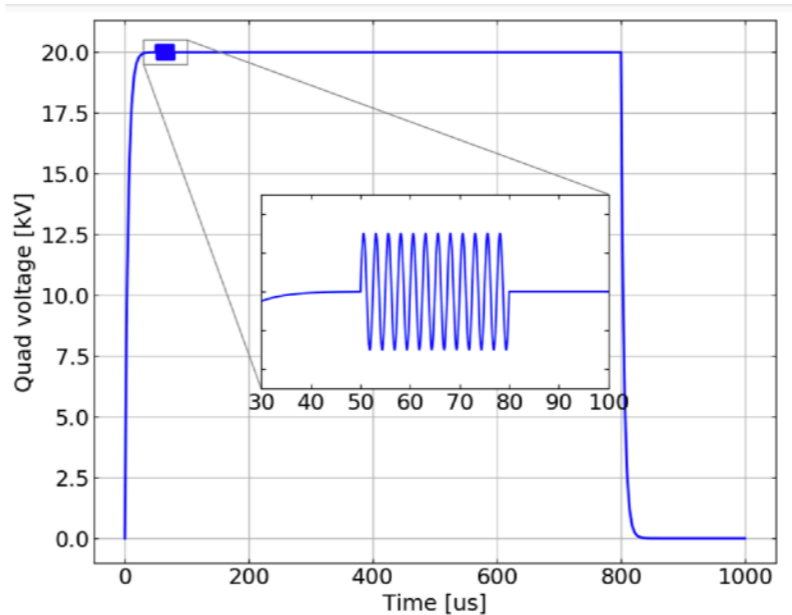
Original idea from Yuri F. Orlov and Yannis Semertzidis (Muon g-2 Note #431). By applying RF dipole or quadrupole electric field; (by kicking the beam out of phase with CBO)

- Reduce CBO Amplitude (Due to an imperfect kicker system, the beam executes CBO oscillations with a large amplitude)
- Reduce muon loss by scraping the beam

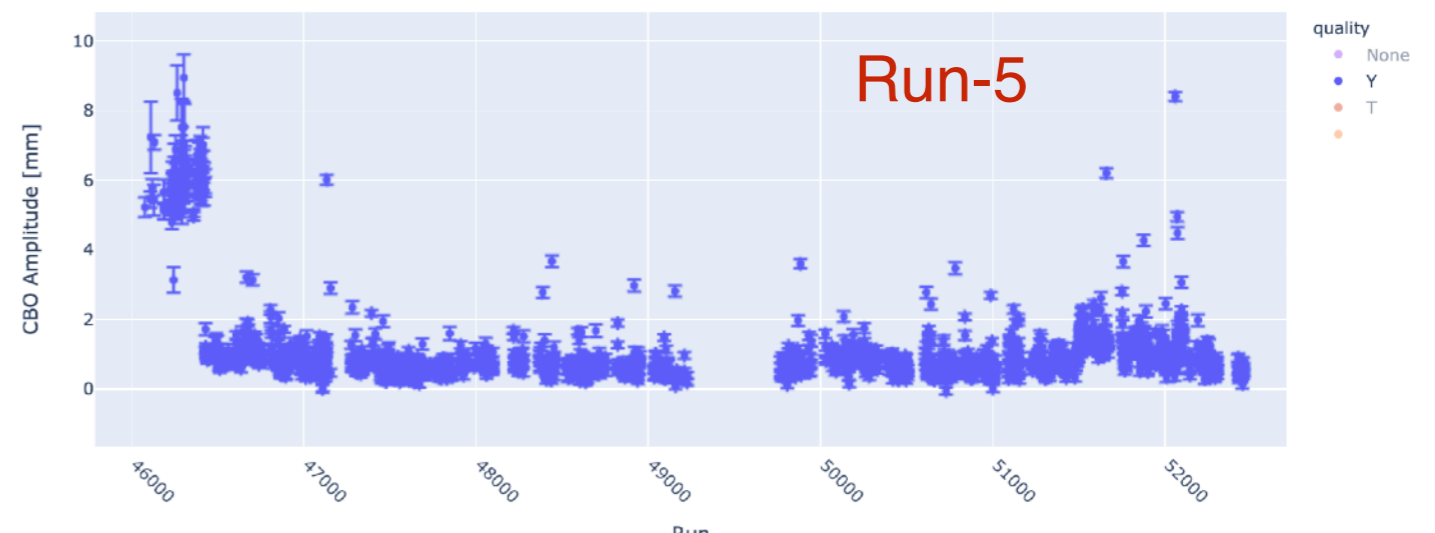
RF can be applied through the quad plates



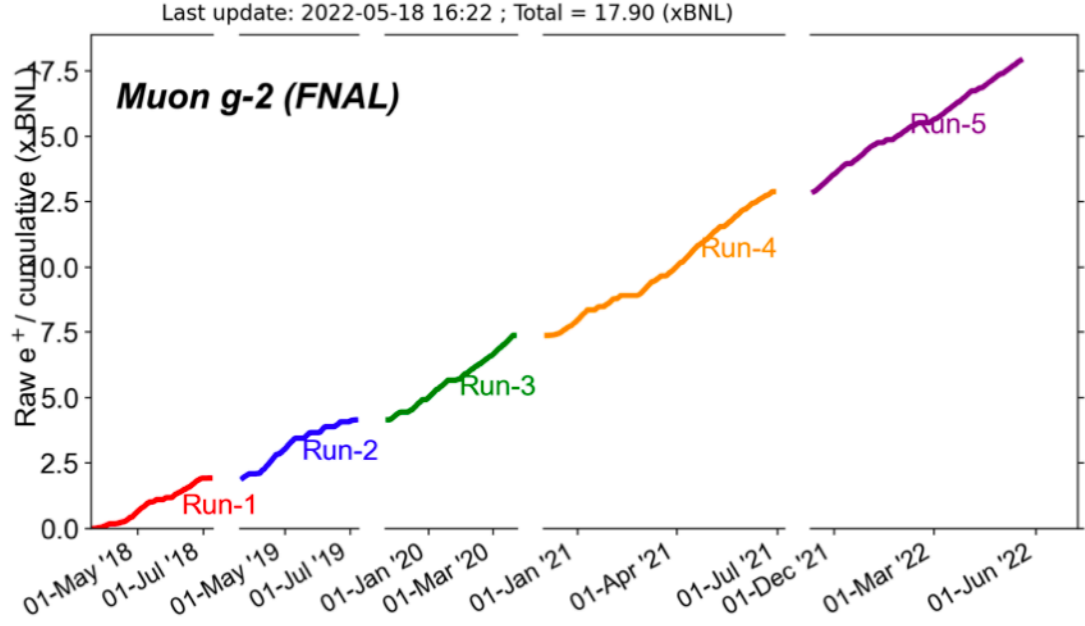
O Kim et al
New J. Phys. 22 (2020) 063002



CBO Amplitude: 5-6mm->0.5-1mm
 Muon Loss : factor of 4 reduction

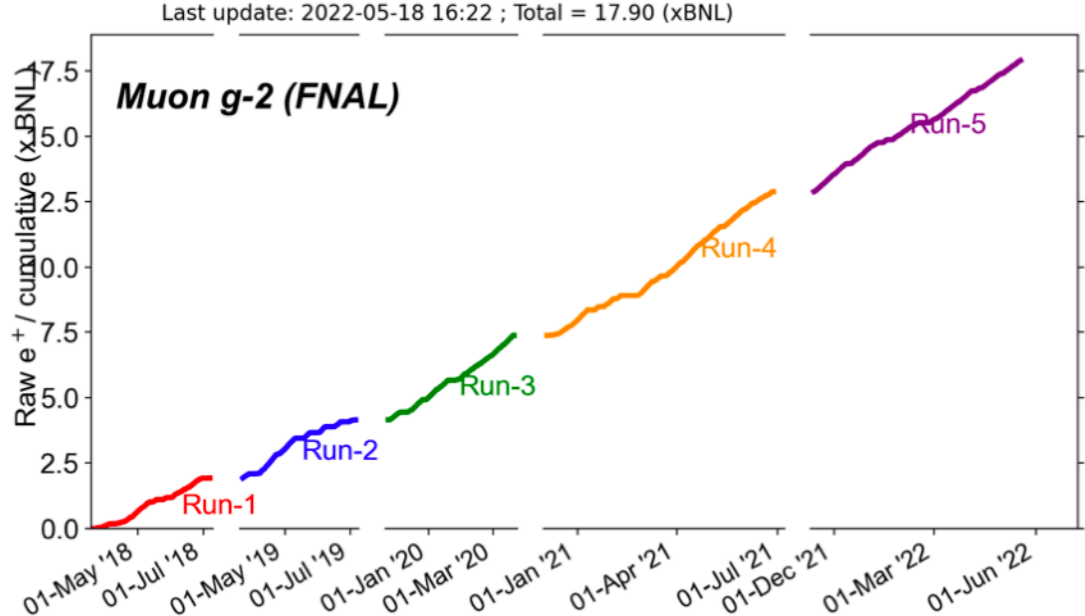


Improvements on the g-2 uncertainty

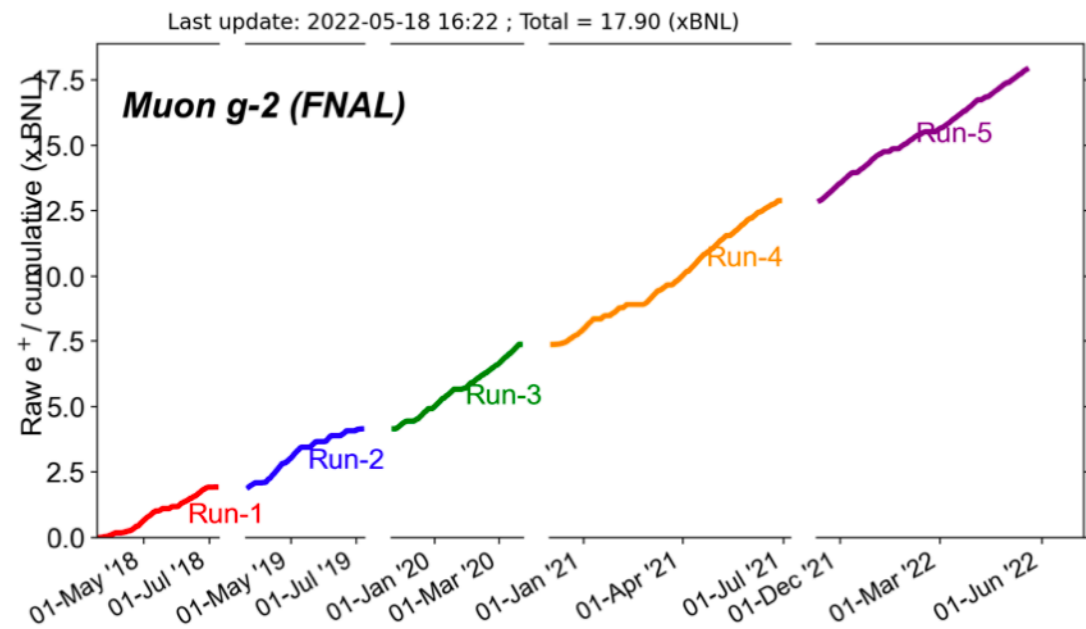


Improvements on the g-2 uncertainty

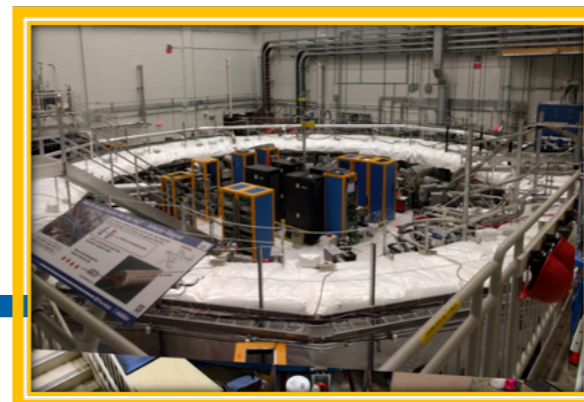
- Run-5 started in November 2021
 - Improved kick: Most recent part of Run-3 had a perfectly centered beam owing to improved kicker system.



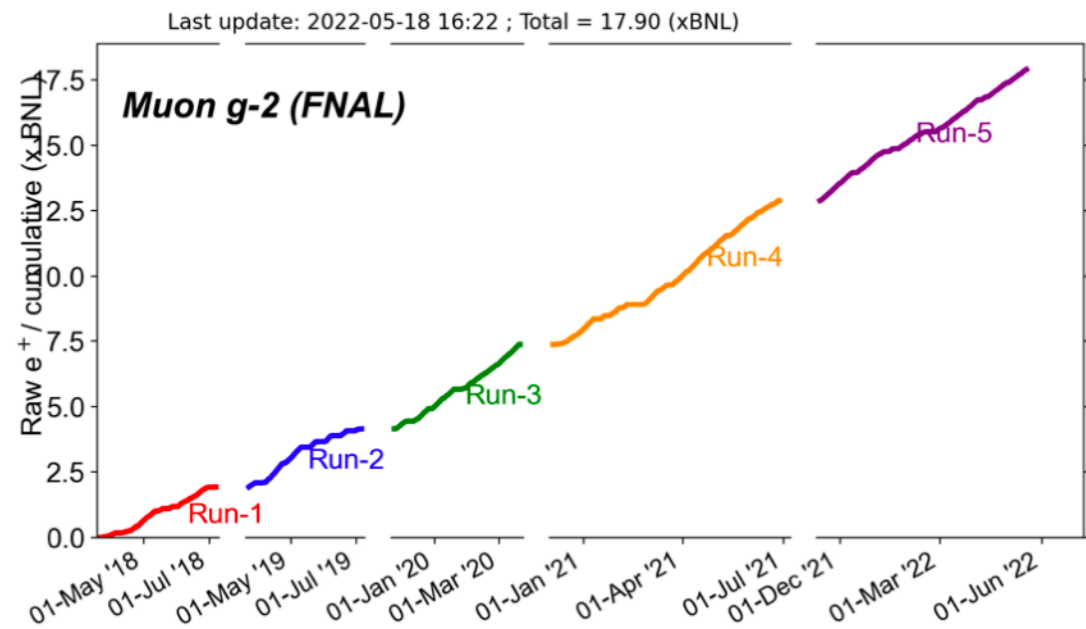
Improvements on the g-2 uncertainty



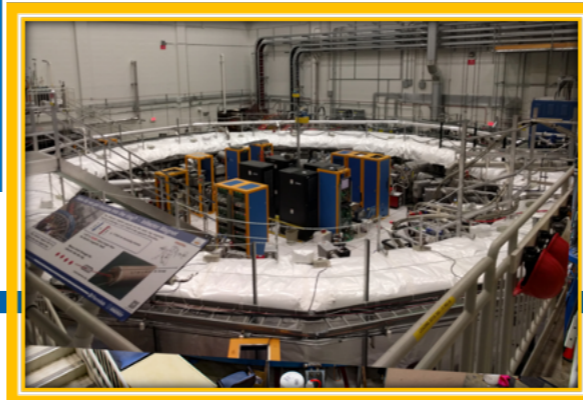
- Run-5 started in November 2021
 - Improved kick: Most recent part of Run-3 had a perfectly centered beam owing to improved kicker system.
 - Improved field stability: More stable temperature and better magnet insulation.



Improvements on the g-2 uncertainty

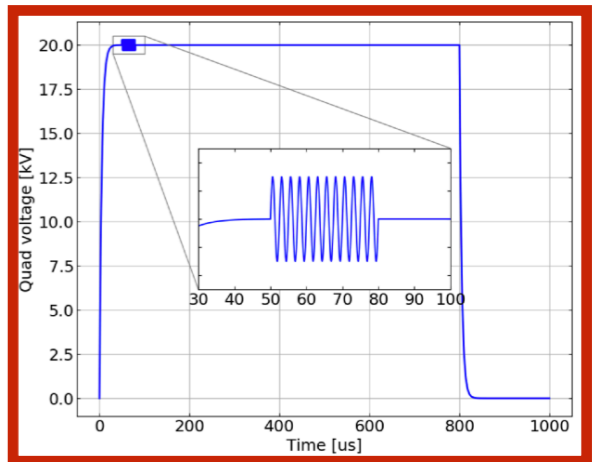
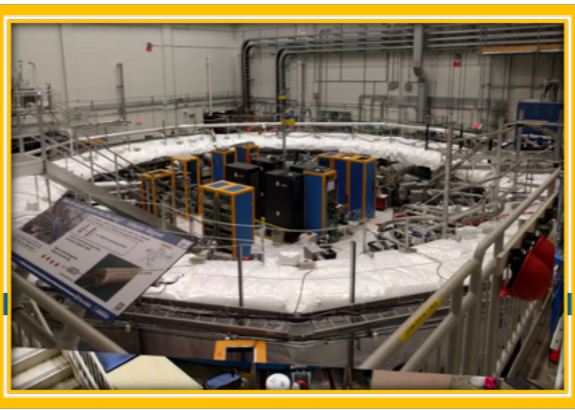
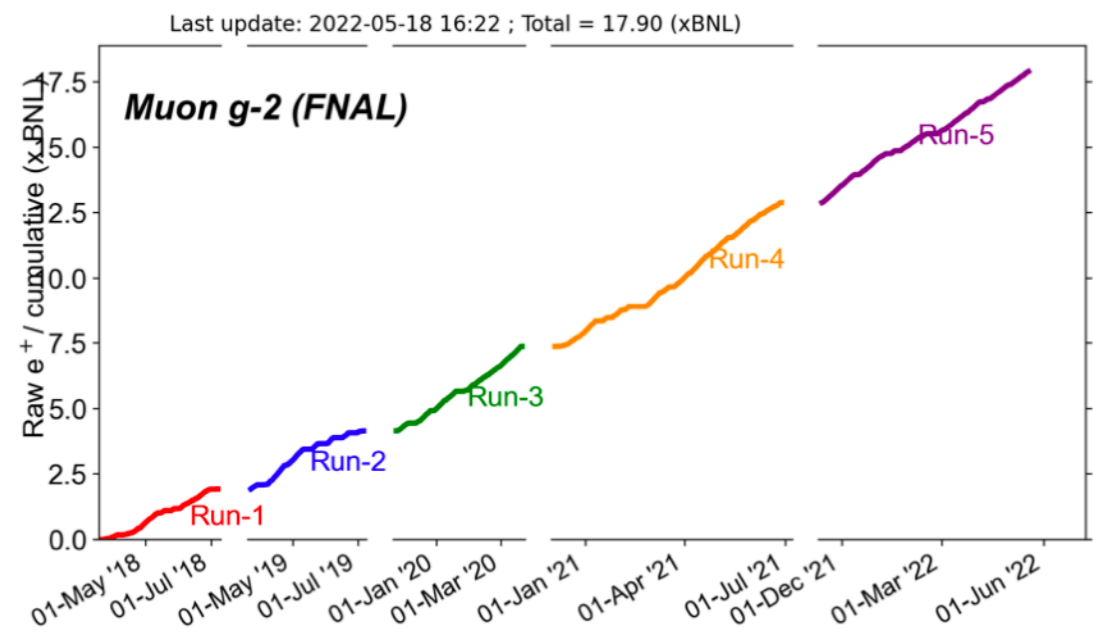


- Run-5 started in November 2021
 - Improved kick: Most recent part of Run-3 had a perfectly centered beam owing to improved kicker system.
 - Improved field stability: More stable temperature and better magnet insulation.
 - Damaged HV resistors were replaced after Run-1



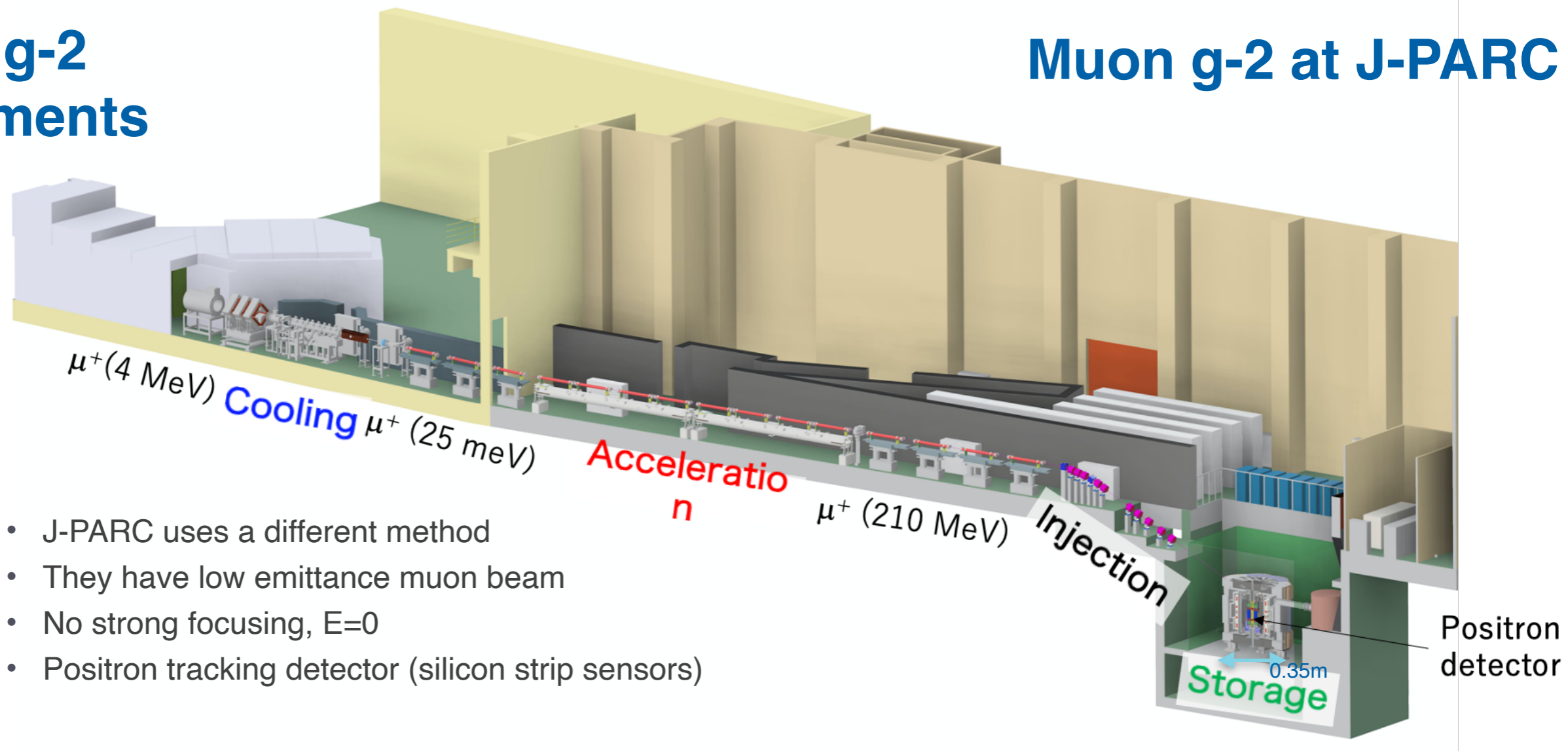
Improvements on the g-2 uncertainty

- Run-5 started in November 2021
 - Improved kick: Most recent part of Run-3 had a perfectly centered beam owing to improved kicker system.
 - Improved field stability: More stable temperature and better magnet insulation.
 - Damaged HV resistors were replaced after Run-1
 - RF System is fully integrated in Run-5



Future g-2 Experiments

Muon g-2 at J-PARC



- J-PARC uses a different method
- They have low emittance muon beam
- No strong focusing, $E=0$
- Positron tracking detector (silicon strip sensors)

- Electric field will be eliminated by using reaccelerated thermal muon beam
- Lower momentum muon beam + compact storage region with highly uniform magnetic field
- Tracking detector for decay positrons \rightarrow reduced pile-up + able to measure the momentum direction of positrons.
- Final Goal is to reach **0.46ppm** \rightarrow **0.1ppm** on a_μ
- Beam line construction has started and commissioning is expected to start in 2027